Gluon radiation beyond Poisson using MHV techniques

Andriniaina Narindra Rasoanaivo

Thesis Presented for the Degree of
DOCTOR OF PHILOSOPHY

Department of Physics
University of Cape Town

November 2017

Dedicated to

Mom and Dad

Gluon radiation beyond Poisson using MHV techniques

Andriniaina Narindra Rasoanaivo

Submitted for the degree of Doctor of Philosophy
November 2017

Abstract

For the first time, MHV techniques are applied to radiative energy loss processes in QCD. First, we provide a pedagogical introduction to MHV techniques with explicit computational example on $q\bar{q} \to gg$ cross section and splitting functions which reproduces known results. Next, we derive the multiple photon emissions current to reproduce the Poisson distribution of photon radiated from a high energetic quark. Then we derive the equivalent current for the case of multiple gluon emissions in vacuum. We then use the previous result to compute the two gluon correlation. We also study the radiation current induced from a change in the color state of an energetic quark: we start with the case of 1, 2, and 3 gluon induced radiations and then conjecture the analytic expression for n gluon emissions. We then prove this conjecture for the case where the emitted gluons are symmetric and antisymmetric under gluon permutations.

Declaration

The work in this thesis is based on research carried out at the Department of Physics, University of Cape Town, South Africa. No part of this thesis has been submitted elsewhere for any other degree or qualification and it is all my own work unless referenced to the contrary in the text.

Acknowledgements

First I would like to thank my supervisor, Dr. W. A. Horowitz, for his continuous support during these three years I was at UCT. His insightful comments and patience are a source of tremendous motivation, and his dedication to physics has inspired me for going forward. "Thank you Will for making me who I am today, for inviting me to UCT; it was a wonderful academic experience."

I am extremely grateful for financial support from the University of Cape Town - Science Faculty PhD Fellowship that has allowed me to pursue this PhD. I also thank the SA-CERN collaboration, the NRF, and the UCT URC for additional support. I would also like to thank the UCT Physics Department; especially those who facilitated my integration into the department: Ben Meiring for those endless physics discussions, and Judith Alcock-Zeilinger for being a wonderful officemate.

I would like to thank Faraniaina Rasolofoson and Andriamanankasina Ramanantoanina for the support during these past three years at UCT. I also thank Volazafy Lydie Yannick for the encouragement she offered.

Last and not least, let me thank my parents and my sister. "*Misaotra betsaka tamin'ireo fankaherezana sy fanohanana ara-tsaina izay nomenareo ary koa ny fahatokisana izay nampetrakareo tamiko. Ny hazo no vanon-ko lakana, ny tany naniriany no tsara.*"

Contents

List of Figures

List of Tables

Introduction *1*

In the beginning of the twentieth century, the two main pillars of the modern physics, quantum mechanics (QM) and special relativity (SR), were formulated. In 1900, the notion of quanta was proposed by Max Planck [1] as a solution to the black-body radiation problem and a decade later became the quantum theory that describes the physics of atomic levels. Special relativity, on the other hand, was introduced by Albert Einstein [2] in 1905 to resolve the inconsistency of Newtonian mechanics with Maxwell's equations of electromagnetism. Despite the success that the two theories achieved, it is necessary for QM and SR to be combined to understand subatomic matter. The resulting theory of this unification is quantum field theory [3].

Today, as a relativistic extension of quantum mechanics, quantum field theory (QFT) has become a mathematical framework to describe three of the fundamental forces: the electromagnetic interaction, the weak interaction and the strong interaction. The electromagnetic (EM) force, one of the two significant forces in everyday life, was the first to be promoted into QFT and is called quantum electrodynamics (QED) [4, 5]. This theory describes the interactions between charged particles via photon exchange, the mediator of the force. The weak and strong interactions are nuclear forces and occur only at the subatomic level. The weak interaction is responsible for the β decay that converts a neutron into a proton or the other way around [6, 7]. In the language of field theory the weak force is mediated by the massive $W^{\pm}$ and Z bosons just as the photon mediates the electromagnetic force in QED. Finally, the strong interaction is the force that keeps protons and neutrons bound together in the nucleus, and it is described by the QFT known as quantum

chromodynamics (QCD), a theory that explains the interaction of color charged particles, quarks and gluons [8].

On top of been able to describe the three fundamental forces, QFT, as a mathematical framework, has successfully combined those three formulations into a single theory known as the Standard Model (SM) and leads to the classification of all known elementary particles. Successfully explaining many experimental results and precisely predicting a wide variety of phenomena, SM has become established as a well-tested physics theory [9–11].

1.1 Road to QCD

The idea of a strong nuclear interaction arose right after the discovery of the neutron by Chadwick in 1932 [12]; this discovery indicated that nuclei consist of protons and neutrons and for this reason the strong force, with a short range interaction, has to be strong enough to counter the electromagnetic repulsion between protons. In 1935, Yukawa came up with the meson theory in which the short range force could be understood as an exchange of a virtual meson [13]. This mediator particle predicted by the meson theory was indeed observed: the π-meson discovered in 1947 [14]. Shortly after finding the π-meson, many other mesons were observed from cosmic rays [15, 16]. Following the discovery of mesons, enormous experimental progress was made toward the understanding of the strong force alongside with theoretical developments.

Gell-Mann [17] and Nishijima [18] introduced a new quantum number, strangeness, which can explain why certain particles produced in strong interactions had a longer lifetime than expected. The theoretical cornerstone was when Gell-Mann and Ne'eman showed that hadrons could be classified into multiplets of the irreducible representation of the $SU(3)$ group, the Eightfold Way classification [19–21].

In 1964, Gell-Man [22] and independently Zweig [23] proposed the existence of a substructure in the assumption that baryons are bound states of those new constituents, while mesons are bound states of two. Gell-Mann named these hypothetical substructure particles *quarks*. Quarks were later accepted to be the fundamental

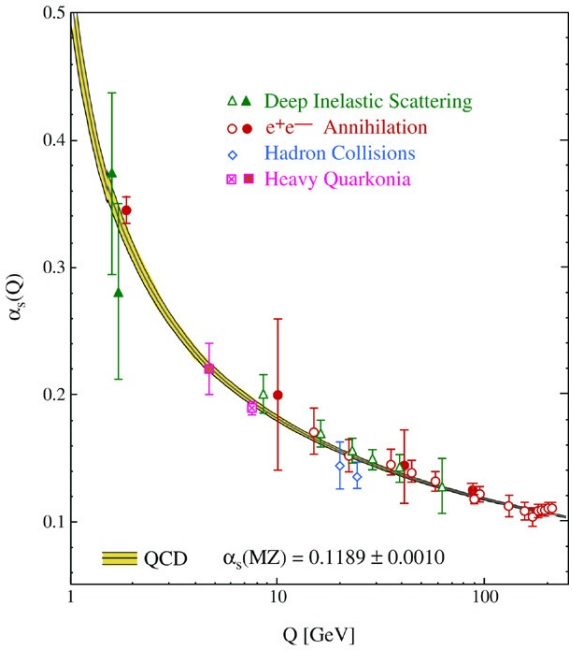

Figure 1.1: The running strong coupling constant, $\alpha_s(Q)$ [32].

building blocks of baryonic matter. Quarks are fermions with fractional charge, and at the time there were three kinds known: one with charge $2/3$ is called "up" (u), one with charge $-1/3$ is called "down" (d) and one more with charge $-1/3$ called "strange" (s).

The quark model had numerous predictions found to be in good agreement with data. On the other hand, Han and Nambu [24] and Miyamoto [25] pointed out that on top of the different flavors of quarks they have to occur in three different states in order to obey spin statistics. This new quantum number was named color; hence a quark can have a color red, blue or green. The final step that led from the quark model to quantum chromodynamics was the introduction of a non-Abelian gauge field by Fritzsch and Gell-Mann [26]; they named the particles of the field gluons, which carry color from one quark to another. The discovery of three jet events at DESY (Deutsches Elektronen-Synchrotron) confirmed the existence of gluons and determined their spin to be one [27, 28].

Despite the resemblance between the strong and electromagnetic interaction, electric-color charge and photon-gluon mediator, the non-Abelian nature of QCD leads to a number of phenomenological differences. Color confinement, simply called

confinement [29], is a phenomenon that color charge cannot be isolated; therefore quarks and gluons are constrained to be bound into hadrons. Unlike QED, the coupling strength of QCD is strong at large distance scales while it decreases as the length scale decreases, equivalent to an increasing in energy scale. The weakening of the coupling at high energies is known as the asymptotic freedom of QCD [30, 31]. See Fig. 1.1 for an illustration of the running of the QCD coupling with energy, $\alpha_s(Q)$. The discovery of asymptotic freedom leads to the prediction of the existence of deconfined quarks and gluons at high temperature ($T \gg \Lambda_{QCD}$) and density ($\rho \gg \Lambda^4_{QCD}$).

1.2 Quark gluon plasma

1.2.1 Theoretical prediction

Quark gluon plasma (QGP) is the name given to the QCD state of matter characterized by an equilibrium system of deconfined quarks and gluons. QGP can be predicted as a direct implication of the asymptotic freedom. At very high temperatures and/or very high densities the interactions between quarks and gluons get smaller and smaller, see Fig. 1.1, and at some point ($T \gg \Lambda_{QCD}$) the interactions are small enough that quarks and gluons are no longer bound together, deconfined.

At this scale $T \gg \Lambda_{QCD}$, chiral symmetry is a symmetry of QCD since the mass of the quarks (u and d) are very small compared to Λ_{QCD} and become negligible. However, these masses are relatively important at low energy which leads to a spontaneous breaking of the chiral symmetry; and since phase transitions can be described by spontaneous symmetry breaking then a phase transition is expected at some critical temperature T_c [33].

At low energy, the non-Abelian nature of the strong force makes the theory hard to solve; it may even impossible to get an analytical solution. However, the lattice formulation of QCD (LQCD) by Wilson subsequently enabled numerical techniques to address QCD nonperturbatively. In this approach, space-time is discretized on a lattice with which numerical predictions are performed, and then the continuum results are recovered by taking the lattice spacing to zero. Based on intense

computational work from LQCD [34], it has been shown that the phase transition from hadronic to deconfined QGP will take place at a critical temperature around $T_c \sim 154MeV$; see Fig. 1.2.

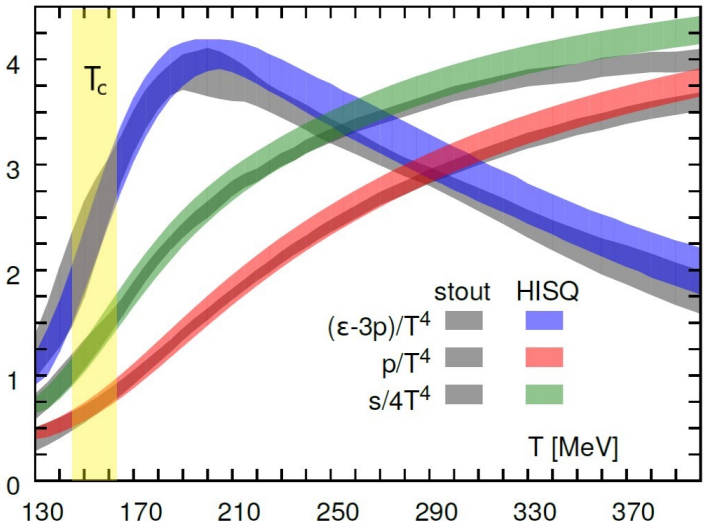

Figure 1.2: Lattice QCD results for the trace anomaly, the pressure, and the entropy density as a function of T [35].

1.2.2 Experimental observation

A few microseconds after the Big Bang, the temperature of the universe was above the critical temperature T_C necessary for QGP to have existed [33]. The Relativistic Heavy Ion Collider (RHIC) at Brookhaven National Laboratory in the United States began operations in 2000 to recreate and study in the laboratory this extremely hot and dense matter. In 2010, the Large Hadron Collider (LHC) at CERN in Switzerland also started a heavy ion collision program with a much higher collision energy $\sim TeV$. Side by side, RHIC and LHC experiments led to a conclusive evidence for the formation of a "quark-gluon plasma (QGP)" [36–38, 41].

- *Strangeness production:* In nature, ordinary matter is mainly composed of light quarks (u,d). However in the QGP, heavy flavors will be produced via gluon-gluon fusion which is increased by the high density of gluons. The abundance of strange quarks is a typical signature for QGP production since the strange quark's mass is comparable to the critical temperature T_c for the QCD phase

transition. Fig. 1.3 shows an enhancement of strange baryons produced in Pb-Pb collisions with respect to pp collisions in which the enhancement increases with the strangeness content, from Λ to $\Omega + \overline{\Omega}^{*}$, and increases also with the number of participants N_{part}. The number of participants is the number of nucleons that undergo at least one collision during a nucleus-nucleus collisions.

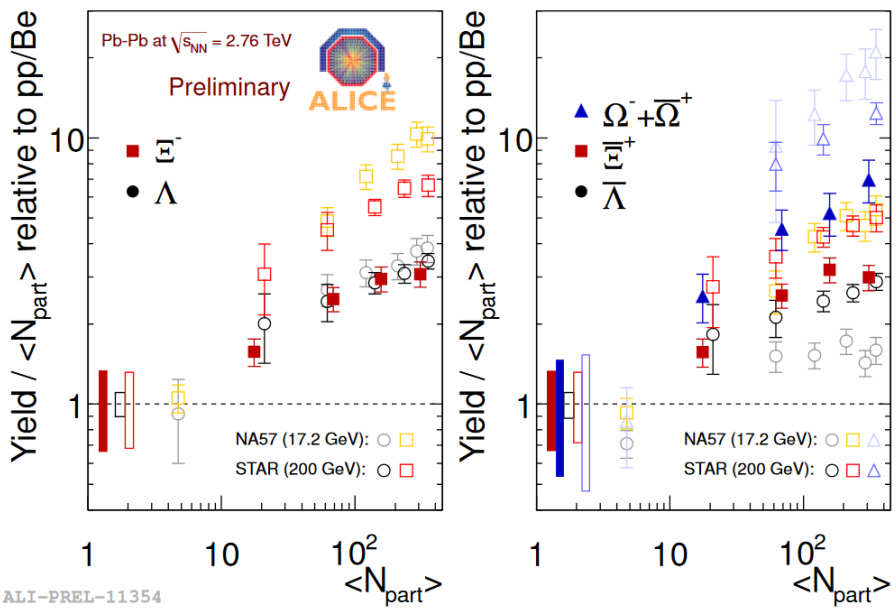

Figure 1.3: Integrated yields of strange baryons produced in Pb-Pb collisions at $\sqrt{s_{NN}} = 2.76TeV$ [39].

- *Collective flow:* The second signature of QGP is the detection of a collective behavior which cannot be explained from a superposition of independent nucleus-nucleus collisions. In a non-central collision, a hot and dense fireball is formed in an ellipsoid shape perpendicular to the plane containing the centers and the velocities of two colliding nuclei, the reaction plane. This asymmetry leads to a pressure gradient which explains the collective motion of the particles emitted with respect to the reaction plane. In experiments the asymmetry is measured by the elliptic flow, v_2, which is a measure of how the flow is not uniform along the azimuthal angle around the beam direction. This elliptic flow v_2 is defined as the second harmonic coefficient of the azimuthal Fourier

decomposition of the momentum distribution,

$$\frac{dN}{p_T dp_T dy d\phi} = \frac{dN}{p_T dp_T dy}\left(1 + 2\sum_{n=1}^{\infty} v_n \cos[n\phi]\right) \tag{1.1}$$

In Fig. 1.4, the elliptic flow produced in Pb-Pb collisions is shown. It is evident from the plot that the flow increase with the centrality, which is related to the initial overlap of the colliding nuclei Fig. 1.5, up to 50%.

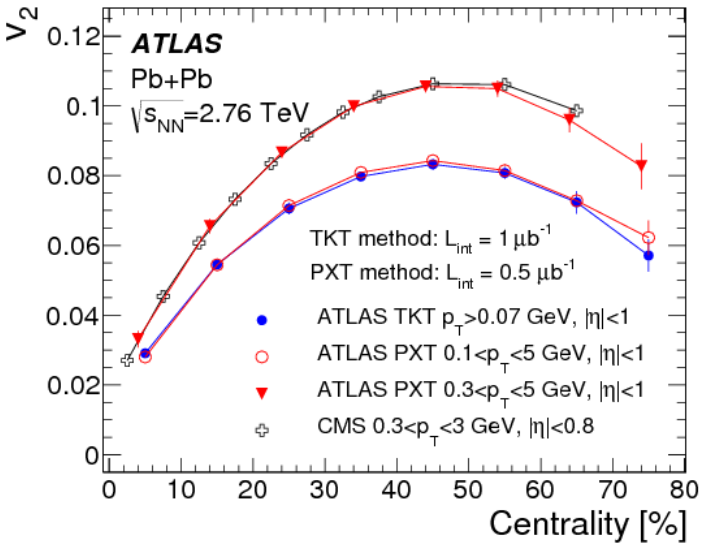

Figure 1.4: Centrality dependence of elliptic flow v_2 in Pb-Pb collisions at $\sqrt{s_{NN}} = 2.76TeV$ [40].

- *Jet Quenching:* Highly collimated clusters of particles, produced from hard scatterings known as jets, are also produced in heavy ion collisions. The partonic nature of those jets makes them sensitive to the presence of a medium and provides an external probe of the system. The fact that partons lose energy dramatically in a medium of high color charge density leads to an observable

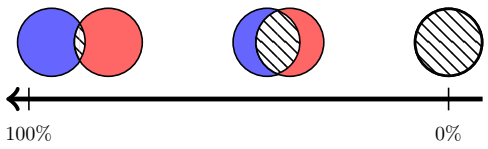

Figure 1.5: Initial overlap area of the nuclei as function of centrality.

suppression in the number of detected particles at a specific momentum compared to reference collisions without a QGP medium. Quantitative evaluation of the suppression is made using the "nuclear modification factor", R_{AA}, the ratio of the measured semi-inclusive yield to the point-like scaled proton-proton cross section,

$$R_{AA} = \frac{1}{N}\frac{d\sigma_{AA}}{d\sigma_{pp}}. \tag{1.2}$$

Fig. 1.6 shows the experimental results for R_{AA} in Au-Au collisions measured by PHENIX for direct γ, π^0, and η [42]. The interpretation of this suppression as a dense-medium effect acting on partonic matter is supported by the fact that 1) there is no dependence on the final state hadronic mass and 2) the direct photons do not show a suppression, since they do not interact with the partonic matter.

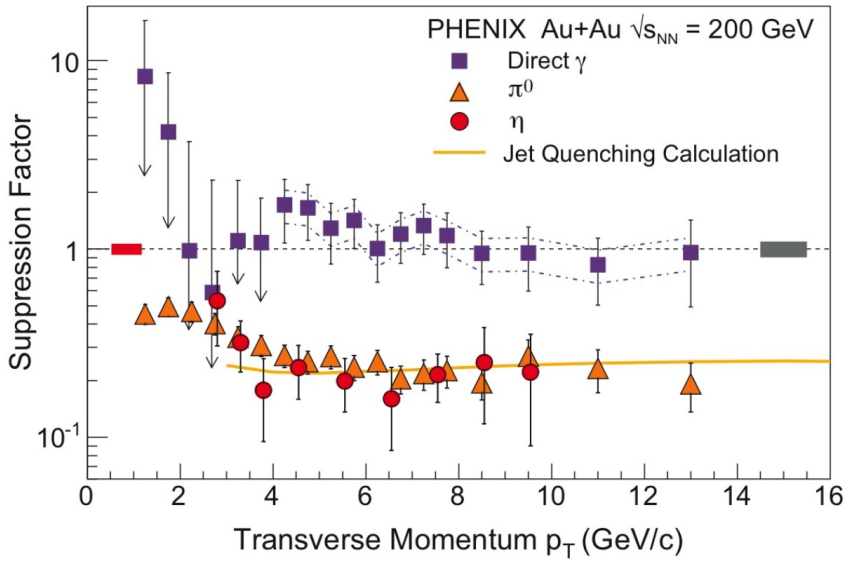

Figure 1.6: The nuclear modification factor R_{AA} as a function of transverse momentum p_T measured in central Au+Au collisions at RHIC γ, π^0, and η [42].

1.3 Motivation

Much progress has been made in the theoretical understanding of the properties of the probed plasma at RHIC and LHC.

On one hand is the picture of the strong force as weakly coupled ($\alpha_s \ll 1$). Then quarks and gluons are approximately free, which makes perturbative QCD (pQCD) calculations the most appropriate tool to describe the probed medium. Perturbative QCD calculations are very successful for describing the energy loss of a high-momentum parton passing through a medium [43–48]. On the other hand, is a picture in which the strong force is strongly coupled ($\alpha_s \gtrsim 1$) , and thus the plasma is well understood as a strongly coupled fluid (sQGP), not as a free gas as in the pQCD picture. Surprisingly non-perturbative calculations, such as LQCD and AdS/CFT, are very successful tools for describing this strongly coupled plasma behavior of the QGP [49–52]. AdS/CFT is a conjecture that maps a strongly coupled QFT in 4-dimensional spacetime (conformal field theory or CFT) to a weakly coupled string theory in 5-dimensional spacetime (gravity in the anti de sitter or AdS). One of the successful predictions of this approach is the minimal bound for the shear viscosity ratio of the plasma [51, 52], $\eta/s = 1/(4\pi)$.

This thesis is mainly focused on the radiative calculation in the weakly coupled regime in which the physics is pictured by pQCD calculations. In the initial overlap of colliding hadrons, partons with high transverse momentum, $p_T \gg \Lambda_{QCD}$, are produced. Then as the partons propagate though the expanding QGP medium, they will experience multiple interactions with the different constituents of the medium and radiate gluons, which leads to a momentum suppression. In this regime, the momentum of the high-p_T parton is altered by a combination of collisions with medium quasiparticles, which are slightly thermally modified free quarks and gluons [53, 54]. And at relativistic speeds, radiative processes contribute to the majority of the energy lost by the parton [55].

The single emission calculation is one of the most well understood structures in the soft and/or collinear region [53]. In vacuum, the distribution of a single gluon radiation off a quark differs from the spectrum of a photon off an electron only by

a color factor C_F and by the substitution of QED to QCD coupling

$$dN_g = C_F \frac{2\alpha_s}{\pi} \frac{dk_T}{k_T} \frac{dx}{x}, \tag{1.3}$$

where k_T is the transverse momentum of the emitted gluon and $x = \omega/E < 1$ the energy fraction of the radiation. Most of the theoretical development in pQCD-based radiative calculations is centered on the single emission. The GLV (Gyulassy, Levai and Vitev) approach computed the energy loss in a single induced emission with a medium modeled as separated heavy static scattering centers with color screened Yukawa potentials [47, 48]. The ASW (Armesto, Salgado and Wiedemann) approach is also focused on the single induced emission with a collection of heavy static scattering centers with a Debye screened potential as a medium [56].

However, it has been estimated that the number of gluons radiated by a typical high-p_T parton in medium at RHIC or LHC is about 3 [57], which is not less or equal to 1. A more realistic energy loss model must take into account the possibility for multiple gluon emission.

In QED, the distribution of multiple photon emission is surprisingly simple in the soft and collinear region [58]. The photon emissions are independent; the distribution of n photons is given by the product of the individual emissions and follows the Poisson convolution of the single inclusive photon

$$dN_\gamma(n) = \frac{1}{n!} \prod_{i=1}^{n} \frac{2\alpha}{\pi} \frac{dx_i}{x_i} \frac{dk_{Ti}}{k_{Ti}}. \tag{1.4}$$

Unfortunately, the multiple gluon calculation is not as simple as the photon emission, the non-Abelian nature of QCD which is reflected by the gluon self-interaction leads to more complicated structure. But for simplicity, the multiple gluon emission is often approximated to be independent, where the distribution of emitted gluons follows a Poisson distribution, with the mean given by the single gluon spectrum. And most of the actual phenomenological calculations and Monte Carlo implementations rely on this independent gluon emission approximation [56, 59–61].

The AMY (Arnold, Moore, Yaffe) energy loss approach models the medium to be composed by quark and gluon quasi-particles in which the interactions are described by hard thermal loop field theory [62, 63]. In its formulation, AMY uses

the emission rate equation to generate multiple radiation, thus keeping track of the decreasing energy of the jet. Similarly, the higher-twist (HT) calculation [64,65] uses a medium-modified DGLAP evolution to calculate multiple gluon emission in which the evolution equation keeps track of the gradual degradation of the jet energy. By keeping track of the energy degradation AMY and HT go beyond the most naive assumption of multiple gluon emissions from a single gluon emission. The focus of this thesis is to advance energy loss theory in a different direction, laying the foundation for deriving multiple induced n-medium gluon emissions in which the non-Abelian nature of QCD is included, i.e. radiated gluons can themselves radiate gluons.

Research has shown that independent emissions do occur in a vacuum cascade process where the angular of the multiple emissions are strongly ordered ($\theta_1 > \cdots > \theta_n$) [66, 67]. Recently, there has been partial progress in computing the momentum distribution of two radiated gluons in-medium beyond this ordering from which a parton undergoing multiple scattering in a QGP medium [68–70].

In this thesis, our main focus is to provide a different framework, using the maximal helicity violating (MHV) techniques, in which the multiple gluon distribution could be computed beyond the Poisson approximation. Poissonian behaviour is a typical characteristic of Abelian emission so any deviation from the independent emission prediction will be referred as a "non-Abelian correction". We compute multiple gluon radiations from an off-shell quark, derived beyond strong ordering. The non-abelian correction will induce multiple particle correlations which are important to understand non-flow anisotropy produced in heavy ion collision. And such correlation could also be used to improve vacuum Monte Carlo showering which are very important for jet showering calculation and for understanding the QCD background.

It is important to mention that this is not the first time that MHV techniques were introduced in heavy ion calculations. The first attempt was done in [71]; in that work, instead of a quark, the high-p_T parton was chosen to be a gluon. The main difference between our work and that of [71] is in the application of the MHV formula. In the procedure of squaring amplitude, [71] assumed that the square of a sum of MHV terms is the sum of the square, thus losing information on non-Abelian

effects.

1.4 Why MHV thechniques?

In this section we want to give a brief history of the development of the MHV thechniques, and motivate why it is useful to study energy loss in heavy ion collision.

With the standard Feynman diagrammatic methods, the number of diagrams becomes out of hand as the number of gluons increases. For example in $e^+e^- \to q\bar{q} + ng$, the number of tree level diagrams needed for a generic number of radiated gluons is summarized in Tab. 1.1.

# Gluons	1	2	3	$\cdots$	n
# Diagrams	2	8	48	$\cdots$	$n!2^n$

Table 1.1: Number of diagram needed in function of gluon legs.

In 1986, Parke and Taylor [72] conjectured that a very complicated Feynman diagram expansion for multi-gluon scattering amplitudes could be simplified to a very compact form if helicity conservation is maximally violated. In the case of multi-gluon amplitudes such simplicity occurs when $n-2$ gluons have the same helicity and the other two have the opposite helicity. In 1988, the conjecture was proved by Berends and Giele [73], and they also showed that with some choice of kinematic variables, spinor helicity variables, the Parke-Taylor formula for the MHV gluons can be written as

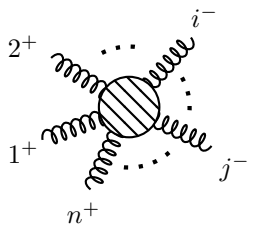

$$= \tilde{g}^{n-2} \frac{\langle ij \rangle^4}{\langle 12 \rangle \langle 2n \rangle \cdots \langle (n-1)n \rangle \langle n1 \rangle}, \tag{1.5}$$

where $\tilde{g} = \sqrt{2}g$ and the bracket notation will be defined in Section 3.2 Today, the maximal helicity violating techniques is known as a spinor helicity based formalism which relies on the chirality of QCD. At a scale $Q \gtrsim T_c$, the chiral symmetry of QCD is restored which makes the MHV formalism useful for pQCD-based calculation.

1.5 Outline of thesis

In the next chapter, we start with the QCD Lagrangian to review the Feynman diagrammatic approach for computing scattering amplitudes. For illustration, we compute the amplitude associated to $q\bar{q} \to gg$ scattering. We show, from a diagrammatic perspective, that the color and kinematic degrees of freedom of the amplitude can be factorized into ordered color factors and partial amplitudes.

In Chapter 3 we review the spinor helicity formalism for massless gauge theories and introduce the spinor helicity variables. These new variables make the on-shell condition of massless particles manifest at any stage of QCD calculations. In terms of the spinor variables, we investigate the partial amplitudes associated to $q\bar{q} \to gg$ according to its helicity configuration. The understanding of this simple process leads us to introduce the concept of maximal helicity violating (MHV) amplitudes for higher order processes like $q\bar{q} \to ng$.

In Chapter 4 we show that the computational efficiency of the MHV techniques makes the $2 \to 2$ cross section computation simple. This chapter is also used to familiarize the reader with MHV calculations. In this chapter we perform our first radiative calculation: we compute the probabilities of finding a gluon in a given parton; these probabilities are known as splitting functions. Independently from these computation, we introduce the photon decoupling in order to incorporate photons in the MHV calculation.

In Chapter 5 we focus on the multiple radiation quest. We start with the computation of single photon emission current, and then use MHV to perform a rigorous derivation to show the independent emission of photons. Similarly with the photon, we derives the single gluon emission current then generalize the computation to multiple gluon emission.

In Chapter 6 we recall the multiple gluon emission current computed from the previous chapter and consider the case of two gluon emissions. We compute the distribution for two gluon emissions in the vacuum and derive the non-Abelian correction to an assumption of independent emission. This non-Abelian effect leads to a correlation between the two gluon emissions that we compare to the two-particle

correlation measured by ALICE from p-Pb collisions.

In Chapter 7 we study the case of induced radiation from a single gluon absorption. In this picture, radiation can be induced from two distinct mechanisms: 1) the incoming gluon provide the necessary energy to make the quark off-shell then induce radiation; 2) the incoming gluon color charge will flip/rotate the color of the quark that will induce a second type of radiation. In this chapter we investigate more on the second mechanism in which we derive the multiple gluon radiation current induced from such color flip.

We conclude the thesis in Chapter 8 which is followed by Appendices (A-F) where we include several important detailed calculations.

Quantum chromodynamics 2

In this chapter, we review the computation of scattering amplitudes using the standard diagrammatic methods of QCD. First, we recall the QCD Lagrangian to illustrate the different possible interactions between particles. Then we explore how the color and kinematic degrees of freedom of QCD amplitudes can be factorized from each other in a $2 \to 2$ process and conclude the chapter with the color and kinematic decomposition for multiple gluon amplitudes.

2.1 QCD Lagrangian

Quantum chromodynamics (QCD) is the quantum field theory of the strong interaction. Reviews of QCD basics can be found in any standard QFT textbook e.g. [58, 74]. QCD describes the force that binds color object quarks and gluons to hadrons and mesons. QCD is described by a non-Abelian $SU(3)$ gauge theory with which the color charges of the theory are given by the generators of the gauge group. For massless QCD the Lagrangian is defined as

$$\mathcal{L}_{QCD} \equiv i\overline{\psi}\not{D}\psi - \frac{1}{4}F^a_{\mu\nu}F^{a\mu\nu}, \tag{2.1}$$

where ψ is the field related to the quark. In fact the quark field has two omitted indices: one is a spinor index that runs from 1 to 4, meaning that the quarks and anti-quarks are spin 1/2 particles; the other one is a color index running from 1 to 3, since the quarks live in the fundamental representation of the gauge group $SU(3)$. On the other hand, the Lorentz 2-tensor $F^a_{\mu\nu}$ is the gluon field strength

tensor associated to a gluon with a color index a, where $a = \{1, \ldots, 8\}$, and is defined as

$$F^a_{\mu\nu} \equiv \partial_\mu A^a_\nu - \partial_\nu A^a_\mu + g f^{abc} A^b_\mu A^c_\nu \tag{2.2}$$

Here the Lorentz vector A^a_μ are the 8 gluon fields that live in the adjoint representation of $SU(3)$, g is the coupling constant of QCD and f^{abc} is the structure constant of the algebra where $[T_a, T_b] = i f_{abc} T_c$. Here T_a's represent the generators of the group $SU(3)$. The Lagrangian Eq. (2.1) contains two types of local interactions. First the quark-gluon interaction, which is hidden in the covariant derivative $\not{D}$ defined as

$$\not{D} \equiv \gamma^\mu D_\mu \equiv \gamma^\mu \partial_\mu - i g \gamma^\mu T_a A^a_\mu. \tag{2.3}$$

Second, the self gluon interactions, which are folded into the term $F^a_{\mu\nu} F^{a\mu\nu}$ and that give rise to three and four gluon interactions. The gauge boson self-interactions are the effect of the non-Abelian nature of the theory which makes QCD different from QED. In the perturbative regime, $g \ll 1$, diagrammatic expansions are used to illustrate the interactions among quarks and gluons in order to compute the amplitude of a given scattering process. In momentum space the Feynman rules for the different vertices are shown below

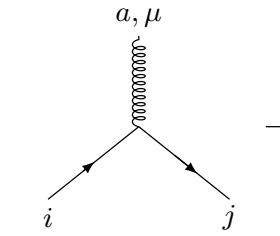

$$\longrightarrow \quad -ig\gamma^\mu (T_a)_{ij}$$

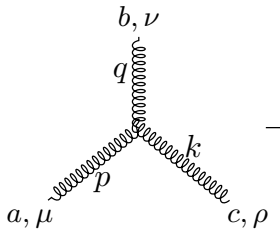

$$\longrightarrow \quad -g f^{abc} [(q-k)^\mu g^{\nu\rho} + (k-p)^\nu g^{\rho\mu} + (p-q)^\rho g^{\mu\nu}] \tag{2.4}$$

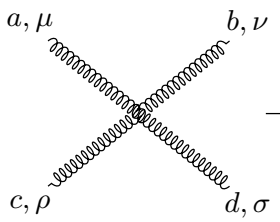

$$\begin{aligned} \longrightarrow \quad & ig^2[\, f^{abe} f^{cde} (g^{\mu\rho} g^{\nu\sigma} - g^{\mu\sigma} g^{\nu\rho}) \\ & + f^{ace} f^{bde} (g^{\mu\nu} g^{\rho\sigma} - g^{\mu\sigma} g^{\nu\rho}) \\ & + f^{ade} f^{bce} (g^{\mu\nu} g^{\rho\sigma} - g^{\mu\rho} g^{\nu\sigma})] \end{aligned}$$

For a local theory, interactions are mediated by particle exchanges, where in the language of Feynman diagrams such exchanges are represented by propagators between

two vertices. In QCD there are two types of propagators: the fermion propagator represented by solid line and the gluon propagator represented by helix line as shown below

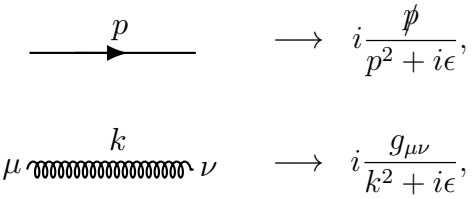

$$\longrightarrow \quad i\frac{\not{p}}{p^2+i\epsilon}, \qquad \longrightarrow \quad i\frac{g_{\mu\nu}}{k^2+i\epsilon}, \tag{2.5}$$

where for the gluon propagator we use the Feynamn gauge as described in [58].

External lines in a diagram represent the initial and final states of particles and are described by the polarizations. The spinors $u_h(p)$ and $\bar{u}_h(p)$ are respectively the polarizations of the incoming and the outgoing quark of momentum p_μ with helicity $h = \pm 1/2$, while the spinors $\bar{v}_h(p)$ and $v_h(p)$ are the the respective polarizations of the incoming and outgoing anti-quark with momentum p_μ with helicity $h = \pm 1/2$, and last $\varepsilon_\mu(h,k)$ and $\varepsilon^*_\mu(h,k)$ are respectively the vector polarization associated to the incoming and outgoing gluon of momentum k_μ with helicity $h = \pm 1$.

For massless fermions the polarizations $u_h(p)$ and $v_h(p)$ are connected through the relation $v_\pm(p) = u_\mp(p)$ which relates the polarization of an incoming fermion to the polarization of outgoing anti-fermion of an opposite helicity. Similarly between $\bar{u}_h(p)$ and $\bar{v}_h(p)$ they satisfy the relation $\bar{v}_\pm(p) = \bar{u}_\mp(p)$, and these relations are a manifestation of crossing symmetry. The four component spinor $u_h(p)$ and $\bar{u}_\mp(p)$ obey to the following equations

$$\not{p}u_h(p) = 0 \quad \text{and} \quad \bar{u}_h(p)\not{p} = 0, \tag{2.6}$$

these equations are known as Dirac equations and they are normalized by the following helicity sum

$$\sum_h u_h(p)\bar{u}_h(p) = \not{p}. \tag{2.7}$$

On the other hand the crossing symmetry for the polarization vector is given by $\varepsilon^*_\mu(\pm,k) = \varepsilon_\mu(\mp,k)$ which relates the polarization of incoming to outgoing gluon. Polarization vectors are constrained to be transverse to the gluon propagation, and this leads to a gauge redundancy in the theory,

$$k_\mu\, \varepsilon^\mu(\pm,k) = 0. \tag{2.8}$$

In this thesis, polarization vectors are normalized as follows

$$\varepsilon^{\mu}(h_1,k)\,\varepsilon_{\mu}(h_2,k)=\delta_{h_1h_2}-1. \tag{2.9}$$

2.2 Properties of scattering amplitudes

In this section, we are going to compute a generic $2\to 2$ scattering amplitude using the standard Feynman diagrammatic calculation. Then by rearranging the diagrams we will factorize the kinematic and color degrees of freedom.

2.2.1 Color and kinematic degrees of freedom

Consider the annihilation process where a quark and an antiquark collide and produce two gluons. At tree level, three diagrams contribute to the corresponding amplitude,

$\mathcal{M}(q\bar{q}\to gg) =$ 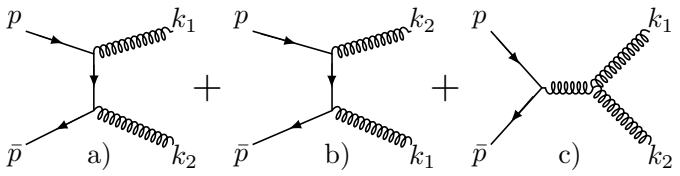

. (2.10)

Here p denotes the momentum of the incoming quark with polarization $u(p)$, $\bar{p}$ the momentum of the antiquark with polarization $\bar{v}(\bar{p})$, and k_1 and k_2 are the momenta of the produced gluons respectively with polarization ε_1 and ε_2. The helicity of the individual polarizations are suppressed, and ε_i is shorthand for the polarization vector $\varepsilon(k_i)$.

The analytical expression of the individual diagrams are obtained by using the Feynman rules and expressed as follows

- diagram a):

$$\begin{aligned}\mathcal{M}_{\mathrm{a}} &= ig^2 T_{a_1}T_{a_2}\frac{\bar{v}(\bar{p})\not{\varepsilon}_2^{*}(\not{p}-\not{k}_1)\not{\varepsilon}_1^{*}u(p)}{2p.k_1}\\ &= iT_{a_1}T_{a_2}K_{\mathrm{a}}(1,2)\end{aligned} \tag{2.11}$$

- diagram b):

$$\begin{aligned}\mathcal{M}_{\rm b} &= ig^2 T_{a_2} T_{a_1} \frac{\bar{v}(\bar{p}) \not{\varepsilon}_1^* (\not{p} - \not{k}_2) \not{\varepsilon}_2^* u(p)}{2p.k_2} \\ &= iT_{a_2} T_{a_1} K_{\rm b}(1,2)\end{aligned} \tag{2.12}$$

- diagram c):

$$\begin{aligned}\mathcal{M}_{\rm c} &= -g^2 f_{a_1 a_2 b} T_b \frac{\bar{v}(\bar{p}) \left((-\not{k}_1 + \not{k}_2) \varepsilon_1^*.\varepsilon_2^* - 2\not{\varepsilon}_2^* k_2.\varepsilon_1^* + 2\not{\varepsilon}_1^* k_1.\varepsilon_2^* \right) u(p)}{2k_1.k_2} \\ &= iT_{a_1} T_{a_2} K_{\rm c}(1,2) - iT_{a_2} T_{a_1} K_{\rm c}(1,2)\end{aligned} \tag{2.13}$$

where $K_{\rm a}(1,2)$, $K_{\rm b}(1,2)$ and $K_{\rm c}(1,2)$ are respectively the kinematics associated to the diagrams a), b) and c) in Eq. (2.10), and the T_a's are the color charges carried by the individual gluons where $a = \{1, \ldots, 8\}$. From the definition above, one can check the following properties of the kinematics

$$K_{\rm a}(1,2) = K_{\rm b}(2,1) \quad \text{and} \quad K_{\rm c}(1,2) = -K_{\rm c}(2,1). \tag{2.14}$$

Since the full amplitude is the sum of the three contributions; and from Eq. (2.11, 2.12, 2.13) the kinematics can grouped according to the ordering of the color charges, i.e. either $T_{a_1} T_{a_2}$ or $T_{a_2} T_{a_1}$,

$$\mathcal{M}(q\bar{q} \to gg) = iT_{a_1} T_{a_2} A(p,1,2,\bar{p}) + iT_{a_2} T_{a_1} A(p,2,1,\bar{p}), \tag{2.15}$$

where the color ordered amplitude $A(p,i,j,\bar{p})$, also called a partial amplitude, is just purely kinematic and defined as

$$A(p,i,j,\bar{p}) \equiv K_{\rm a}(i,j) + K_{\rm c}(i,j). \tag{2.16}$$

2.2.2 Gauge invariance of $A(p,1,2,\bar{p})$

In QFT, scattering amplitudes are a fundamental quantity that connect theory predictions and experimental measurements. Here we are going to show that the partial amplitude, introduced in Eq. (2.16), is a gauge invariant quantity. For that purpose, it is useful to decompose the partial amplitude $A(p,1,2,\bar{p})$ into two contractions of two Lorentz vectors as follows

$$A(p,1,2,\bar{p}) = \varepsilon_{1\mu}^* A^\mu(p,1,2,\bar{p}). \tag{2.17}$$

Similarly the kinematic piece $K_{\rm a}(1,2) = \varepsilon^*_{1\mu} K^\mu_{\rm a}(1,2)$, such that

$$K^\mu_{\rm a}(1,2) = g^2 \frac{\bar{v}(\bar{p}) \not{\varepsilon}^*_2 (\not{p} - \not{k}_1) \gamma^\mu u(p)}{2p.k_1}, \tag{2.18}$$

and the kinematic piece $K_{\rm c}(1,2) = \varepsilon^*_{1\mu} K^\mu_{\rm c}(1,2)$, such that

$$K^\mu_{\rm c}(1,2) = g^2 \frac{\bar{v}(\bar{p}) \left(-\not{k}_1 \varepsilon_2^{\mu *} - \not{\varepsilon}^*_2 k_2^\mu + \gamma^\mu k_1.\varepsilon^*_2 \right) u(p)}{k_1.k_2}. \tag{2.19}$$

Therefore

$$A^\mu(p,1,2,\bar{p}) = K^\mu_{\rm a}(1,2) + K^\mu_{\rm c}(1,2). \tag{2.20}$$

This factorization of $A(p,1,2,\bar{p})$ in Eq. (2.17) is useful for showing the invariance of the amplitude Eq. (2.17) under the gauge transformation $\varepsilon^\mu_1 \to \varepsilon^\mu_1 + \omega k^\mu_1$, for any constant ω. Therefore, in order to be invariant under gauge transformation, $k_{1\mu} A^\mu(p,1,2,\bar{p})$ has to vanish. It can be checked that

$$k_{1\mu} K^\mu_{\rm a} = g^2 \bar{v}(\bar{p}) \not{\varepsilon}^*_2 u(p) \quad \text{and} \quad k_{1\mu} K^\mu_{\rm c} = -g^2 \bar{v}(\bar{p}) \not{\varepsilon}^*_2 u(p). \tag{2.21}$$

Then, one can conclude that

$$k_{1\mu} A^\mu(p,1,2,\bar{p}) = 0, \tag{2.22}$$

that is to say the partial amplitude is a gauge invariant quantity and Eq. (2.22) is known as the Ward identity. The partial amplitude $A(p,1,2,\bar{p})$ can be computed using the same set of Feynman rules, as introduced in [75], from which the color dependence of the vertex is removed from the vertex rules Eq. (2.4):

- the quark-antiquark-gluon vertex: $-ig\gamma^\mu$,
- and the 3-gluon vertex: $-ig(p-q)^\rho g^{\mu\nu} + (q-k)^\rho g^{\nu\rho} + (k-p)^\nu g^{\rho\mu}$, (2.23)
- and the 4-gluon vertex: $ig^2(2g^{\mu\rho}g^{\nu\sigma} - g^{\mu\nu}g^{\rho\sigma} - g^{\mu\sigma}g^{\nu\rho})$.

The external and internal lines remain with same rules, but in addition a specific order as to be considered for the diagram to reproduce the ordering of the color charges,

$A(p,1,2,\bar{p}) =$ 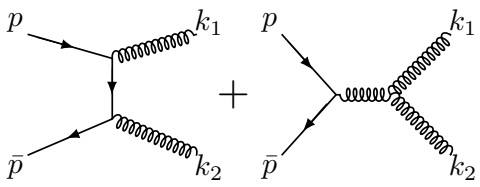 . (2.24)

In summary, we have considered the amplitude associated to $q\bar{q} \to gg$, then showed that the color part of the amplitude can be separated from the partial amplitude which is purely kinematics. In the next section, we will show how to generalize this color kinematic decomposition to $q\bar{q} \to ng$ amplitudes.

2.3 Color kinematic decomposition

In this section, we will generalize the color kinematic decomposition in Eq. (2.15) to multiple gluon productions out of $q\bar{q}$ annihilation. In an other word, we are going to factorized the color degrees of freedom of a given amplitude from the kinematic degree of freedom. And as we have already seen in Eq. (2.13) the color factor associated to the diagram c) in Eq. (2.10) is equal to the difference of the color factor of the diagram a) and b). Diagrammatically this difference can be represented as

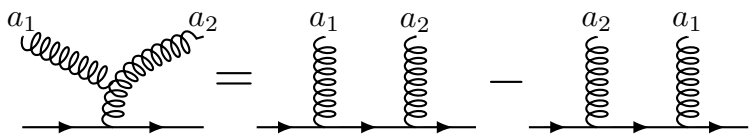

. (2.25)

Also written as $f_{a_1 a_2 b} T_b = -i[T_{a_1}, T_{a_2}]$, this relation was the key for the decomposition Eq. (2.15). A similar transformation can be done for any multiple gluon vertex of a given diagram where all structure constants f_{abc} contracted with a color charge T_c will be transformed into commutators of color charges. For illustration, let us consider the color factor associated to a particular diagram below which contributes to the production of six gluons from a quark line,

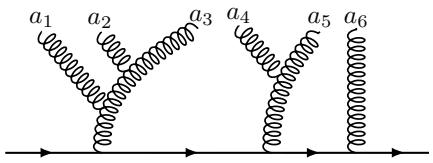

$$= \left(T_{b_1} f_{a_1 b_2 b_1} f_{a_2 a_3 b_2}\right) \left(T_{b_3} f_{a_4 a_5 b_3}\right) T_{a_6}. \qquad (2.26)$$

Then from this expression, each $f_{abc}T_c$ will be replaced, one by one, by a commutator as in Eq. (2.25). Once it is expressed only in terms of the different color charges, the commutators can be expanded explicitly so it will become a linear combination

of the different strings of T_a's

$$\begin{aligned}[T_{a_1},[T_{a_2},T_{a_3}]][T_{a_4},T_{a_5}]T_{a_6} &= T_{a_1}T_{a_2}T_{a_3}T_{a_4}T_{a_5}T_{a_6} - T_{a_1}T_{a_2}T_{a_3}T_{a_5}T_{a_4}T_{a_6} \\ &- T_{a_1}T_{a_3}T_{a_2}T_{a_4}T_{a_5}T_{a_6} + T_{a_1}T_{a_3}T_{a_2}T_{a_5}T_{a_4}T_{a_6} - T_{a_2}T_{a_3}T_{a_1}T_{a_4}T_{a_5}T_{a_6} \\ &+ T_{a_2}T_{a_3}T_{a_1}T_{a_5}T_{a_4}T_{a_6} + T_{a_3}T_{a_2}T_{a_1}T_{a_4}T_{a_5}T_{a_6} - T_{a_3}T_{a_2}T_{a_1}T_{a_5}T_{a_4}T_{a_6}.\end{aligned} \tag{2.27}$$

In a more general way, given a diagram $\mathcal{D}$ the associated color factor $C_{\mathcal{D}}$ could be written only in terms of the generator T_a. Starting from the vertex closer to the quark line, the contracted structure constants $f_{abc}T_c$ will be transformed into commutators; i.e. the gluon vertices will be replaced one by one as in Eq. (2.25). Similarly, the same procedure could be applied for the four gluon vertex in which the color factor is be written in terms of $f_{abe}f_{cde}$. Contracted with a generator, $f_{abe}f_{cde}T_a$ will be replaced as $[T_b,[T_c,T_d]]$. This procedure will lead to a general expression of the type

$$C_{\mathcal{D}} = \sum_{\mathcal{P}_n} U^{\mathcal{D}}_{12\cdots n}(T_{a_1}T_{a_2}\cdots T_{a_n}), \tag{2.28}$$

the coefficients $U^{\mathcal{D}}_{12\cdots n}$ are some numbers that depend only on the diagram $\mathcal{D}$ and the sum over $\mathcal{P}_n$ represent the sum over the permutation of the n gluon-indices. On the other hand, a given diagram $\mathcal{D}$ is a combination of a color coefficient $C_{\mathcal{D}}$ and a kinematic piece $K_{\mathcal{D}}$ as in (2.11); i.e. $\mathcal{D} = C_{\mathcal{D}}K_{\mathcal{D}}$. Knowing that the full amplitude is equal to the sum of all diagrams $\mathcal{D}$, and via Eq. (2.28) all terms with the same color ordered charge $(T_{a_1}T_{a_2}\cdots T_{a_n})$ will be grouped and yields

$$\mathcal{M}(q\bar{q}\to ng) = \sum_{\mathcal{P}_n}(T_{a_1}T_{a_2}\cdots T_{a_n})A(p,1,2,\ldots,n,\bar{p}), \tag{2.29}$$

where $A(p,1,2,\ldots,n,\bar{p})$ will be called the partial amplitude, also known as the color ordered amplitude, and is given by a linear combination of the kinematic pieces and is a generalization of Eq. (2.16)

$$A(p,1,2,\ldots,n,\bar{p}) \equiv \sum_{\mathcal{D}} U^{\mathcal{D}}_{12\cdots n}K_{\mathcal{D}}(1,2,\ldots,n). \tag{2.30}$$

The decomposition of the amplitude in Eq. (2.29) is called the color kinematic decomposition, which is a factorization of the color degrees of freedom from the kinematics. The structure of the color decomposition may change from one process to another depending on the color flow; for example as shown in [76], the color

decomposition for the case of purely gluonic amplitudes will have a trace structure $\mathrm{tr}\,(T_{a_1}T_{a_2}\cdots T_{a_n})$ instead of the ordered color charge in Eq. (2.29).

Through this chapter, we have considered the production of two gluons from quark anti-quark annihilation. With the QCD Feynman rules we computed the related amplitude in order to decompose the color and kinematic degrees of freedom as in Eq. (2.15), and generalized the decomposition to $q\bar{q} \to ng$. This decomposition structure Eq. (2.29) is one of the fundamental building blocks of the technique we use through this work, MHV. The partial amplitudes can be evaluated using a new set of Feynman rules as for Eq. (2.24); however in the next chapter we will show that for massless theories there is an efficient way to evaluate these amplitudes.

Spinor helicity formalism 3

In the previous chapter, we emphasized the fact that color degrees of freedom of QCD amplitudes can be decoupled from the kinematics, and that is the first step toward the MHV techniques. In this chapter, we explore more on the structure of the kinematics, partial amplitudes. We first review the spinor representation of momenta and then introduce to a new set spinor variables and use these variable to formulate the MHV amplitude from $q\bar{q} \to gg$ to multiple gluons. Reviews of the spinor helicity technique can be found in [77, 78].

3.1 Spinor representation

Recall that there are two inequivalent spin-1/2 representations of the Lorentz group $SO(3,1)$: $(1/2,0)$ and $(0,1/2)$. Elements of these representation are respectively the left-handed spinor, ξ_a and ξ^a, and the right-handed spin-1/2 particles, $\xi^\dagger_{\dot{a}}$ and $\xi^{\dagger\dot{a}}$. Further, recall that one can represent a Lorentz four vector p^μ as an object acting on either of these vector spaces through the mapping

$$p_{a\dot{b}} \equiv p^\mu \left(\sigma_\mu\right)_{a\dot{b}} \quad \text{and} \quad p^{\dot{a}b} \equiv p^\mu \left(\tilde{\sigma}_\mu\right)^{\dot{a}b}, \tag{3.1}$$

where $\sigma_\mu = (1, \vec{\sigma})$ and $\tilde{\sigma}_\mu = (1, -\vec{\sigma})$ with $\vec{\sigma}$ the Pauli matrices

$$\sigma_1 = \begin{pmatrix} 0 & 1 \\ 1 & 0 \end{pmatrix}, \quad \sigma_2 = \begin{pmatrix} 0 & -i \\ i & 0 \end{pmatrix}, \quad \sigma_3 = \begin{pmatrix} 1 & 0 \\ 0 & -1 \end{pmatrix}. \tag{3.2}$$

Therefore, the $p_{a\dot{b}}$ matrix representation of the momentum p^μ can be written as

$$p_{a\dot{b}} = \begin{pmatrix} p_0 - p_3 & -p_1 + ip_2 \\ -p_1 - ip_2 & p_0 + p_3 \end{pmatrix}, \tag{3.3}$$

where the Lorentz index μ can be lowered using the metric $g_{\mu\nu} = \text{diag}(+,-,-,-)$.

With these two representations, the invariant mass of a momentum is obtained from a determinant and the scalar product from a trace,

$$p^\mu p_\mu = \det(p_{a\dot{b}}) \quad \text{and} \quad p.q = \frac{1}{2}\text{tr}\left(q^{\dot{a}c} p_{c\dot{b}}\right). \tag{3.4}$$

It is important to mention that $q^{\dot{a}c}$ can be recovered by raising the left and right handed spinor indices with respect to the two dimensional Levi-Civita symbols ϵ^{ab} and $\epsilon^{\dot{a}\dot{b}}$

$$q^{\dot{a}b} = \epsilon^{ab}\epsilon^{\dot{a}\dot{b}} q_{a\dot{b}}, \tag{3.5}$$

where the the antisymmetric Levi-Civita tensors are chosen to be

$$\epsilon^{12} = \epsilon^{\dot{1}\dot{2}} = -\epsilon_{12} = -\epsilon_{\dot{1}\dot{2}} = 1. \tag{3.6}$$

One can also construct a bispinor representation as a direct sum of the left and right handed spin-1/2 represenations $(1/2, 0) \oplus (0, 1/2)$. In the Weyl basis in this representation the slashed momentum $\not{p}$ is defined by

$$\not{p} \equiv \begin{pmatrix} 0 & p_{a\dot{b}} \\ p^{\dot{a}b} & 0 \end{pmatrix} \tag{3.7}$$

that acts on the different Weyl spinors, elements of the representation. A Weyl spinor $u_h(p)$ can be decomposed into left and right handed spinors $u_h(p) \equiv (u_a, u^{\dot{a}})$; therefore the Dirac equation introduced in Eq. (2.6) becomes

$$\begin{pmatrix} 0 & p_{a\dot{b}} \\ p^{\dot{a}b} & 0 \end{pmatrix} \begin{pmatrix} u_c \\ u^{\dot{c}} \end{pmatrix} = 0 \Leftrightarrow \begin{cases} p^{\dot{a}c} u_c = 0 \\ p_{a\dot{c}} u^{\dot{c}} = 0. \end{cases} \tag{3.8}$$

Eq. (3.8) are called the Weyl equations. The right and left handed spinors are decoupled, which reflects the fact that the theory is invariant under chiral transformations.

3.2 Spinor variables

In the standard Feynman description, external particles are described by the helicity h and momentum vector p_μ. At any stage of a computation one has to remember the on-shell condition for external particles, $p^2 = m^2$. The goal of this section is to introduce a new parametrization for the matrix representation Eq. (3.3) that makes the on-shell condition for massless particles, $p^2 = 0$, manifest.

3.2.1 Parametrization of momenta

As mentioned in Eq. (3.4), the invariant mass is given by the determinant of $p_{a\dot{b}}$, which is equal to zero for massless particles. From linear algebra, zero determinant is equivalent to the rank of $p_{a\dot{b}}$ being equal to one; i.e. the two columns of the matrix are proportional to each other, and $p_{a\dot{b}}$ can be written as a product of two spinors [77, 78]

$$p_{a\dot{b}} = \lambda_a \widetilde{\lambda}_{\dot{b}}, \tag{3.9}$$

in matrix form $p_{a\dot{b}}$ is written as

$$\begin{pmatrix} p_0 - p_3 & -p_1 + ip_2 \\ -p_1 - ip_2 & p_0 + p_3 \end{pmatrix} = \begin{pmatrix} \lambda_1 \widetilde{\lambda}_{\dot{1}} & \lambda_1 \widetilde{\lambda}_{\dot{2}} \\ \lambda_2 \widetilde{\lambda}_{\dot{1}} & \lambda_2 \widetilde{\lambda}_{\dot{2}} \end{pmatrix}. \tag{3.10}$$

Here the momentum $p_{a\dot{b}}$ is parametrized by the variables λ_a and $\widetilde{\lambda}_{\dot{b}}$ which respectively transforms as a left and right handed spinor and are known as *spinor variables*. Such a parametrization is not possible for the case of a massive particle, which means the parametrization (or factorization) Eq. (3.9) is an explicit manifestation of the on-shellness of the massless particle.

Let $q_{a\dot{b}} = \mu_a \widetilde{\mu}_{\dot{b}}$ be the on-shell representation of a null momentum q_μ. Since the scalar product between two momenta is given by the trace Eq. (3.4), then in terms of spinor variables the scalar product is

$$p.q = \frac{1}{2}\left(\epsilon^{ab}\lambda_a\mu_b\right)\left(\epsilon^{\dot{a}\dot{b}}\widetilde{\lambda}_{\dot{a}}\widetilde{\mu}_{\dot{b}}\right). \tag{3.11}$$

In this expression, the product between the left and right handed spinors are decoupled from each other into two separate products which are both antisymmetric.

The left handed and the right handed spinor products are represented by angle and square brackets

$$\langle pq\rangle \equiv \epsilon^{ab}\lambda_a\mu_b \quad \text{and} \quad [pq] \equiv \epsilon^{\dot{a}\dot{b}}\widetilde{\lambda}_{\dot{a}}\widetilde{\mu}_{\dot{b}}. \tag{3.12}$$

In the Weyl representation $p_{a\dot{b}}$ is Hermitian for a real momentum p_μ; therefore $\widetilde{\lambda} = \lambda^*$ and $[pq] = \langle pq\rangle^*$ for real p_μ.

There are many properties between spinors but here are some useful identities that we will use to simplify algebraic expressions. Consider n null momenta $k_{i\mu}$ and let $k_{ia\dot{a}} = \lambda_{ia}\widetilde{\lambda}_{i\dot{a}}$ be the corresponding on-shell representation

- *The brackets are linear:* Even through the brackets are antisymmetric they still preserve the linearity of the scalar products, $k_{l\mu}(\alpha_i k_i^\mu + \alpha_j k_j^\mu) = \alpha_i k_l.k_i + \alpha_j k_l.k_j$. One can see that

$$\begin{aligned}\langle \lambda_l, \alpha\lambda_i + \beta\lambda_j\rangle &= \epsilon^{ab}\lambda_{la}(\alpha\lambda_{ib} + \beta\lambda_{jb}) \\ &= \alpha\langle\lambda_l\lambda_i\rangle + \beta\langle\lambda_l\lambda_j\rangle.\end{aligned} \tag{3.13}$$

- *Momentum scaling:* There are different ways of writing a scaling αk_μ in terms of spinor variables; in this work we use the symmetric scaling in order to preserve the relation $\widetilde{\lambda} = \lambda^*$,

$$\alpha_i k_{ia\dot{a}} = \left(\sqrt{\alpha_i}\lambda_{ia}\right)\left(\sqrt{\alpha_i}\widetilde{\lambda}_{i\dot{a}}\right) \tag{3.14}$$

- *Schouten identity:* Since spinors live in a two dimensional vector space, three different spinors, $\{\lambda_j, \lambda_k, \lambda_l\}$, cannot be independent from each other. One finds the following identity for any $\lambda_i, \lambda_j, \lambda_k, \lambda_l$

$$\langle ij\rangle\langle kl\rangle + \langle ik\rangle\langle lj\rangle + \langle il\rangle\langle jk\rangle = 0. \tag{3.15}$$

- *Vanishing product:* Since angle brackets are antisymmetric products then the product of two non-zero spinors vanishes if and only if the two spinors are proportional to each other

$$\langle ij\rangle = 0 \Leftrightarrow \lambda_{ia} = \alpha\lambda_{ja}. \tag{3.16}$$

As mentioned above, angle brackets and square brackets are conjugates to each other; therefore similar relations hold for the square brackets by complex conjugation.

3.2.2 Parametrization of polarizations

For completeness it is also necessary to parametrize the polarization, spinor and vector, in terms of these new variables. Before we continue to this parametrization, it is necessary to remind the readers that the spinor variables, λ and $\widetilde{\lambda}$, are different from the spinors initial/final states of fermions, $u(p)$ and $\bar{u}(p)$, which we call *spinor polarizations*.

Spinor polarization

As mentioned in the previous section, the polarization for massless fermions can be decomposed into right and left handed spinors $(u_a, u^{\dot{a}})$; each handed spinors has to satisfy the Weyl equations. However the matrix $p_{a\dot{b}}$ is now parametrized in terms of spinor variables, λ_a and $\widetilde{\lambda}_{\dot{b}}$, therefore the Weyl equations Eq. (3.8) are reduced to

$$\langle pu\rangle = \lambda^a u_a = 0 \quad \text{and} \quad [pu] = \widetilde{\lambda}_{\dot{a}} u^{\dot{a}} = 0. \tag{3.17}$$

Here the spinor variables are non-zero. Thus in order to satisfy these equations the right and left handed polarization have to be respectively proportional to λ and $\widetilde{\lambda}$. To fix the constant of proportionality one can use the helicity sum relation in Eq. (2.7) to find that $u_h(p) = (t\lambda_a, t^{-1}\widetilde{\lambda}^{\dot{a}})$, where t is an arbitrary non-zero constant that leaves $p_{a\dot{b}}$ invariant. Thus any choice of t will be a solution, and two different choices of t are related by the transformation called *the little group* action. For simplicity, we can fix the redundancy by taking $t = 1$. Then the right and left handed polarization are given by

$$u_- = \begin{pmatrix} \lambda_a \\ 0 \end{pmatrix} \quad \text{and} \quad u_+ = \begin{pmatrix} 0 \\ \widetilde{\lambda}^{\dot{a}} \end{pmatrix}, \tag{3.18}$$

where $\widetilde{\lambda}^{\dot{a}} = \varepsilon^{\dot{a}\dot{b}}\widetilde{\lambda}_{\dot{b}}$ and similarly with $\lambda^a = \varepsilon^{ab}\lambda_b$, we can write $p^{\dot{a}b} = \widetilde{\lambda}^{\dot{a}}\lambda^b$. For completeness the parametrization of the different spinor states are obtained through

$$\bar{u}_\pm = u_\pm^\dagger \gamma^0 \quad \text{and} \quad v_\pm = u_\mp. \tag{3.19}$$

Vector polarization

We introduced the polarization vector associated to a gluon in Eq. (2.8, 2.9). The polarization can be either $\varepsilon^-_\mu(k)$ or $\varepsilon^+_\mu(k)$, where $\varepsilon^\pm_\mu \varepsilon^{\pm\mu} = 0$. As mentioned in Eq. (3.9), any null vector can be represented as a product of two spinor variables in the spinor representation as an ansatz

$$\varepsilon_{a\dot{b}}(k;q) = \mu_a \widetilde{\mu}_{\dot{b}}, \tag{3.20}$$

where μ_a and $\widetilde{\mu}_{\dot{b}}$ are respectively a right and left handed reference spinors. The transversality condition $k^\mu \varepsilon^\pm_\mu = 0$ implies either $\mu_a = z_1 \lambda_a$ or $\widetilde{\mu}_{\dot{a}} = z_2 \widetilde{\lambda}_{\dot{a}}$ where λ_a and $\widetilde{\lambda}_{\dot{a}}$ are the spinor variables associated to the momentum k_μ of the gluon and z_i are some normalization constants.

These two solutions reflect the fact that there are two possible orientations of the helicity. The normalization factors z_i are fixed by the normalization $\varepsilon^+_\mu(k)\varepsilon^{-\mu}(k) = -1$ from Eq. (2.9), and we find

$$\varepsilon^1_{a\dot{a}}(k;\widetilde{\mu}) = \sqrt{2}\frac{\lambda_a \widetilde{\mu}_{\dot{a}}}{[k\widetilde{\mu}]} \quad \text{and} \quad \varepsilon^2_{a\dot{a}}(k;\mu) = \sqrt{2}\frac{\mu_a \widetilde{\lambda}_{\dot{a}}}{\langle k\mu\rangle}, \tag{3.21}$$

where $\varepsilon^1_{a\dot{a}}$ and $\varepsilon^2_{a\dot{a}}$ are the two possible polarizations that satisfy Eq. (2.8) and Eq. (2.9). The helicity choice, i.e. ε^- and ε^+, between the two solutions is fixed with the little group action on $\varepsilon^\pm_{a\dot{a}}$, as introduced in [79]. The same way as $u_h(p)$ transforms under the little group, any polarization $\mathcal{P}_h(k)$ of a particle with momentum k and helicity h will transform as

$$\mathcal{P}_h(k) \xrightarrow{(t\lambda, t^{-1}\widetilde{\lambda})} t^{-2h}\mathcal{P}_h(k). \tag{3.22}$$

Therefore,

$$\varepsilon^-_{a\dot{a}}(k;q) = \sqrt{2}\frac{\lambda_a \widetilde{\mu}_{\dot{a}}}{[kq]} \quad \text{and} \quad \varepsilon^+_{a\dot{a}}(k;q) = \sqrt{2}\frac{\mu_a \widetilde{\lambda}_{\dot{a}}}{\langle kq\rangle}, \tag{3.23}$$

where μ and $\widetilde{\mu}$ are combined into a reference momentum given by $q_{a\dot{b}} = \mu_a \widetilde{\mu}_{\dot{b}}$. From these expressions, one can see that the reference momentum q is not physical since these expression were derived for an arbitrary $q \neq k$. However, two different choices of references, q and q', are related by a gauge transformation

$$\varepsilon^-_{a\dot{a}}(k;q) - \varepsilon^-_{a\dot{a}}(k;q') = \omega^- k_{a\dot{a}}, \tag{3.24}$$

where ω^- is some scalar factor given by

$$\omega^- = \sqrt{2}\frac{[qq']}{[qk][kq']}. \tag{3.25}$$

In a similar way the same relation holds with the positive helicity $\varepsilon^+_{a\dot{a}}(k;q)$ with a factor $\omega^+ = (\omega^-)^*$.

3.2.3 Helicity projections

The goal of this section is to simplify the transition from the standard Lorentz invariant quantity, like $\bar{v}_h(\bar{p})\not{k}u_h(p)$, to the spinor helicity brackets notation by using helicity projections. Starting with the fact that a polarization $u(p)$ splits into Weyl spinors, see Eq. (3.8), the gamma matrices would be represented by

$$\gamma^0 = \begin{pmatrix} 0 & \mathbb{1} \\ \mathbb{1} & 0 \end{pmatrix} \quad \text{and} \quad \gamma^i = \begin{pmatrix} 0 & \sigma^i \\ -\sigma^i & 0 \end{pmatrix}. \tag{3.26}$$

Therefore, one can define projectors $\mathbf{P}_\pm$ that project the spinor into the Weyl spinors u_- and u_+ such that $u_\pm = \mathbf{P}_\pm u(p)$,

$$\mathbf{P}_- = \begin{pmatrix} \mathbb{1} & 0 \\ 0 & 0 \end{pmatrix} \quad \text{and} \quad \mathbf{P}_+ = \begin{pmatrix} 0 & 0 \\ 0 & \mathbb{1} \end{pmatrix}; \tag{3.27}$$

these are the helicity projectors with which $\mathbf{P}_i\mathbf{P}_j = \delta_{ij}\mathbf{P}_i$ and $\mathbf{P}_- + \mathbf{P}_+ = \mathbb{1}$. The helicity projectors $\mathbf{P}_\pm$ project a particle into the state where the helicity is $h = \pm 1/2$. However, by crossing symmetry, $\mathbf{P}_\pm$ will project an antiparticle $v(p)$ into the state with helicity $h = \mp 1/2$; that is to say $\mathbf{P}_\pm v(p) = v_\mp$.

Recall that the polarization of the outgoing particle and incoming antiparticle are respectively defined as $\bar{u} = u^\dagger\gamma^0$ and $\bar{v} = v^\dagger\gamma^0$. From these definition, we can find the action of the projectors on these spinors $\bar{u}$ and $\bar{v}$ by using the applying the same definition on $\bar{u}_\pm$ and $\bar{v}_\pm$

$$\begin{aligned} \bar{u}_\pm &= (\mathbf{P}_\pm u)^\dagger\gamma^0 = u^\dagger\mathbf{P}_\pm\gamma^0 = \bar{u}\mathbf{P}_\mp \\ \bar{v}_\pm &= (\mathbf{P}_\mp v)^\dagger\gamma^0 = v^\dagger\mathbf{P}_\mp\gamma^0 = \bar{v}\mathbf{P}_\pm. \end{aligned} \tag{3.28}$$

In the above derivations, we used the fact that the projectors are Hermitian and $\mathbf{P}_\pm\gamma^0 = \gamma^0\mathbf{P}_\mp$. The final piece is to decompose a Weyl matrix $\not{k}$, defined in Eq. (3.7),

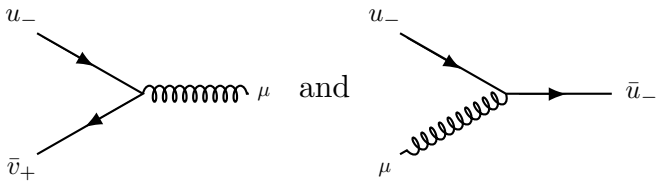

Figure 3.1: Helicity flow along fermion lines.

in terms of the projectors $\mathbf{P}_\pm$. It is straight forward to check that

$$\not{k} = \mathbf{P}_+ \not{k} \mathbf{P}_- + \mathbf{P}_- \not{k} \mathbf{P}_+, \tag{3.29}$$

where in terms of spinor variables we have

$$\mathbf{P}_+ \not{k} \mathbf{P}_- = \begin{pmatrix} 0 & 0 \\ \widetilde{\lambda}^{\dot{a}} \lambda^b & 0 \end{pmatrix} \quad \text{and} \quad \mathbf{P}_- \not{k} \mathbf{P}_+ = \begin{pmatrix} 0 & \lambda_a \widetilde{\lambda}_{\dot{b}} \\ 0 & 0 \end{pmatrix}. \tag{3.30}$$

The orthogonality of the projectors, $\mathbf{P}_+ \mathbf{P}_- = 0$, leads to the fact that a particle or antiparticle in a state of helicity h will have a zero projection into the state of opposite helicity $-h$, which can be understood by $\mathbf{P}_\pm u_\mp = \bar{v}_\pm \mathbf{P}_\mp = 0$. Thus with all these concepts of projection in hand, one can find how $\bar{v}_h(\bar{p}) \not{k} u_h(p)$ would be written in terms of angle and square brackets for given helicities,

$$\begin{aligned} \bar{v}_+(\bar{p}) \not{k}_i u_-(p) &= [\bar{p} i] \langle i p \rangle \equiv [\bar{p} | \not{k}_i | p \rangle \\ \bar{v}_-(\bar{p}) \not{k}_i u_+(p) &= \langle \bar{p} i \rangle [i p] \equiv \langle \bar{p} | \not{k}_i | p]. \end{aligned} \tag{3.31}$$

Here the notation $[\bar{p}|\not{k}_i|p\rangle$ reflects the fact that the $\not{k}$ is projected in the right-left component $\mathbf{P}_+ \not{k} \mathbf{P}_-$ and the right part is contracted with a right-handed spinor through the square bracket and the left part is contracted with a left-handed spinor through the angle bracket, and similarly for the $\langle \bar{p}|\not{k}_i|p]$.

Helicity flow:

The interpretation of the equations Eq. (3.31) is that in massless theory a tree vertex keeps the helicity conserved along a fermion line as in Fig. 3.1. This conservation is a consequence of the decomposition in Eq. (3.29): consider an incoming quark with a polarization u_- where an interaction through a three vertex will contract the fermion with $\bar{v}$ for an incoming antiquark or $\bar{u}$ for an outgoing fermion.

The decomposition Eq. (3.29) of gamma matrices, $\gamma^\mu = \mathbf{P}_+\gamma^\mu\mathbf{P}_- + \mathbf{P}_-\gamma^\mu\mathbf{P}_+$, will fix the helicity of $\bar{v}$ for given $\bar{u}$'s helicity,

$$\begin{aligned}\bar{v}\gamma^\mu u_- &= \bar{v}\mathbf{P}_+\gamma^\mu\mathbf{P}_-u_- = \bar{v}_+\mathbf{P}_+\gamma^\mu\mathbf{P}_-u_- = \bar{v}_+\gamma^\mu u_-,\\ \bar{u}\gamma^\mu u_- &= \bar{u}\mathbf{P}_+\gamma^\mu\mathbf{P}_-u_- = \bar{u}_-\mathbf{P}_+\gamma^\mu\mathbf{P}_-u_- = \bar{u}_-\gamma^\mu u_-.\end{aligned} \tag{3.32}$$

Momentum conservation:

Here we want to write the momentum conservation of four vector momenta in terms of angle and square brackets. Starting with the conservation relation $\sum \not{k}_{\text{initial}} = \sum \not{k}_{\text{final}}$, we sandwich the left and right side of the relation with $\bar{v}_+(r)$ and $u_-(s)$ where r and s are some arbitrary momenta. With the relation Eq. (3.31), the momentum conservation can be written as

$$\sum_{i=\text{initial}} [ri]\langle is\rangle = \sum_{f=\text{final}} [rf]\langle fs\rangle. \tag{3.33}$$

Useful relations from helicity projections

- Consider a chain of slashed momenta, $\not{k}_1\not{k}_2\cdots\not{k}_n$, of length n-odd. One can insert $\mathbb{1} = \mathbf{P}_- + \mathbf{P}_+$ in between two momenta and by considering Eq. (3.29) we can find

$$\not{k}_1\not{k}_2\cdots\not{k}_n = \mathbf{P}_+\not{k}_1\mathbf{P}_-\not{k}_2\cdots\mathbf{P}_+\not{k}_n\mathbf{P}_- + \mathbf{P}_-\not{k}_1\mathbf{P}_+\not{k}_2\cdots\mathbf{P}_-\not{k}_n\mathbf{P}_+. \tag{3.34}$$

- From Eq. (3.34), if we contract the chain of momenta in the far left with $\bar{v}_+(\bar{p})$ and in the right by $u_-(p)$. The same way as Eq. (3.31), we can find

$$\bar{v}_+(\bar{p})\not{k}_1\not{k}_2\cdots\not{k}_n u_-(p) = [\bar{p}|\not{k}_1\not{k}_2\cdots\not{k}_n|p\rangle = [\bar{p}1]\langle 12\rangle[23]\cdots\langle np\rangle, \tag{3.35}$$

  and similarly

$$\bar{v}_-(\bar{p})\not{k}_1\not{k}_2\cdots\not{k}_n u_+(p) = \langle\bar{p}|\not{k}_1\not{k}_2\cdots\not{k}_n|p] = \langle\bar{p}1\rangle[12]\langle 23\rangle\cdots[np], \tag{3.36}$$

  the different combinations with $\bar{u}(\bar{p})$, $v(p)$ and their corresponding helicities are related to Eq. (3.36, 3.35) by crossing symmetry Eq. (3.19).

- The last relation is to express a trace of slashed momenta in terms of brackets. This can be shown by expanding $\not{p}$ as in Eq. (2.7), and the trace will contract the polarizations with the different momenta

$$\begin{aligned}\mathrm{tr}\left(\not{p}\not{k}_1\not{k}_2\cdots\not{k}_n\right) &= \mathrm{tr}\left([u_+(p)\bar{u}_+(p)+u_-(p)\bar{u}_-(p)]\not{k}_1\not{k}_2\cdots\not{k}_n\right)\\ &= \mathrm{tr}\left([u_+(p)\bar{v}_-(p)+u_-(p)\bar{v}_+(p)]\not{k}_1\not{k}_2\cdots\not{k}_n\right)\\ &= \mathrm{tr}\left(u_+(p)\bar{v}_-(p)\not{k}_1\not{k}_2\cdots\not{k}_n\right)+\mathrm{tr}\left(u_-(p)\bar{v}_+(p)\not{k}_1\not{k}_2\cdots\not{k}_n\right)\\ &= \bar{v}_-(p)\not{k}_1\not{k}_2\cdots\not{k}_n u_+(p)+\bar{v}_+(p)\not{k}_1\not{k}_2\cdots\not{k}_n u_-(p)\\ &= \langle p|\not{k}_1\not{k}_2\cdots\not{k}_n|p]+[p|\not{k}_1\not{k}_2\cdots\not{k}_n|p\rangle.\end{aligned} \tag{3.37}$$

  In the first equality we use Eq. (2.7) to replace $\not{p}$ in terms of spinors $u_\pm$ and $\bar{u}_\pm$, then we use the crossing symmetry relation in Eq. (3.19) to obtain the second equality. Then with the linear and cyclic properties of the trace we can derive the last relation.

An application of these useful relations is the computation of the $q\bar{q}\to g$ partial amplitude. Using the color free Feynman rules in Eq. (2.23), we can find

$$A(p,1,\bar{p}) = -ig\,\bar{v}(\bar{p})\not{\varepsilon}_1^*u(p) = -ig[\bar{p}|\not{\varepsilon}_1^*|p\rangle, \tag{3.38}$$

where $u(p)$ be the polarization of the quark with momentum p, $\bar{v}(\bar{p})$ be the polarization of the anti-quark with momentum $\bar{p}$, and ε_1^μ be the polarization of the gluon with momentum k_1. Say the helicity of the quark is $-1/2$. Then the helicity flow in Eq. (3.32) will impose that the helicity of the anti-quark will be $+1/2$. By applying the relation in Eq. (3.35) we can find

$$\begin{aligned}A(p,1^-,\bar{p}) = -ig[\bar{p}|\not{\varepsilon}_{1-}^*|p\rangle &= -ig\sqrt{2}\frac{\langle p1\rangle[\bar{p}q]\langle 1p\rangle}{\langle p1\rangle[1q]}\\ &= -ig\sqrt{2}\frac{\langle p1\rangle\cancel{[\bar{p}q]}\langle 1p\rangle}{\langle p\bar{p}\rangle\cancel{[\bar{p}q]}}\\ &= i\tilde{g}\frac{\langle p1\rangle^3\langle\bar{p}1\rangle}{\langle p1\rangle\langle 1\bar{p}\rangle\langle\bar{p}p\rangle},\end{aligned} \tag{3.39}$$

where in the first line we substitute ε_{1-}^* using Eq. (3.23) with q the reference momentum of the polarization. Then going from the first line to the second line, we use the momentum conservation introduced in Eq. (3.33): $\langle p1\rangle[1q] = \langle p\bar{p}\rangle[\bar{p}q]$. Similarly

for the case where the gluon has a $+1$ helicity, we find

$$\begin{aligned} A(p,1^+,\bar{p}) = -ig[\bar{p}|\not{\epsilon}^*_{1+}|p\rangle &= -ig\sqrt{2}\frac{[\bar{p}1][\bar{p}1]\langle qp\rangle}{[\bar{p}1]\langle 1q\rangle} \\ &= -ig\sqrt{2}\frac{[\bar{p}1]^2\cancel{\langle qp\rangle}}{\cancel{\langle qp\rangle}[p\bar{p}]} \\ &= -i\tilde{g}\frac{[\bar{p}1]^3[p1]}{[p1][1\bar{p}][\bar{p}p]}. \end{aligned} \tag{3.40}$$

The amplitude in Eq. (3.39) and Eq. (3.40) will be used as the initial conditions of the recursion in Section 3.4 in order to generate higher order amplitudes. As discussed in [75] any 3-point amplitudes, like $q\bar{q} \to g$, are only non-zero if and only if the momenta are complex.

3.3 Partial amplitude $A(p,1,2,\bar{p})$

Now that the new kinematic variables have been introduced with the color decomposition, let us consider again the partial amplitude for the generic process of quark antiquark annihilation into two gluons. We are going to compute the partial amplitude Eq. (2.16) for different helicity configurations. We then translate the expressions for the kinematic terms $K_{\rm a}$ and $K_{\rm c}$ in terms of the spinor variables by substituting the scalar product with angle and square brackets and the polarizations with their spinor representations.

We first recall that helicity is conserved along a massless fermion line. Therefore in the annihilation processes, the incoming quark and antiquark necessarily have opposite helicity. For this computation the helicity of the quark is chosen to be $-1/2$ and by conservation the helicity of the antiquark is fixed to be $+1/2$.

3.3.1 Case 1: The two gluons have the same helicity

Let the helicities of the gluons be equal to -1. Since the partial amplitude is gauge invariant, as shown in Section 2.2.2, we are free to choose the reference momenta q_1 and q_2 of the vector polarizations. Here we fix the reference momenta to be the same and equal to p; thus

$$\varepsilon_1^-.\varepsilon_2^- = \frac{\langle 12\rangle[q_1q_2]}{[1q_1][2q_2]} \propto [q_1q_2] = 0. \tag{3.41}$$

Start with the diagram *a)* where the kinematic term is given in Eq. (2.11). We first substitute the polarization in terms of brackets as in Eq. (3.31), then by considering the fact that we are in a gauge where $q_1 = q_2 = p$, the whole expression will collapse into a single term,

$$\begin{aligned} K_{\rm a}(1^-,2^-) &= g^2 \frac{[\bar{p}|\not{\epsilon}_2^* \not{p} \not{\epsilon}_1^*|p\rangle - [\bar{p}|\not{\epsilon}_2^* \not{k}_1 \not{\epsilon}_1^*|p\rangle}{2p.k_1} \\ &= -2g^2 \frac{[\bar{p}q_2]\langle 21\rangle[1q_1]\langle 1p\rangle - [\bar{p}q_2]\langle 2p\rangle[pq_1]\langle 1p\rangle}{\langle p1\rangle[p1][1q_1][2q_2]} \\ &= 2g^2 \frac{[\bar{p}p]\langle 21\rangle}{[p1][2p]}. \end{aligned} \tag{3.42}$$

Then with the diagram *c)*, the kinematic piece is given by Eq. (2.13). With the exact same steps as for the diagram *a)* we obtain

$$\begin{aligned} K_{\rm c}(1^-,2^-) &= -2g^2 \frac{[\bar{p}p]\langle 21\rangle}{[p1][2p]} \frac{\langle p1\rangle[1p] + \langle p2\rangle[2p]}{\langle 12\rangle[21]} \\ &= -2g^2 \frac{[\bar{p}p]\langle 21\rangle}{[p1][2p]} \frac{\langle p\bar{p}\rangle[\bar{p}p]}{\langle 12\rangle[21]} \\ &= -2g^2 \frac{[\bar{p}p]\langle 21\rangle}{[p1][2p]}. \end{aligned} \tag{3.43}$$

To get to the second line we use momentum conservation, Eq. (3.33). To get to the third line we again use momentum conservation, where $p.\bar{p} = k_1.k_2 \Leftrightarrow \langle p\bar{p}\rangle[\bar{p}p] = \langle 12\rangle[21]$.

Back to the partial amplitude, we can see that $K_{\rm a} = -K_c$ for the case where the two gluons have helicity -1. The partial amplitude for that case then vanishes, and so does the case where the two gluons have $h_1 = h_2 = +1$,

$$A(p^-, 1^{\mp}, 2^{\mp}, \bar{p}^+) = 0. \tag{3.44}$$

3.3.2 Case 2: The two gluons have different helicities

Now let the helicity of the first gluon be $h_1 = -1$ so the second one is $h_2 = +1$. We basically perform the same steps as in the previous calculation with the same gauge where q_1 and q_2 are both equal to p.

The expression of $K_{\rm a}$ is obtained straight from the substitution of variables with some simple simplification

$$K_{\rm a} = 2g^2 \frac{[\bar{p}2]\langle 1p\rangle}{[p1]\langle 2p\rangle}. \tag{3.45}$$

However for K_c after the substitution, it requires the use of momentum conservation in order to write the expression as follows

$$K_c = -2g^2 \frac{\langle p1\rangle^3\langle\bar{p}1\rangle}{\langle\bar{p}p\rangle\langle p1\rangle\langle 12\rangle\langle 2\bar{p}\rangle} - 2g\frac{[\bar{p}2]\langle 1p\rangle}{[p1]\langle 2p\rangle}. \tag{3.46}$$

Then by summing the results for K_a and K_c, the partial amplitude for $h_1 = -1$ and $h_2 = +1$ is equal to the following expression

$$A(p^-, 1^-, 2^+, \bar{p}^+) = -2g^2 \frac{\langle p1\rangle^3\langle\bar{p}1\rangle}{\langle p1\rangle\langle 12\rangle\langle 2\bar{p}\rangle\langle\bar{p}p\rangle}. \tag{3.47}$$

This result is very compact and remarkably expressed only with the angle bracket. It can also be shown that interchanging the helicities of the gluons, where $h_1 = +1$ and $h_2 = -1$, will lead to a similar expression with the only difference in the numerator where the labels 1 become 2,

$$A(p^-, 1^+, 2^-, \bar{p}^+) = -2g^2 \frac{\langle p2\rangle^3\langle\bar{p}2\rangle}{\langle p1\rangle\langle 12\rangle\langle 2\bar{p}\rangle\langle\bar{p}p\rangle}. \tag{3.48}$$

3.4 Maximal helicity violating amplitudes

Now that we have a general idea for how the standard Feynman diagram formalism can be simplified using the spinor helicity variables to compute the amplitude for $q\bar{q} \to gg$, let us generalize the computation for n gluon productions. To do so, it is necessary to introduce the Britto, Cachazo, Feng and Witten, or BCFW, recursion.

In the original formulation [80, 81], the BCFW recursion was introduced to compute multiple gluon scattering amplitudes from only 3-point amplitudes. The recursion was used to show that tree amplitudes for process involving only gluons with the following helicity configurations vanish:

$$\begin{aligned} A_n^{gluon}(1^\pm, 2^\pm, \ldots, n^\pm) &= 0, \\ A_n^{gluon}(1^\pm, \ldots, i^\mp, \ldots, n^\pm) &= 0. \end{aligned} \tag{3.49}$$

Since helicity is the projection of the spin onto the direction of momentum, then to make sense with these helicity configurations, all gluons are considered to be outgoing; and, if needed, the physical states of incoming gluons can be recovered by crossing symmetry. With that convention the recursion is formulated as

$$A_n^{gluon} = \sum_{m,h} A_{m+1}^{gluon}(\hat{1}, 2, \ldots, m, \hat{q}_m^h)\frac{1}{q_m^2}A_{n-m+1}^{gluon}(-\hat{q}_m^{-h}, m{+}1, \ldots, n{-}1, \hat{n}), \tag{3.50}$$

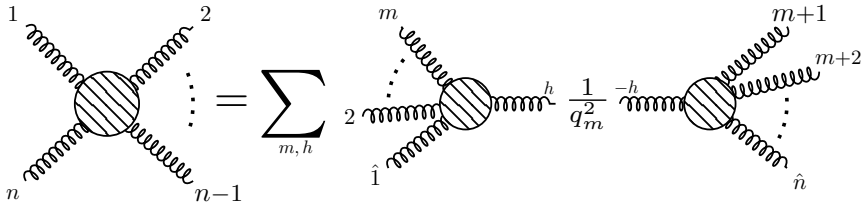

Figure 3.2: Diagrammatic representation of the BCFW recursion.

such that $\hat{q}_m^2 = 0$. In this recursion, the amplitude is factorized into two sub-amplitudes, and summed over different configurations of splitting the two amplitudes and all possible helicities of the exchanged gluon; see Fig. 3.2.

In this recursion, the momenta k_1 and k_n are shifted and denoted by $\hat{k}_1$ and $\hat{k}_n$. These shifts are performed in such a way that momentum conservation and the on-shell conditions are preserved. Thus $\hat{k}_1 = \lambda_1(z)\widetilde{\lambda}_1(z)$ and $\hat{k}_n = \lambda_n(z)\widetilde{\lambda}_n(z)$ with

$$\begin{aligned} \lambda_1(z) &= \lambda_1 & \lambda_n(z) &= \lambda_n - z\lambda_1 \\ \widetilde{\lambda}_1(z) &= \widetilde{\lambda}_1 + z\widetilde{\lambda}_n & \widetilde{\lambda}_n(z) &= \widetilde{\lambda}_n, \end{aligned} \tag{3.51}$$

where z is a complex parameter fixed by the on-shell condition of the intermediate momentum, $\hat{q}_m^2 = 0$, with

$$\hat{q}_m = -(\hat{k}_1 + k_2 + \cdots + k_m) = k_{m+1} + \cdots + k_{n-1} + \hat{k}_n. \tag{3.52}$$

And in this original formulation, the initial conditions of the recursion are given by the following 3 gluons amplitudes:

$$A(1^-, 2^-, 3^+) = i\tilde{g}\frac{\langle 12\rangle^4}{\langle 12\rangle\langle 23\rangle\langle 31\rangle}, \quad \text{and} \quad A(1^+, 2^+, 3^-) = -i\tilde{g}\frac{[12]^4}{[12][23][31]}. \tag{3.53}$$

To extend this recursion into the case of quark antiquark scattering, in this thesis we will consider the following convention:

1. we keep the original convention where all gluons are considered to be outgoing,
2. in contrast to the gluons, we consider all fermions to be incoming,
3. we will use the same momentum shifts as in the original formulation Eq. (3.51), in order to complexify the amplitude, that is to say we shift two gluons.

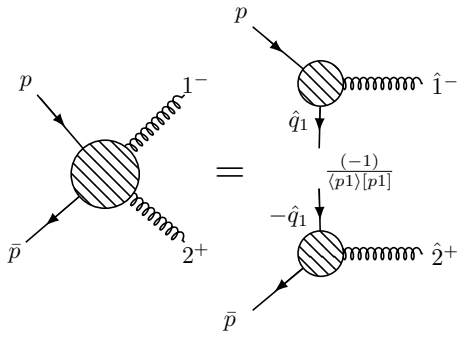

Figure 3.3: BCFW term for $q\bar{q} \to gg$.

We then use exactly the same recursion as in Eq. (3.50) in addition with a quark antiquark pair. Therefore, the amplitude is given by the sum of all possible ways to factorize it into two sub-amplitudes by keeping the two shifted momenta separated. The recursion will be then written as

$$\begin{aligned} A(p,1,\ldots,n,\bar{p}) = &\sum_{m,h} A(p,\hat{1},2,\ldots,m,\hat{q}^h_{1m},\bar{p})\frac{1}{q^2_{1m}}A(-\hat{q}^{-h}_{1m},m{+}1,\ldots,\hat{n},) \\ &+\sum_{m,h} A(\hat{1},2,\ldots,m,\hat{q}^h_{2m})\frac{1}{q^2_{2m}}A(p,-\hat{q}^{-h}_{2m},m{+}1,\ldots,\hat{n},\bar{p}) \\ &+\sum_{m} A(p,\hat{1},2,\ldots,m,\hat{\bar{q}}_{3m})\frac{1}{q^2_{3m}}A(-\hat{q}_{3m},m{+}1,\ldots,\hat{n},\bar{p}), \end{aligned} \tag{3.54}$$

where $\hat{q}^h_{1m}$ and $\hat{q}^h_{2m}$ are intermediate gluon momenta of helicity $h = \pm 1$, while the $\hat{q}_{3m}$ and $\hat{\bar{q}}_{3m}$ are respectively the intermediate quark and anti-quark momenta.

In addition to the original initial conditions Eq. (3.53), we will also need the single gluon production amplitudes $A(p,1^+,\bar{p})$ and $A(p,1^-,\bar{p})$,

$$A(p,1^-,\bar{p}) = i\tilde{g}\frac{\langle p1\rangle^3\langle\bar{p}1\rangle}{\langle p1\rangle\langle 1\bar{p}\rangle\langle\bar{p}p\rangle}, \quad \text{and} \quad A(p,1^+,\bar{p}) = -i\tilde{g}\frac{[\bar{p}1]^3[p1]}{[p1][1\bar{p}][\bar{p}p]}. \tag{3.55}$$

These amplitudes are obtained straight from the qqg vertex contracted with the respective polarizations; see Eq. (3.39) and Eq. (3.40).

The two gluon production amplitude can be recovered using the recursion. As shown in Fig. 3.3, there is only one BCFW term to consider. With the initial condition Eq. (3.55) we computed $A(p,1^-,2^+,\bar{p})$ in Appendix C.1 and found

$$A(p,1^-,2^+,\bar{p}) = -\tilde{g}^2\frac{\langle p1\rangle^3\langle\bar{p}1\rangle}{\langle p1\rangle\langle 12\rangle\langle 2\bar{p}\rangle\langle\bar{p}p\rangle} = -\tilde{g}^2\frac{[\bar{p}2]^3[p2]}{[p1][12][2\bar{p}][\bar{p}p]}. \tag{3.56}$$

For the most general case where we have n gluon production, we showed in Appendix C.2.1 that if all the gluons have the same helicity the amplitude will vanish, $A(p, 1^{\pm}, 2^{\pm}, \ldots, n^{\pm}, \bar{p}) = 0$. We also computed the maximal helicity violating amplitudes in Appendix C.2.2 and found that

$$\begin{aligned} A(p, 1^{+}, \ldots, I^{-}, \ldots, n^{+}, \bar{p}) &= (i\tilde{g})^{n} \frac{\langle pI\rangle^{3}\langle \bar{p}I\rangle}{\langle p1\rangle\langle 12\rangle \ldots \langle n\bar{p}\rangle\langle \bar{p}p\rangle} \\ A(p, 1^{-}, \ldots, I^{+}, \ldots, n^{-}, \bar{p}) &= (i\tilde{g})^{n} \frac{[\bar{p}I]^{3}[pI]}{[p1][12]\ldots[n\bar{p}][\bar{p}p]}, \end{aligned} \tag{3.57}$$

and since they maximally violated helicity conservation, $|\Delta h| = n - 1$, they are respectively called MHV and $\overline{\text{MHV}}$. This formula is an extension of the Parke-Taylor formula Eq. (1.5), where instead of purely gluonic amplitudes we also include a quark anti-quark pair.

3.5 Summary

In summary to avoid diagrammatic complication, see for example in Tab. 1.1, we introduced the spinor variables Eq. (3.9) as a new parametrization of the kinematics, and showed that the two gluon production amplitude can be written in a very compact way, Eq. (3.47). We introduced the BCFW recursion relation that relates an n gluon amplitude to two $m + 1$ and $n - m + 1$ gluon sub-amplitudes. We generalized this recursion relation to include a $q\bar{q}$ pair. Then using this new recursion relation we generalized our two gluon production amplitude calculation to n gluons, $q\bar{q} \to ng$.

4 *MHV calculations*

In the previous chapters, we illustrated some of the properties of QCD in order to present the two main foundations of the MHV techniques, the color kinematic decomposition and the spinor helicity parametrization of the kinematics. In this chapter, we investigate further some physical observables in order to help familiarize the reader more with the MHV techniques. We first compute the transition probability for the quark anti-quark annihilation to two gluons. Then we show how MHV can reproduce the gluon splitting probability by studying the collinear behavior of the amplitude. Splitting functions have been studied in MHV calculations, for example see [82], but in this thesis, we present this calculation in a new and very natural way using MHV techniques. Last we show how to incorporate photons in the technique.

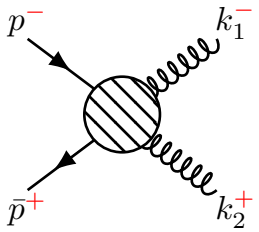

Figure 4.1: Diagram contributing to $q\bar{q} \to gg$ scattering.

4.1 Transition probability $q\bar{q} \to gg$

We first recall that the transition probabilities are defined as the moduli squared of transition amplitudes $\mathcal{M}$. With the amplitude for the process $q\bar{q} \to gg$ in hand, we wish to compute the amplitude squared. Consider the incoming quark and antiquark of momenta p and $\bar{p}$ and respectively with helicities $-1/2$ and $+1/2$ to scatter to produce two gluons of momenta k_1 and k_2, respectively, with helicities -1 and $+1$ as presented in Fig. 4.1. In terms of brackets, the associated Mandelstam variables to this process are

$$\begin{aligned} s &= (p+\bar{p})^2 = (k_1+k_2)^2 = \langle p\bar{p}\rangle[p\bar{p}] = \langle 12\rangle[12] \\ t &= (p-k_1)^2 = (\bar{p}-k_2)^2 = -\langle p1\rangle[p1] = -\langle \bar{p}2\rangle[\bar{p}2] \\ u &= (p-k_2)^2 = (\bar{p}-k_1)^2 = -\langle p2\rangle[p2] = -\langle \bar{p}1\rangle[\bar{p}1]. \end{aligned} \tag{4.1}$$

From the color decomposition Eq. (2.15), the corresponding amplitude is given by the sum of two partial amplitudes weighed with the ordered color charge,

$$\mathcal{M}(1^-, 2^+) = T_{a_1}T_{a_2}A(p, 1^-, 2^+, \bar{p}) + T_{a_2}T_{a_1}A(p, 2^+, 1^-, \bar{p}). \tag{4.2}$$

To square the amplitude, recall the fact that the square and angle brackets are complex conjugates of each other, and the average over the color states leads to a trace over the $SU(3)$ generators

$$\mathrm{tr}\,|\mathcal{M}|^2 = C_1 \sum_{\mathcal{P}_2} \left|A(p, 1^{h_1}, 2^{h_2}, \bar{p})\right|^2 + C_2 \sum_{\mathcal{P}_2} A(p, 1^{h_1}, 2^{h_2}, \bar{p})A^*(p, 2^{h_2}, 1^{h_1}, \bar{p}) \tag{4.3}$$

where h_i denotes the helicity of the gluon labelled by i, and the sum over $\mathcal{P}_2$ is the sum over the permutations of the gluon label, and the coefficients C_1 and C_2 are given by

$$\begin{aligned} C_1 &= \mathrm{tr}\,(T_{a_1}T_{a_2}T_{a_2}T_{a_1}) = C_A C_F \\ C_2 &= \mathrm{tr}\,(T_{a_1}T_{a_2}T_{a_1}T_{a_2}) = -C_F/2, \end{aligned} \tag{4.4}$$

are the color factors that emerge from the trace. The full detailed computation is done in Appendix D which shows how the kinematics can be written as

$$\begin{aligned} \sum_{\mathcal{P}_2} \left|A(p, 1^{h_1}, 2^{h_2}, \bar{p})\right|^2 &= \tilde{g}^4 \left(\frac{t}{u} - 2\frac{t^2}{s^2}\right), \\ \sum_{\mathcal{P}_2} A(p, 1^{h_1}, 2^{h_2}, \bar{p})A^*(p, 2^{h_2}, 1^{h_1}, \bar{p}) &= 2\tilde{g}^4 \frac{t^2}{s^2}. \end{aligned} \tag{4.5}$$

By putting all the pieces together, the color averaged amplitude for a quark anti-quark scattering into gluons with $+1$ and -1 helicity can be written in terms of the Mandelstam variables as

$$\mathrm{tr}\,|\mathcal{M}|^2 = \tilde{g}^4 C_A C_F^2 \left(\frac{t}{u} - \frac{C_A}{C_F}\frac{t^2}{s^2}\right). \tag{4.6}$$

In practice, the two gluons are indistinguishable; then adding the case where the two gluons are interchanged, $t \leftrightarrow u$, will make the helicity final state indistinguishable. This is the same as summing over the helicities of the final state gluons as in the standard Feynman computation. We find that

$$\mathrm{tr}\,\left|\overline{\mathcal{M}}\right|^2 = \tilde{g}^4 C_A C_F^2 \left(\frac{t}{u} + \frac{u}{t} - \frac{C_A}{C_F}\frac{t^2+u^2}{s^2}\right). \tag{4.7}$$

Here we don't need to explicitly average over the initial helicity state of the quarks, since swapping the helicities of the incoming q and $\bar{q}$ leaves the results in Eq. (4.7) unchanged. Therefore Eq. (4.7) is properly averaged over the initial quark anti-quark states and summed over the final gluon states.

The differential cross section associated to $q\bar{q} \to gg$ is a well known result. So one can compare Eq. (4.7) from the result computed using the usual Feyanman diagrammatic expansion in [58, 83], and see that the MHV calculation is a reliable and a very efficient method to compute not only the amplitude but also its modulus squared.

It is important to mention that any $2 \to 2$ scattering process is fully characterized by MHV amplitudes, as done in this section. In the case of a $2 \to n$ scattering process, $n > 2$, various non-MHV helicity configurations are needed to fully characterized the process. However, to simplify the calculation, we will restrict our calculation to the MHV configurations throughout this thesis. This restriction is also motivated by the suppression of the non-MHV contribution for small angle emission, which dominates the radiation spectrum.

4.2 Splitting function

In a $2 \to 2$ process where hard parton jets are produced, one cannot see the sub-structure of the jets in which a parton splits in two or more parton jets with a very

small angular separation; i.e. two jets emitted at a very small $k_\perp$ will be observed as a single jet. The probability for the jet to split into two subjects is called splitting function $P(z)$, where z is the fraction of energy of the parent carried by one of the subjects.

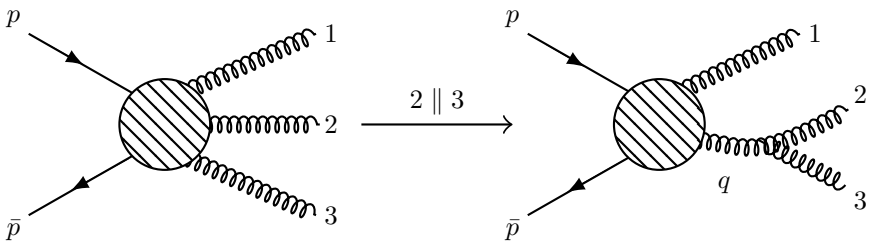

Figure 4.2: Standard splitting factorization from $q\bar{q} \to ggg$.

In order to compute the splitting function $P_{gg}(z)$, where a gluon splits into two gluons, we consider the amplitude $\mathcal{M}(1,2,3)$ corresponding to $q\bar{q} \to ggg$ and then take k_2 to be parallel to k_3; see Fig. 4.2. By taking $k_2 \parallel k_3$, we enhance the diagram in which a gluon splits into k_2 and k_3 by the near on-shellness of its propagator, a property independent of MHV techniques. To begin with we are going to parametrize the momenta as

$$k_2 = zq + k_\perp \quad \text{and} \quad k_3 = (1-z)q - k_\perp, \tag{4.8}$$

where q is the total momentum of the observed parton jet with $q = k_2 + k_3$ while the momentum fraction z runs from 0 to 1. The transverse component $k_\perp$ of the momentum is taken to be small for the splitting, and as $k_\perp \to 0$, the momenta k_2 and k_3 tend to be parallel, and the brackets $\langle 23\rangle$ and $[23]$ will go to zero. From the structure of the MHV amplitude (3.57), one sees that $\langle 23\rangle$ and $[23]$ are in the denominators of the MHV and $\overline{\text{MHV}}$ of the amplitudes $A(p,1,2,3,\bar{p})$ and $A(p,2,3,1\bar{p})$ respectively. Thus a singularity occurs in this collinear region for these two partial amplitudes. For the two amplitudes $A(p,2,1,3,\bar{p})$ and $A(p,3,1,2,\bar{p})$, there is no singularity as these two amplitudes do not have $\langle 23\rangle$ or $[23]$ in the denominator; these two amplitudes will be then suppressed compare to the other partial amplitudes.

Now we are going to see how the amplitude for three gluon production will be reduced to a lower order production in the collinear region, $k_\perp \to 0$. First let us translate the parametrization Eq. (4.8) in terms of spinor variables. In this collinear

region where $k_\perp \to 0$ the momenta k_2 and k_3 will become $k_2 = zq$ and $k_3 = (1-z)q$. Taking $q = \mu_a \widetilde{\mu}_{\dot{a}}$ to be the on-shell parent gluon, we find that

$$\begin{cases} \lambda_{2a} \simeq \sqrt{z}\,\mu_a \\ \widetilde{\lambda}_{2\dot{a}} \simeq \sqrt{z}\,\widetilde{\mu}_{\dot{a}} \end{cases} \quad \text{and} \quad \begin{cases} \lambda_{3a} \simeq \sqrt{1-z}\,\mu_a \\ \widetilde{\lambda}_{3\dot{a}} \simeq \sqrt{1-z}\,\widetilde{\mu}_{\dot{a}}. \end{cases} \tag{4.9}$$

From this point of this section, the symbol " $\simeq$ " will denote the asymptotic behavior in the collinear limit region. Now in terms of amplitudes, we can notice that the partial amplitudes for the processes have to be either MHV or $\overline{\text{MHV}}$, since the helicities of the three gluons cannot be all the same. Let us first consider the amplitude $A(p, 1^-, 2^+, 3^+, \bar{p})$ which is an MVH and then substitute k_2 and k_3 with respect to Eq. (4.9)

$$\begin{aligned} A(p, 1^-, 2^+, 3^+, \bar{p}) &= (i\tilde{g})^3 \frac{\langle p1\rangle^3 \langle \bar{p}1\rangle}{\langle p1\rangle\langle 12\rangle\langle 23\rangle\langle 3\bar{p}\rangle\langle \bar{p}p\rangle} \\ &\simeq (i\tilde{g})^3 \frac{\langle p1\rangle^3 \langle \bar{p}1\rangle}{\langle p1\rangle\langle 1q\rangle\langle q\bar{p}\rangle\langle \bar{p}p\rangle} \frac{1}{\langle 23\rangle} \frac{1}{\sqrt{z(1-z)}} \\ &\simeq A(p, 1^-, q^+, \bar{p}) \frac{i\tilde{g}}{\langle 23\rangle} \frac{1}{\sqrt{z(1-z)}}. \end{aligned} \tag{4.10}$$

In the second line, we just substitute the variables according to Eq. (4.9), and by considering the linearity of the bracket Eq. (3.13) we factorize the z dependence by keeping the bracket $\langle 23\rangle$ which is the singular part of the amplitude. In the last line, we can identify the MHV amplitude $A(p, 1^-, q^+, \bar{p})$ and consider the remaining part to compute the splitting probability. The same manipulation can be done for any helicity configuration of $A(p, 1, 2, 3, \bar{p})$, which leads to the results summarized in Tab. 4.1.

In the case of $A(p, 2, 3, 1, \bar{p})$ the z dependencies remain the same as in $A(p, 1, 2, 3, \bar{p})$; this cyclic rotation of the ordering of gluons will leads to a swap between the momenta q and k_1 in the lower point amplitude, $A(p, q, 1, \bar{p})$. Here by lower point amplitude we mean an amplitude with one fewer external gluon. And finally, we can see from Tab. 4.1 that swapping k_2 and k_3 induces an overall sign flip, a manifestation of the antisymmetric property of the brackets $\langle 23\rangle$ and $[23]$ that leads to a commutator structure $[T_{a_2}, T_{a_3}]$ in the full amplitude. Combining the pieces together into the full amplitude, for $(1^-, 2^+, 3^+)$ one obtains the following factorization

$$\mathcal{M}(1^-, 2^+, 3^+) \simeq \Big[T_{a_1} T_a A(1^-, q^+) + T_a T_{a_1} A(q^+, 1^-)\Big] i \frac{f_{a_2 a_3 a}}{\langle 23\rangle} \frac{i\tilde{g}}{\sqrt{z(1-z)}}. \tag{4.11}$$

$A(p,1^-,2^+,3^+,\bar{p})$	$\longrightarrow$	$A(p,1^-,q^+,\bar{p})\frac{i\tilde{g}}{\langle 23\rangle}\frac{1}{\sqrt{z(1-z)}}$
$A(p,1^-,2^+,3^-,\bar{p})$	$\longrightarrow$	$A(p,1^-,q^+,\bar{p})\frac{i\tilde{g}}{[23]}\frac{z^2}{\sqrt{z(1-z)}}$
$A(p,1^-,2^-,3^+,\bar{p})$	$\longrightarrow$	$A(p,1^-,q^+,\bar{p})\frac{i\tilde{g}}{[23]}\frac{(1-z)^2}{\sqrt{z(1-z)}}$
$A(p,1^+,2^-,3^-,\bar{p})$	$\longrightarrow$	$A(p,1^+,q^-,\bar{p})\frac{i\tilde{g}}{[23]}\frac{1}{\sqrt{z(1-z)}}$
$A(p,1^+,2^-,3^+,\bar{p})$	$\longrightarrow$	$A(p,1^+,q^-,\bar{p})\frac{i\tilde{g}}{\langle 23\rangle}\frac{z^2}{\sqrt{z(1-z)}}$
$A(p,1^+,2^+,3^-,\bar{p})$	$\longrightarrow$	$A(p,1^+,q^-,\bar{p})\frac{i\tilde{g}}{\langle 23\rangle}\frac{(1-z)^2}{\sqrt{z(1-z)}}$

Table 4.1: Factorization of $A(p,1,2,3,\bar{p})$ when k_2 and k_3 become collinear for all different helicity configurations.

We can identify from Eq. (4.2) that the terms in the bracket are equal to $\mathcal{M}(1^-,q^+)$, which is the amplitude for $q\bar{q}\to gg$. We can also see that at the amplitude level the splitting function and the lower point amplitude are still entangled since we still have a summation over the a color index "a". However, when we square the amplitude and sum over the color states by considering the fact that

$$\sum_{a_2,a_3} f_{a_2a_3a}f_{a_2a_3b} = C_A\delta_{ab}, \tag{4.12}$$

the splitting will become independent of the lower amplitude. We find

$$\mathrm{tr}\left|\mathcal{M}(1^-,2^+,3^+)\right|^2 \simeq \mathrm{tr}\left|\mathcal{M}(1^-,q^+)\right|^2 \frac{\tilde{g}^2}{2k_2.k_3}\frac{C_A}{z(1-z)}. \tag{4.13}$$

We can perform the exact same procedure for the other helicity configurations, and summing the six different configurations yields

$$\mathrm{tr}\left|\overline{\mathcal{M}}(1,2,3)\right|^2 \simeq \mathrm{tr}\left|\overline{\mathcal{M}}(1,q)\right|^2 \frac{8\pi\alpha}{q^2}P_{gg}(z), \tag{4.14}$$

where the splitting function $P_{gg}(z)$ is given by

$$P_{gg}(z) = 2C_A\left[z(1-z)+\frac{1-z}{z}+\frac{z}{1-z}\right]. \tag{4.15}$$

Similarly, we can compute the probability for a quark to split into a quark and a gluon using the same methods. Starting with $\mathcal{M}(1,2,3)$, we can take a gluon with k_3 to be collinear to the quark p. And as for P_{gg}, the full amplitude will be dominated by the partial amplitudes with $\langle p3\rangle$ and $[p3]$ in the denominator,

since these brackets will tend to zero as $k_3 \to p$. These partial amplitudes are $A(3^+, 1^-, 2^+)$, $A(3^+, 1^+, 2^-)$, $A(3^-, 1^+, 2^-)$, $A(3^-, 1^-, 2^+)$, and their respective $1 \leftrightarrow 2$ swaps.

In the asymptotic limit, the parametrizations are given by $p \simeq (1-z)p_s$ and $k_3 \simeq zp_s$, where p_s is the momentum of the parent quark. After the substitution of p and k_3 in the partial amplitudes as in Eq. (4.10), we combine them into the full amplitudes: $\mathcal{M}(1^-, 2^+, 3^+)$, $\mathcal{M}(1^+, 2^-, 3^+)$, $\mathcal{M}(2^+, 1^-, 3^+)$, and $\mathcal{M}(2^-, 1^+, 3^+)$. Squaring and averaging over colors and helicities gives

$$\mathrm{tr}\left|\overline{\mathcal{M}}(1,2,3)\right|^2 \simeq \mathrm{tr}\left|\overline{\mathcal{M}}(1,2)\right|^2 \frac{8\pi\alpha}{p_s^2} P_{gq}(z), \tag{4.16}$$

where the splitting function $P_{gq}(z)$ is

$$P_{gq}(z) = C_F \left[\frac{1+(1-z)^2}{z}\right]. \tag{4.17}$$

As mentioned in [84], $P_{AB}(z)$ can be interpreted as the probability of finding a parton of type "A" in a parton of type "B" with a momentum fraction z of the parent parton and a transverse momentum much less than the energy scale of the parent. Based on the calculation made in [58, 84], one can see the simplicity of the computation using MHV techniques.

4.3 Photon decoupling

Up to this point, we have discussed amplitudes for pure QCD processes. However, in this section we will discuss a critical behavior of the QCD amplitude under which a gluon will be constrained to become a photon, this is called "photon decoupling". Such a procedure was first introduced in [85] and usually called $U(1)$ decoupling in purely gluon amplitude calculations as in [87]. To begin with, we consider the fact that both photons and gluons are massless spin-one particles, which means they have the same polarization structure Eq. (3.23). Thus the kinematics of gluons and the kinematics of photons will be described by the same representation.

To incorporate a photon as an external particle of a given amplitude, the only operation is to replace the color factor $(T_a)_{ij}$ by the quantity $\delta_{ij}Qe/g$. The kronecker delta δ_{ij} comes from the fact that quark-photon vertex preserves the color of the

quark, and the factor Qe/g changes the QCD coupling g to Qe, where e is the QED coupling and Q is the fractional charge of the quark. For illustration, let us consider the three gluon production process and decouple one gluon in order to compute the amplitude for $q\bar{q} \to gg\gamma$. We start with the expression of the amplitude $\mathcal{M}(1,2,3)$, then we replace T_{a_3} with Qe/g,

$$\mathcal{M}(1^-,2^+,3^+_\gamma) = \frac{Qe}{g}\sum_{\mathcal{P}_3} T_{a_1}T_{a_2}A(p,1^-,2^+,3^+,\bar{p}). \tag{4.18}$$

We can see that the color part of the amplitude cannot "see" the presence of the photon labelled by "3"; this procedure will allow us to explicitly sum all possible permutations of the photon without changing the structure of the color factor,

$$\sum_{\mathcal{P}_2} T_{a_1}T_{a_2}\left[A(p,1^-,2^+,3^+,\bar{p}) + A(p,1^-,3^+,2^+,\bar{p}) + A(p,3^+,1^-,2^+,\bar{p})\right]. \tag{4.19}$$

And with the expression of the MHV amplitude in Eq. (3.57), we can see that this kinematic term in the brackets is proportional to the the following,

$$\begin{aligned}
&\frac{\langle p1\rangle^3\langle\bar{p}1\rangle}{\langle p1\rangle\langle 12\rangle\langle 23\rangle\langle 3\bar{p}\rangle} + \frac{\langle p1\rangle^3\langle\bar{p}1\rangle}{\langle p1\rangle\langle 12\rangle\langle 23\rangle\langle 3\bar{p}\rangle} + \frac{\langle p1\rangle^3\langle\bar{p}1\rangle}{\langle p1\rangle\langle 12\rangle\langle 23\rangle\langle 3\bar{p}\rangle} \\
&= \frac{\langle p1\rangle^3\langle\bar{p}1\rangle}{\langle p1\rangle\langle 12\rangle\langle 2\bar{p}\rangle}\left(\frac{\langle 2\bar{p}\rangle}{\langle 23\rangle\langle 3\bar{p}\rangle} + \frac{\langle 12\rangle}{\langle 13\rangle\langle 32\rangle} + \frac{\langle p1\rangle}{\langle p3\rangle\langle 31\rangle}\right) \\
&= \frac{\langle p1\rangle^3\langle\bar{p}1\rangle}{\langle p1\rangle\langle 12\rangle\langle 2\bar{p}\rangle}\frac{\langle p\bar{p}\rangle}{\langle p3\rangle\langle 3\bar{p}\rangle}.
\end{aligned} \tag{4.20}$$

In the first equality we factored out an expression so the part remaining in the bracket can be combined from the applications of the following triangle relation, which is a direct consequence of the Schouten identity,

$$\frac{\langle p1\rangle}{\langle p3\rangle\langle 31\rangle} + \frac{\langle 12\rangle}{\langle 13\rangle\langle 32\rangle} = \frac{\langle p2\rangle}{\langle p3\rangle\langle 32\rangle}. \tag{4.21}$$

Then by combining everything back to the amplitude Eq. (4.18), we see that the amplitude is factorized into two terms. One term depends only on the gluon degrees of freedom while the other term depends only on the photon degrees of freedom. This factorization is a manifestation of the photon decoupling in which the gluon and the photon act on the quark respectively via the adjoint representation of $SU(3)$ and via $U(1)$. Explicitly the amplitude is factorized as follows

$$\mathcal{M}(1^-,2^+,3^+_\gamma) = \mathcal{M}(1^-,2^+)\frac{Q\tilde{e}\langle p\bar{p}\rangle}{\langle p3\rangle\langle 3\bar{p}\rangle}. \tag{4.22}$$

4.4 Summary

As introduced in the begin of the chapter, this chapter showed how MHV techniques work to compute some observable quantities and also to study some structures of QCD amplitudes. First, we computed $q\bar{q} \to gg$ scattering to the cross section level, we showed the simplicity and efficiency of the technique by comparing with the textbook results using standard Feynman diagram approaches. Second, we used the process $q\bar{q} \to ggg$ to review the collinear behavior of QCD amplitudes and rederived the splitting functions P_{gg} and P_{gq} using MHV. P_{gg} and P_{gq} are, respectively, the probability to find a gluon in a gluon and a gluon in a quark jet. We presented the splitting function computations in a very pedagogical way to remove the ambiguities from different MHV manuscripts in which they use more than one different process to compute the different helicity configuration for a single splitting. And last, we introduced the photon decoupling that converts asymptotic states of gluons into photons. This decoupling will be used in the next chapter to rederive the multiple photon emissions spectrum. We will also use the absorption of a photon to produce a virtuality to an on-shell quark, thus inducing gluon radiation.

5 *Vacuum radiation*

Theoretical accuracy often requires including higher order radiative corrections, which leads to precise experimental tests. A perfect example is the prediction of the anomalous magnetic moment of the electron. The QED calculation matches the experimental precision with an order of 10^{-12}; see [88]. Computing higher order corrections is not just about precision, but it also helps to reveal measurements that are sensitive to radiation. In the electroweak sector, as discussed in [89], initial state radiation leads to a reduced effective center of mass energy for hard scattering processes, which changes the shape of the measured Z resonance in $e^+e^- \to Z \to 2f$.

In heavy ion physics, a precise understanding of jet energy loss is needed to characterize the QGP. Such an understanding requires a theoretical computation of multiple gluon emission, one of the mechanisms that lead to jet suppression, both in vacuum and in medium. The main goal of this chapter is to compute the multiple gluon radiation current in the vacuum. Before doing so, it useful to review a simpler case, multiple photon radiation. It is also important to specify that from this point in this thesis the term collinear radiation is used to refer to a photon (or a gluon) radiated at a very small angle where a photon (or a gluon) of momentum k will have $k_\perp \ll k_\parallel$.

5.1 Single photon emission

Let us first compute the single inclusive photon emission for an accelerated charged particle. The calculation will provide us with an opportunity to use the spinor

helicity formalism in the context of a well-known calculation [58]. We will introduce the use of MHV techniques, which require all initial and final state particles to be on-shell, in the next section. From classical electrodynamics it has been understood that an accelerated charge radiates photon. In the case of a sudden change of momentum, say from p to $\bar{p}$, a charged particle induces a current J that leads to the radiation of photons. In QED, the same current can be derived from a generic amplitude in which an additional soft photon will be taken to be collinear along the direction of the charged particle; see Fig. 5.1. Then, if we consider a quark as the charged particle, the induced current is given by

$$J(1) = -Qe\left(\frac{\bar{p}_\mu}{\bar{p}.k_1} - \frac{p_\mu}{p.k_1}\right)\varepsilon^\mu(k_1) + \mathcal{O}(k_{1\perp}). \tag{5.1}$$

Here J represents the current associated to a single bremsstrahlung photon. In the field theory description such a current is generally obtained from soft collinear factorizations, such that

$$\mathcal{M}_1(1) = J(1)\mathcal{M}_0. \tag{5.2}$$

Qe is the electrical charge of the quark, p the initial momentum, $\bar{p}$ the momentum after radiation and $\varepsilon(k_1)$ the polarization vector of the emitted photon with momentum k_1. We can express this current in terms of spinor variables using the duality vector to spinor representation,

$$J(1^+) = Q\tilde{e}\frac{\langle p\bar{p}\rangle}{\langle p1\rangle\langle 1\bar{p}\rangle}. \tag{5.3}$$

To derive Eq. (5.3), we start from Eq. (5.1) and substitute the different momenta with their respective spinor variables, Eq. (3.9). We also consider that the photon has a " $+1$" helicity, where the polarization is given by $\varepsilon^+_{a\dot{a}}(k_1;q_1)$ as defined in Eq. (3.23). For the Lorentz contraction we used the relation $\langle p1\rangle[p1] = 2p.k_1$ defined in Eq. (3.11). Then the expression was simplified with the Schouten identity Eq. (3.15).

We would like to draw special attention to the two following features of this expression. First, the current doesn't depend on the reference q_1, a manifestation of the gauge invariance property of the current. Second, the current has the exact same expression as in the photon decoupling Eq. (4.22) which means that the soft

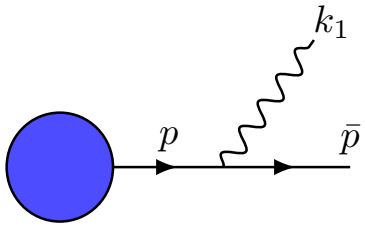

Figure 5.1: Photon emitted from an off-shell quark.

collinear photon will be factorized out of any QCD amplitude in the same way as Eq. (4.20).

A similar treatment can be done for a photon with " -1" helicity, where the polarization is $\varepsilon^{-}_{a\dot{a}}(k_1; q_1)$. The result is quite similar, with an exchange of angle-brackets to square-brackets,

$$J(1^-) = Q\tilde{e}\frac{[p\bar{p}]}{[p1][1\bar{p}]}. \tag{5.4}$$

In order to obtain the momentum distribution for emitting a photon off an off-shell quark, we need to compute the modulus squared of the current and sum over the two different helicities states,

$$\begin{aligned} dN(k_1) &= \frac{Q^2\tilde{e}^2}{(2\pi)^3}\frac{d^3k_1}{2\omega_{k_1}}\left(\left|\frac{\langle p\bar{p}\rangle}{\langle p1\rangle\langle 1\bar{p}\rangle}\right|^2 + \left|\frac{[p\bar{p}]}{[p1][1\bar{p}]}\right|^2\right) \\ &= \frac{Q^2\tilde{e}^2}{(2\pi)^3}\frac{d^3k_1}{2\omega_{k_1}}\frac{p.\bar{p}}{(p\cdot k_1)(\bar{p}\cdot k_1)} \\ &= \frac{Q^2\tilde{e}^2}{(2\pi)^3}\frac{d^3k_1}{\omega_{k_1}}\frac{1}{(1-\cos^2\theta)} \\ &= \frac{Q^2\alpha_e}{\pi}\frac{dx}{x}\frac{dk_\perp}{k_\perp}\frac{d\phi}{2\pi}. \end{aligned} \tag{5.5}$$

The structure of this distribution shows the enhancement of soft-collinear photon radiation. This distribution is divergent in two ways: first as ω_{k_1} tends to zero, in which the energy fraction $x = \omega_{k_1}/\omega_p$ goes to zero, and second as $\vec{k}_1$ goes collinear to the quark line, where the transverse momentum $k_\perp$ goes to zero. Equation (5.5) recovers the Sudakov double logarithm as in [58]. Note that here the off-shellness of the quark is absorbed into the Born amplitude $\mathcal{M}_0$, which will be non-zero and will be able to radiate a photon if and only if the momentum p of the internal quark has a small virtuality produced by the absorption of an incoming photon

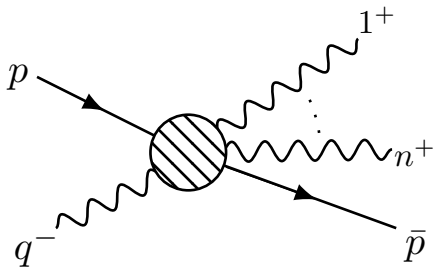

Figure 5.2: Multiple photon radiation off a quark.

5.2 Multiple photons

The application of MHV techniques to study QED processes was first introduced in [85] and was reviewed in [86] for calculations beyond MHV. In this section, we use MHV to generalize the single photon radiation for multiple n photon emissions and rederive the Poisson distribution of multiple photon emissions. We are unaware of such a calculation in which the MHV amplitude was squared and the emission processes were shown to be independent and given by the Poisson distribution. In order to realize such a generalization, consider the following situation: a highly energetic quark with a momentum p absorbs a photon of momentum q with helicity "-1." This absorption will induce a virtuality which will be reduced by photon emissions. As long as the virtuality is non-zero the quark will radiate more photons; see Fig. 5.2. The momenta of the radiated photons are labelled from 1 to n, and all have the same helicities equal to "$+1$."

Restricting all outgoing photons or gluons to have the same helicity simplifies the computation of the distribution. One can show that contributions when one, two, or more outgoing gluons having a different helicity, which correspond to NMHV, NNMHV, etc, diagrams, are suppressed in the soft and collinear limit we are exploring.

The aim of this section is not just to compute the multiple photon emission current but also to show that it is given by the product of individual single photon emissions. The scattering amplitude for such radiation can be computed with Eq. (2.29) in which the $n+1$ gluons are decoupled to photons; that is to say all the

T_a's are replaced by Qe/g and the amplitude becomes purely QED:

$$\begin{aligned}\mathcal{M}(1^+,\ldots,n^+,q^-) &= \left(\frac{Qe}{g}\right)^{n+1}\sum_{\mathcal{P}_{n+1}} A(p,1^+,\cdots,n^+,q^-,\bar{p}) \\ &= Q\tilde{e}\frac{\langle pq\rangle^3\langle\bar{p}q\rangle}{\langle pq\rangle\langle q\bar{p}\rangle\langle\bar{p}p\rangle}J_n(1^+,2^+,\ldots,n^+)\end{aligned} \tag{5.6}$$

On the right hand side of the first equality we have a sum over the permutation of the $n+1$ photons, where the incoming photon is labelled by q. To get the second equality we explicitly summed over all possible permutations of q as in the photon decoupling from Eq. (4.19) to the factorization Eq. (4.20). Then as a result, the incoming photon is factorized out from the n emitted photons and the J_n part that depends on the emitted photons will be defined as our current

$$J_n(1^+,2^+,\ldots,n^+) = (Q\tilde{e})^n\sum_{\mathcal{P}_n}\frac{\langle p\bar{p}\rangle}{\langle p1\rangle\langle 12\rangle\cdots\langle n\,\bar{p}\rangle}, \tag{5.7}$$

which includes a sum over the permutations of the emitted n photons.

Now let us first investigate the simplest case where the quark radiates only $n=2$ photons, and then we will show by induction that the multiple photon current is indeed equal to the product of the single emissions Eq. (5.3). For two photons the permutation can be explicitly written as two terms. By putting the two terms over a common denominator we can simplify the expression using the Schouten identity,

$$\begin{aligned}J_2(1^+,2^+) &= \frac{(Q\tilde{e})^2\langle p\bar{p}\rangle}{\langle p1\rangle\langle 12\rangle\langle 2\bar{p}\rangle} + \frac{(Q\tilde{e})^2\langle p\bar{p}\rangle}{\langle p2\rangle\langle 21\rangle\langle 1\bar{p}\rangle} \\ &= \frac{Q\tilde{e}\langle p\bar{p}\rangle}{\langle p1\rangle\langle 1\bar{p}\rangle}\frac{Q\tilde{e}\langle p\bar{p}\rangle}{\langle p2\rangle\langle 2\bar{p}\rangle} \\ &= J_1(1^+)J_1(2^+).\end{aligned} \tag{5.8}$$

As expected, the two photon emissions are independent; the two emissions current is equal to the product of the individual emissions.

For the multiple emissions, let us show that the current J_n can also be factorized into the product of a single emission current J_1 and the multiple emission J_{n-1}. Starting with the expression in Eq. (5.7), we explicitly permute the n-th photon so the permutation sum will be reduced to $\mathcal{P}_{n-1}$,

$$J_n = \sum_{\mathcal{P}_{n-1}}\frac{(Q\tilde{e})^{n-1}\langle p\bar{p}\rangle}{\langle p1\rangle\langle 12\rangle\cdots\langle n{-}1\,\bar{p}\rangle}\left(\frac{Q\tilde{e}\langle p1\rangle}{\langle pn\rangle\langle n1\rangle} + \frac{Q\tilde{e}\langle 12\rangle}{\langle 1n\rangle\langle n2\rangle} + \cdots + \frac{Q\tilde{e}\langle n{-}1\,\bar{p}\rangle}{\langle n{-}1\,n\rangle\langle n\bar{p}\rangle}\right). \tag{5.9}$$

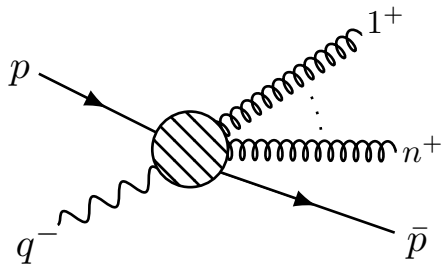

Figure 5.3: Multiple gluon radiation off a quark after absorbing a photon.

In Eq. (5.9) the expression in red is the kernel of J_{n-1}, but it is still coupled with the terms in brackets. The final crucial step is to recall the triangle relation in Eq. (4.21); $n-1$ applications of Eq. (4.21) on the terms in brackets lead to a term that depends only on the n-th photon and can be pulled out of the summation,

$$J_n(1^+,\ldots,n^+) = \left(\sum_{\mathcal{P}_{n-1}} \frac{(Q\tilde{e})^{n-1}\langle p\bar{p}\rangle}{\langle p1\rangle\langle 12\rangle\cdots\langle n{-}1\,\bar{p}\rangle}\right)\frac{Q\tilde{e}\langle p\bar{p}\rangle}{\langle pn\rangle\langle n\bar{p}\rangle}. \tag{5.10}$$

Thus $J_n = J_{n-1}\times J_1$; and by induction, the emission current of indistinguishable photons is then given by the product of the single independent emissions

$$J_n(1^+,\ldots,n^+) = \sum_{\mathcal{P}_n}\frac{(Q\tilde{e})^n\langle p\bar{p}\rangle}{\langle p1\rangle\langle 12\rangle\cdots\langle n\,\bar{p}\rangle} = \prod_{I=1}^{n}\frac{Q\tilde{e}\,\langle p\bar{p}\rangle}{\langle pI\rangle\langle I\bar{p}\rangle}. \tag{5.11}$$

From this expression it is obvious that the distribution of n photon emissions is the product of n single emissions, but normalised by $n!$ that comes with the bosonic phase space of the n final state of photons,

$$dN(k_1,\ldots,k_n) = \frac{1}{n!}\prod_{I=1}^{n} dN(k_I). \tag{5.12}$$

5.3 Gluon radiation

Multiple gluon radiation from an off-shell quark in vacuum is a hard problem. Previous work [90] with traditional pQCD techniques was limited to computing amplitudes with only a few emitted gluons. On the MHV calculation side, previous work [91] were limited to purely gluonic amplitudes. We compute here for the first

time the amplitude for an off-shell quark to emit n gluons in vacuum for n arbitrary using MHV. We square our amplitude in the limit of strong angular ordering and we recover the known results of independent emissions derived using the usual pQCD techniques [66, 67].

An accelerated color charged particle (parton) will radiate gluons just as an electrical charged particle (electron) radiates photons. Thus we can consider the exact same situation where a quark will receive a kick by absorbing a photon, which will induce gluon radiation. The main difference between the two processes is that gluons carry color charge and therefore can also radiate additional gluons.

Starting with the single gluon emission, we consider the amplitude for $q\gamma \to qg$. The different kinematics of the two types of bosons are factorized by the photon decoupling Eq. (4.22) in which the Born $\mathcal{M}(q^-)$ amplitude associated to the photon absorption is separated from the gluon current J; see Fig. 5.3, where q_μ is the momentum of the incoming photon. Let us first derive the single gluon emission amplitude. Starting from Eq. (4.2), and taking into account that one gluon is decoupled into a photon, we have

$$\begin{aligned}\mathcal{M}(1^+, q^-) &= Q\tilde{e}\tilde{g}\left(\frac{T_{a_1}\langle pq\rangle^3\langle\bar{p}q\rangle}{\langle p1\rangle\langle 1q\rangle\langle q\bar{p}\rangle\langle\bar{p}p\rangle} + \frac{T_{a_1}\langle pq\rangle^3\langle\bar{p}q\rangle}{\langle pq\rangle\langle q1\rangle\langle 1\bar{p}\rangle\langle\bar{p}p\rangle}\right)\\ &= \frac{Q\tilde{e}\langle pq\rangle^3\langle\bar{p}q\rangle}{\langle pq\rangle\langle q\bar{p}\rangle\langle\bar{p}p\rangle}\frac{\tilde{g}T_{a_1}\langle p\bar{p}\rangle}{\langle p1\rangle\langle 1\bar{p}\rangle}\\ &= \mathcal{M}(q^-)\frac{\tilde{g}T_{a_1}\langle p\bar{p}\rangle}{\langle p1\rangle\langle 1\bar{p}\rangle},\end{aligned} \tag{5.13}$$

where we used the triangle relation to derive the second line from the first.

Therefore the current for single emission is

$$J_1(1^+) = \frac{\tilde{g}T_{a_1}\langle p\bar{p}\rangle}{\langle p1\rangle\langle 1\bar{p}\rangle}. \tag{5.14}$$

Eq. (5.14) has exactly the same structure as the single photon emission up to a decoupling factor, $T_{a_1} \leftrightarrow (Qe/g)$. At the level of the distribution of real emissions, in which the modulus squared of the current will be traced over the color, we can conclude that the single gluon distribution differs from the single photon case Eq. (5.5) only by the fractional charge to color factor exchange, $Q^2\alpha_e \leftrightarrow C_F\alpha_s$. From these factor differences, we can see also that there are more gluons radiated in QCD than

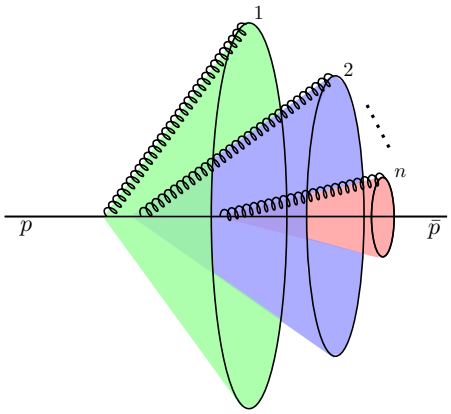

Figure 5.4: Angular ordered gluon emitted off a quark.

photons in QED, since the Q's are a fraction less than 1 and the color factor is $C_F = 4/3$,

$$\langle N_g \rangle > \langle N_\gamma \rangle. \tag{5.15}$$

Despite the duality between these single emissions, the non-Abelian nature of gluons can make a difference for $n > 1$ gluon emissions. However, since the photon carries no color charge, the same factorization Eq. (5.6) still occurs for the absorbed photon in which the photon decouples. The general vacuum radiation current for multiple gluon emission is then given by

$$J_n(1^+, \ldots, n^+) = \tilde{g}^n \sum_{\mathcal{P}_n} (T_{a_1} T_{a_2} \cdots T_{a_n}) \frac{\langle p\bar{p} \rangle}{\langle p1 \rangle \langle 12 \rangle \cdots \langle n\bar{p} \rangle}. \tag{5.16}$$

Eq. (5.16) is quite similar to the multiple photon emissions Eq. (5.7), but what makes the difference is that gluons have non-commutative color charges T_a's. This increases the degrees of freedom by n color degrees of freedom, and makes the multi-gluons calculation more challenging compared to the multiple photon emission.

Let us first consider the case where the emissions are strongly ordered; see Fig. 5.4, in which the opening angle of the radiation is ordered in such a way that $\theta_1 \gg \theta_2 \gg \cdots \gg \theta_n$. Thus, we have $k_{\perp 1} \gg k_{\perp i}$, and one can check that

$$\frac{p.k_i}{p.k_1\, k_1.k_i} \simeq \frac{p.\bar{p}}{p.k_1\, k_1.\bar{p}} + \mathcal{O}(k_{\perp i}/k_{\perp 1}) \quad \text{and} \quad \frac{k_j.k_i}{k_j.k_1\, k_1.k_i} \simeq \mathcal{O}(k_{\perp i}/k_{\perp 1}). \tag{5.17}$$

Then the following relations will be true for $\theta_1 \gg \theta_i$,

$$\frac{\langle pi \rangle}{\langle p1 \rangle \langle 1i \rangle} \simeq \frac{\langle p\bar{p} \rangle}{\langle p1 \rangle \langle 1\bar{p} \rangle} \quad \text{and} \quad \frac{\langle ij \rangle}{\langle i1 \rangle \langle 1j \rangle} \simeq 0. \tag{5.18}$$

In this case, the gluon labelled 1 will not see the other $n-1$ gluons, because viewed from 1 they are not resolved from the parent quark; see Fig. 5.5. It will then follow that

$$\sum_{\mathcal{P}_n} \frac{(T_{a_1}T_{a_2}\cdots T_{a_n})\,\langle p\bar{p}\rangle}{\langle p1\rangle\langle 12\rangle\cdots\langle n\bar{p}\rangle} \simeq \frac{T_{a_1}\,\langle p\bar{p}\rangle}{\langle p1\rangle\langle 1\bar{p}\rangle} \sum_{\mathcal{P}_{n-1}} \frac{(T_{a_2}\cdots T_{a_n})\,\langle p\bar{p}\rangle}{\langle p2\rangle\cdots\langle n\bar{p}\rangle}. \tag{5.19}$$

Once the first gluon is factorized out using Eq. (5.18), we can factorize out the next one that won't see the $n-2$ gluons resolved from $\bar{p}$ and so forth and so on until the n-th gluon. Then under the strong angular ordering shown in Fig. 5.4, the QDC emission current will be reduced into the product of individual emissions, like for QED

$$J_n(1^+,\ldots,n^+) \simeq (T_{a_1}T_{a_2}\cdots T_{a_n}) \prod_{I=1}^{n} \frac{\tilde{g}\langle p\bar{p}\rangle}{\langle pI\rangle\langle I\bar{p}\rangle}. \tag{5.20}$$

The color averaged square of Eq. (5.20) is given by

$$\frac{1}{C_A}\mathrm{tr}\left(\left|J_n(1^+,\ldots,n^+)\right|^2\right) \simeq C_F^n \prod_{I=1}^{n}\left|\frac{\tilde{g}\langle p\bar{p}\rangle}{\langle pI\rangle\langle I\bar{p}\rangle}\right|^2 = \prod_{I=1}^{n}\left|J_n(I^+)\right|^2, \tag{5.21}$$

where the $1/C_A$ is the initial radiation normalization, and Eq. (5.21) reproduces the angular ordered calculation presented in [66, 67].

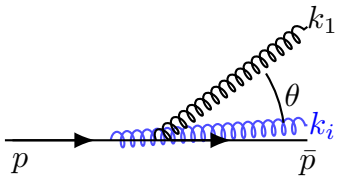

Figure 5.5: k_1 cannot resolve k_i from the parent parton under strong ordering.

5.4 Summary of the chapter

We motivated the study of higher order radiation corrections for precision physics and to unfold some observables that are sensitive to radiation, such as jets in heavy ion collisions. Then we reviewed the single photon emission spectrum from an off-shell quark. We showed that knowing the single photon emission is enough to understand the multiple photon distribution by the use of the decoupling property

of photons. In the last section we showed that the single gluon distribution is comparable to the single photon. The non-Abelian nature of the color charge carried by gluons can lead to major differences in the multiple emission case.

We also showed that under angular ordering the multiple gluon current is reduced to the product of the independent emission in a given order. This ordering breaks the permutation symmetry of the gluons as shown in Eq. (5.20) where we no longer have the sum over the permutations of emitted gluons. In the next chapter we will investigate further the case of two gluon emissions using the general current Eq. (5.16) beyond the assumption of angular ordering.

Particle correlation 6

In this chapter, we would like to find the momentum distribution of two soft and collinear gluons radiated by an off-shell quark.

The radiation current for multiple gluons was introduced in the previous chapter. We showed that under angular ordering the current is reduced to the Abelian result. Here, we analyze the radiation beyond angular ordering as a first test problem as we work to gain insight into the more difficult problem of multiple gluon emission stimulated by multiple scattering in a QGP. There are additional benefits of examining these two gluon emissions from an off-shell quark. First, by quantifying the correlations amongst two gluons emitted that do not have strong angular ordering, we will provide a benchmark for improving vacuum Monte Carlo showering programs. Second, with the two gluon correlation function, we may make a connection with the two particle correlations measured in hadronic collisions.

6.1 Two gluon distribution

In order to compute the distribution for emitting two gluons, we must compute the square of the two gluon emission current, J_2. For soft-collinear emission, the dominant contribution comes from the configuration with both gluons having the same helicity opposite to the photon. From the general expression Eq. (5.16), the two gluon emission current can be expanded as

$$J_2(1,2) = \tilde{g}^2 \left(\frac{T_{a_1} T_{a_2} \langle p\bar{p} \rangle}{\langle p1 \rangle \langle 12 \rangle \langle 2\bar{p} \rangle} + \frac{T_{a_2} T_{a_1} \langle p\bar{p} \rangle}{\langle p2 \rangle \langle 21 \rangle \langle 1\bar{p} \rangle} \right). \tag{6.1}$$

Squaring the current J_2 directly makes the computation complicated since the color factors and the kinematics will mix. To avoid such mixing, we rewrite Eq. (6.1) as a sum over the different permutation symmetries under gluon swap. In the case of two gluon emission, there are two possible configurations: symmetric and antisymmetric under interchange of gluons. We may thus write

$$J_2 = \frac{\tilde{g}^2}{2} C^s_{1,2} J^s_2(1,2) + \frac{\tilde{g}^2}{2} C^a_{1,2} J^a_2(1,2), \tag{6.2}$$

where $C^s_{1,2}$ and $C^a_{1,2}$ are the symmetrized and antisymmetrized color factors and $J^s_2(1,2)$ and $J^a_2(1,2)$ are the symmetrized and antisymmetrized kinematics:

- Color factors

$$\begin{cases} C^s_{1,2} = T_{a_1} T_{a_2} + T_{a_2} T_{a_1} = \{T_{a_1}, T_{a_2}\} \\ C^a_{1,2} = T_{a_1} T_{a_2} - T_{a_2} T_{a_1} = [T_{a_1}, T_{a_2}] \end{cases} \tag{6.3}$$

- Kinematics

$$\begin{cases} J^s_2(1,2) = \dfrac{\langle p\bar{p}\rangle}{\langle p1\rangle\langle 12\rangle\langle 2\bar{p}\rangle} + \dfrac{\langle p\bar{p}\rangle}{\langle p2\rangle\langle 21\rangle\langle 1\bar{p}\rangle} \\ J^a_2(1,2) = \dfrac{\langle p\bar{p}\rangle}{\langle p1\rangle\langle 12\rangle\langle 2\bar{p}\rangle} - \dfrac{\langle p\bar{p}\rangle}{\langle p2\rangle\langle 21\rangle\langle 1\bar{p}\rangle}. \end{cases} \tag{6.4}$$

Then the trace of the modulus square of J_2 is just the sum of the trace squared of the individual term (s and a); i.e. the cross terms' traces vanish. Then the average square of $J_2(1,2)$ will be the square of the individual terms ($C^{s/a}$ and $J^{s/a}$).

6.1.1 Symmetric configuration

For the symmetric case, summing over all possible initial and final color configurations yields the following trace

$$\mathrm{tr}\left(|C^s_{1,2}|^2\right) = \mathrm{tr}\left(\{T_{a_1}, T_{a_2}\}^2\right) = 2C_F^2 C_A - C_F = 4C_A C_F^2 - C_A^2 C_F. \tag{6.5}$$

The symmetrization of the kinematics is analogous to the photon decoupling Eq. (5.11), in which the kinematics is reduced into the product of the two independent emissions. The modulus square of J^s_2 can be written as

$$|J^s_2(1,2)|^2 = \prod_{i=\{1,2\}} \frac{p.\bar{p}}{2(p.k_i)(\bar{p}.k_i)}. \tag{6.6}$$

6.1.2 Antisymmetric configuration

Similarly, summing over initial and final color configurations of the antisymmetric color factor yields

$$\mathrm{tr}\left(|C^a_{1,2}|^2\right) = -\mathrm{tr}\left([T_{a_1}, T_{a_2}]^2\right) = 2C_F^2 C_A + C_F = C_A^2 C_F. \tag{6.7}$$

Since the symmetric part is mainly Abelian, i.e. Eq. (6.6) is the product of individual emission, so we expect information on the non-Abelian QCD nature of gluon coherence effects to emerge from the antisymmetric kinematics. Squaring the antisymmetric kinematic piece we find

$$\begin{aligned} |J_2^a(1,2)|^2 &= \left(\sum_{\mathcal{P}_2} \frac{\epsilon_{12}\langle p\bar{p}\rangle}{\langle p1\rangle\langle 12\rangle\langle 2\bar{p}\rangle}\right)\left(\sum_{\mathcal{P}_2} \frac{\epsilon_{12}[p\bar{p}]}{[p1][12][2\bar{p}]}\right) \\ &= \left(1 + \frac{\mathrm{tr}\left(\not{p}\not{k}_1\not{\bar{p}}\not{k}_2\right)}{2(k_1.k_2)(p.\bar{p})}\right) \prod_{i=\{1,2\}} \frac{p.\bar{p}}{2(p.k_i)(\bar{p}.k_i)}, \end{aligned} \tag{6.8}$$

the details of this computation can be found in Appendix E.1.

6.1.3 Emission distribution

With the above symmetric and antisymmetric results in hand, we may combine everything into the distribution for the emission of two gluons,

$$\begin{aligned} dN(1,2) &= |J_2(1,2)|^2 \prod_{1,2} \frac{d^3k_i}{2\omega_i} \\ &= [1 + C(1,2)]\, dN(1) dN(2), \end{aligned} \tag{6.9}$$

where

$$C(1,2) = \left(\frac{1}{2}\frac{C_A}{C_F}\right) \frac{\mathrm{tr}\left(\not{p}\not{k}_1\not{\bar{p}}\not{k}_2\right)}{4(k_1.k_2)(p.\bar{p})} \quad \text{and} \quad dN(i) = |J_1(i)|^2 \frac{d^3k_i}{2\omega_i}. \tag{6.10}$$

Since $dN(i)$ is the one gluon emission probability related to Eq. (5.14), $C(1,2)$ measures the correlation between the two emitted gluons. The correlation $C(1,2)$ is the main interest of this chapter: it gives the deviation away from the usual Poisson independent emission assumption due to non-Abelian QCD effects.

6.2 Two gluon correlations

In this section we would like to understand more fully the non-Abelian correction, $C(1,2)$, and the phenomenological consequences for the correlations in the emission of two gluons from an off-shell quark. In statistics, the correlation function between two emission events is defined by the ratio between the distribution of getting the two emissions and the product of the two independent emission distributions,

$$\frac{dN(1,2)}{dN(1)dN(2)} - 1 = C(1,2). \tag{6.11}$$

This confirm that $C(1,2)$ defined in the previous section is precisely a correlation function, and will be referred as the two gluon correlation. Note that in the definition of the correlation function above we subtracted the uncorrelated part in order to shift the base line of the correlation and so the correlation vanishes in the Abelian limit.

6.2.1 Color dependence of the correlation

We absorb the color dependence of the correlation function $C(1,2)$ into a factor δ_N that we define as

$$\delta_N \equiv \frac{1}{2}\frac{C_A}{C_F} = \frac{N^2}{N^2-1}. \tag{6.12}$$

In the Abelian limit δ_N vanishes as $C_A \to 0$. One can see in Fig. 6.1 that $\delta_N \to 1$ as $N \to \infty$. For $N = 3$, specific for QCD, the color factor is equal to $\delta_3 = 1.125$. This is to say that from $N = 3$ the correlation function doesn't change much as N grows, and so for the rest of this chapter we will take $\delta_N \approx 1$.

6.2.2 Kinematics of the two gluon correlation function

We can see that $C(1,2)$ is invariant under gluon exchange $(1 \leftrightarrow 2)$ and is singular as the two gluons become collinear. In the distribution Eq. (6.9) one can check that the correlation is dimensionless. Even more, it is invariant under momentum rescaling, so it is useful to express it in terms of angles. But first let us expand the trace in

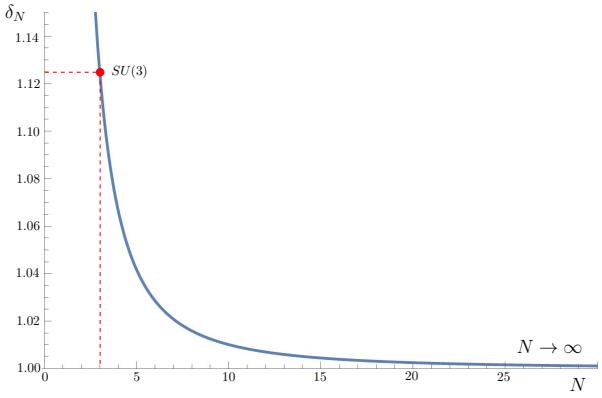

Figure 6.1: Correlation color factor δ_N, Eq. (6.12), for $N \geq 2$.

terms of scalar products:

$$C(1,2) = \frac{\mathrm{tr}\left(\not{p}\not{k}_1\not{\bar{p}}\not{k}_2\right)}{4(k_1\cdot k_2)(p\cdot\bar{p})} = \frac{(p\cdot k_1)(\bar{p}\cdot k_2)+(p\cdot k_2)(\bar{p}\cdot k_1)}{(k_1\cdot k_2)(p\cdot\bar{p})} - 1. \tag{6.13}$$

To evaluate these dot products, we need to define our angular parameters. Let $\bar{p}^\mu \equiv (\omega_P, \vec{P})^\mu$ be the momentum of the off-shell parent quark. After the emission of gluons, the now on-shell quark momentum is $p^\mu = (\omega_p, \vec{p})^\mu$. The deflected quark makes an angle θ_c with respect to the z axis defined by the direction of motion of the off-shell quark of momentum $\vec{P}$; $\vec{P}\cdot\vec{p} = |\vec{P}||\vec{p}|\cos\theta_c$. On the other hand, the i^{th} emitted gluon has a momentum $k_i^\mu = (\omega_i, \vec{k}_i)^\mu$. The emitted gluon makes an angle θ_i with respect to the z axis defined by the off-shell incoming quark and is emitted in a plane at an angle ϕ_i with respect to the plane defined by the incoming off-shell quark and the final on-shell quark. See Fig. 6.2.

In order to parametrize the momenta of the gluons, which are soft and collinear as introduced in the beginning of the chapter, in terms of the angles defined above, let us define the z axis as the spatial direction of motion of the incoming off-shell quark. Let us also define the $x-z$ plane as the plane spanned by the spatial momenta of the incoming quark and the outgoing quark. Then the momenta of the emitted gluons can be written as

$$\vec{k}_i = \omega_i(\sin\theta_i\cos\phi_i\,\hat{x} + \sin\theta_i\sin\phi_i\,\hat{y} + \cos\theta_i\,\hat{z}). \tag{6.14}$$

In terms of these angles, one finds that

$$\frac{(P\cdot k_1)(p\cdot k_2)}{(k_1\cdot k_2)(P\cdot p)} = \frac{(1-\cos\theta_1)\,(1-\cos\theta_c\cos\theta_2-\sin\theta_c\sin\theta_2\cos\phi_2)}{(1-\cos\theta_c)(1-\cos\theta_1\cos\theta_2-\sin\theta_1\sin\theta_2\cos\Delta\phi)}, \tag{6.15}$$

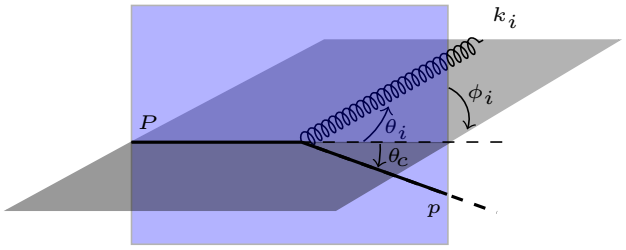

Figure 6.2: Angle parameters for evaluating the two particle correlation $C(1,2)$, Eq. (6.13). ϕ_i is the angle the (blue) plane in which the gluon is emitted makes with respect to the (gray) plane in which the off-shell quark of momentum P is scattered. θ_i is the angle the emitted gluon makes with respect to the z axis defined by the direction of motion of the off-shell quark of momentum P; similarly, θ_c is the angle the scattered quark makes with respect to the z axis.

where $\Delta\phi$ is the azimuthal angle difference between the two gluons. We know that the direction of the parent quark does not change much after radiating away soft-collinear gluons, which is the case we consider here. Eq. (6.15) presents two singularities, first when the two gluons tend to be collinear ($\delta\phi = 0$ and $\theta_1 = \theta_2$), second when the quark is not deflected ($\theta_c = 0$)

In order to understand better these singularities, let us first isolate the θ_c dependence from the collinear divergences induced from the gluon radiations into two separate functions, which we will be denoted by $f(1,2,\theta_c)$ and $g(1,2)$, and defined as follows:

$$\begin{cases} f(1,2,\theta_c) \equiv \dfrac{(1-\cos\theta_1)\,(1-\cos\theta_c\cos\theta_2-\sin\theta_c\sin\theta_2\cos\phi_2)+(1\leftrightarrow 2)}{1-\cos\theta_c} \\ g(1,2) \equiv \dfrac{1}{(1-\cos\theta_1\cos\theta_2-\sin\theta_1\sin\theta_2\cos\Delta\phi)}. \end{cases} \tag{6.16}$$

Since θ_c is small, we may Taylor expand $f(1,2,\theta_c)$ around $\theta_c = 0$ to determine how the correlation function $C(1,2)$ behaves at small θ_c,

$$\begin{aligned} C(1,2) &= f(1,2,\theta_c)\,g(1,2) - 1, \\ &= \left(\sum_{n\in\mathbb{Z}} f_n(1,2)\,\theta_c^n\right)\,g(1,2) - 1 \\ &= \left(\frac{f_{-2}(1,2)}{\theta_c^2} + \frac{f_{-1}(1,2)}{\theta_c} + f_0(1,2)\right)\,g(1,2) - 1 + \mathcal{O}(\theta_c). \end{aligned} \tag{6.17}$$

In terms of the emitted gluon's angles, these coefficient functions are equal to

$$\begin{cases} f_{-2}(1,2) = 4(1-\cos\theta_1-\cos\theta_2+\cos\theta_1\cos\theta_2) \\ f_{-1}(1,2) = 2\cos\phi_1\sin\theta_1(\cos\theta_2-1)+2\cos\phi_2\sin\theta_2(\cos\theta_1-1) \\ f_0(1,2) = \dfrac{1}{3}(1+2\cos\theta_1+2\cos\theta_2-5\cos\theta_1\cos\theta_2). \end{cases} \tag{6.18}$$

Recall the fact that the two gluons are emitted at a very small angle. Then we can expand f_i's in terms of θ_i, and see that up to $\mathcal{O}(\theta^3)$ the expressions in Eq. (6.18) can be simplified:

$$f_{-2} = f_{-1} = 0 \quad \text{and} \quad f_0 = 1-\cos\theta_1\cos\theta_2. \tag{6.19}$$

We may then write the two particle correlation function for the emission of two gluons collinear to the off-shell quark, after some simplification, as

$$C(\theta_1,\theta_2,\Delta\phi) = \frac{\sin\theta_1\sin\theta_2\cos\Delta\phi}{1-\cos\theta_1\cos\theta_2-\sin\theta_1\sin\theta_2\cos\Delta\phi}. \tag{6.20}$$

We can find an even simpler expression by using the pseudorapidities $e^{-\eta_i} \equiv \tan(\theta_i/2)$ of the emitted gluons:

$$C(\Delta\eta,\Delta\phi) = \frac{\cos\Delta\phi}{\cosh\Delta\eta-\cos\Delta\phi}. \tag{6.21}$$

In equation Eq. (6.21) the correlation is expressed in a compact form in which the conformal invariance is explicitly manifest since the correlation is expressed only in terms of angles.

6.2.3 Two particle correlations phenomenology

We would like to compare our two particle correlation Eq. (6.21) with data. We imagine a hadronic collision at a particle accelerator. Then we can think of the incoming parton in Fig. 6.2 as inside one incoming hadron that is subsequently deflected by a small angle in the collision with the opposing hadron. The incoming parton then radiates gluons at a small angle with respect to the incoming hadron. A plot of the two particle correlations amongst the emitted quanta, Eq. (6.21), are shown in the left hand plot of Fig. 6.3. One can see that the near-side correlations are tight in angle ϕ but are long range in rapidity η. We show in the right hand plot

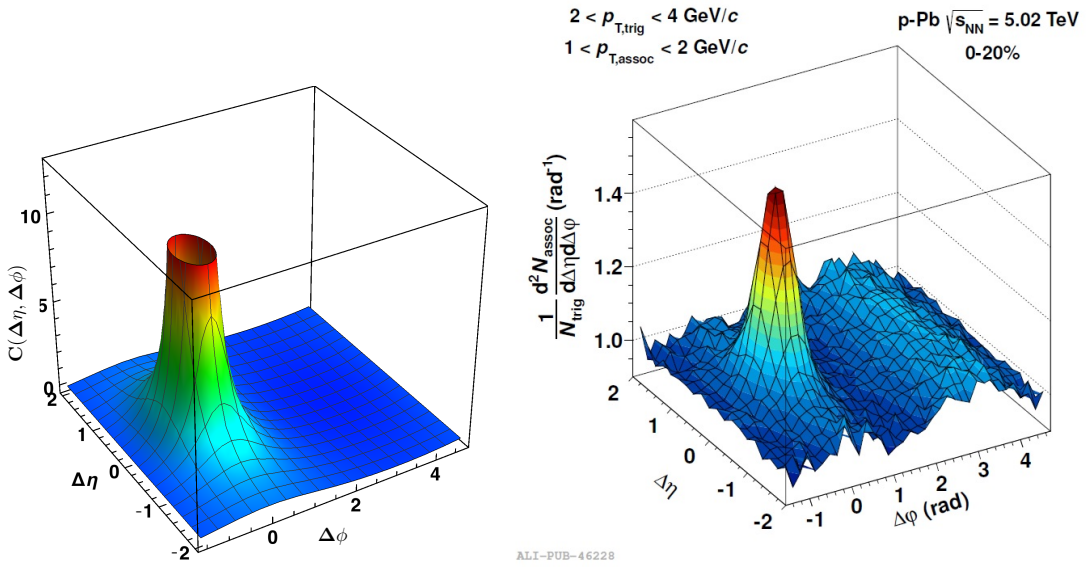

Figure 6.3: The 2-particle correlations from (left) our non-Abelian, two gluon emission expression Eq. (6.21) and from (right) central $p + Pb$ collisions as measured by the ALICE collaboration [92]. Note that the predicted 2-particle correlation plot on the left is not normalized, unlike the experimental result on the right.

of Fig. 6.3 the two particle correlation measurement from central $p + Pb$ collisions at ALICE [92], whose tight angular and long range in rapidity near-side correlation is very similar to our two particle correlation result.

Several comments are in order. Our theoretical prediction is rigorously valid only for small angles of deflection and for small polar angles of emission, θ_i, that allow us to reduce Eq. (6.15) into Eq. (6.21). Since rapidity is defined as $e^{-\eta_i} \equiv \tan(\theta_i/2)$, small θ_i implies large η_i. Our result is thus valid for $\eta_i \gtrsim 0.7$; i.e. our result is valid for arbitrarily large rapidity down to some lower limit. Since the individual η_i can be arbitrarily large, there is no restriction on $\Delta\eta$; therefore $\Delta\eta$ can be arbitrarily large or small depending on the individual η_i. Since we imposed no restriction on the ϕ_i, our result is also valid for all $\Delta\phi$. The comparison between our result and data must be interpreted with caution, though, because there are no rapidity cuts restricting the rapidities on the individual particles $\eta_i \gtrsim 0.7$ in the experimental measurements. And while our correlation in rapidity is much larger than in angle, our result does have an exponential dropoff in $\Delta\eta$ which may be stronger than that

observed in data. Further, a quantitative comparison with data is difficult because our result formally diverges as $\Delta\eta$ and $\Delta\phi$ go to zero, whereas hadronization and detector effects mean that the ALICE data is finite for $\Delta\eta = \Delta\phi = 0$.

However, our result is valid in its regime of applicability and does contribute to the long range in rapidity correlations. An intriguing prediction from our result is that the two particle correlations are conformal; it would be very interesting to see if future two particle correlations measurements reflect our predicted insensitivity to the precise momentum cuts made (modulo detector and hadronization effects).

6.3 Summary

In this chapter we studied the emission of two gluons from an off-shell quark which is important for showering radiation. We found that for non-Abelian QCD, unlike in QED, the emission probability for two gluons is not simply an independent Poisson convolution of the single inclusive gluon emission probability. We explicitly derived the non-Abelian correlations between the two emitted gluons, Eq. (6.10), which simplifies to the manifestly conformal Eq. (6.13) in terms of only the difference in angle, $\Delta\phi$, and rapidity, $\Delta\eta$, between the two emitted gluons for the case of collinear radiation.

We then investigated the phenomenological relevance of our results. A direct comparison between the two gluon correlations we computed and recent ALICE data from central p + Pb collisions shows a surprisingly good qualitative agreement: both distributions display a tight correlation in angle and broad correlation in rapidity. The conformality of our correlations prediction, Eq. (6.13) implies that the shape of the two particle correlations measured in collisions without medium modification will be independent of the momentum cuts made.

We then saw that the absorption of photon can provide the necessary momentum kick to the quark to radiate gluons. However, it is important to ask ourselves how the off-shell-ness produced by the photon absorption would be relevant to a p-A collision despite the qualitative comparison in Fig. 6.3. We know that the more appropriate picture for such collision will be the case where the off-shell-ness is

induced from gluon absorption. In such situation, the absorption of gluon will flip the color state of the quark which will break the decoupling factorization in Eq. (6.1). Therefore, such a color flip will provide an additional source of radiation that needs to be added to the correlation Eq. (6.13) which will be the main motivation for the following Chapter.

7 *Induced radiation*

In the last chapter we showed that gluon emissions are not independent. In order to radiate, we first set up a situation where the virtuality of the quark is produced from a photon absorption. We then decomposed the radiation current into symmetric and anti-symmetric terms under gluon exchange. And as a result we observed that the antisymmetric piece of the decomposition contained information on the non-Abelian effect that produces a correlation between the two gluons.

In this chapter, instead of a photon we will consider a gluon to interact with the quark which will provide a more realistic situation for a gluon radiation in p-A collision. Similarly to the photon case, this interaction with the gluon induces a virtuality to the quark which leads to gluon radiation. In this set up, we consider a highly energetic quark passing through a quark-gluon plasma medium; see Fig. 7.1. The quark then absorbs a gluon, which is approximated here by a free gluon, from the medium that will induce gluon radiation. In our calculation we consider such an absorption via the s-channel for simplicity.

We first consider the general case where a quark absorbs a gluon which will provide the necessary kick to induce the gluon emissions. Then we will show that differently from photon radiation, an infinitely soft interaction with the medium will still induce gluon radiation by color exchange. We explicitly derive the emission currents for the case of one, two and three gluon emissions. Based on these results for one, two, and three gluon emissions, we will conjecture the emission current of induced radiation from a color flip for an arbitrary number of emitted gluons. Further, we will prove our conjectured current is correct for the cases of gluon

emission for which the result is either fully symmetric or fully antisymmetric in the exchange of emitted gluons.

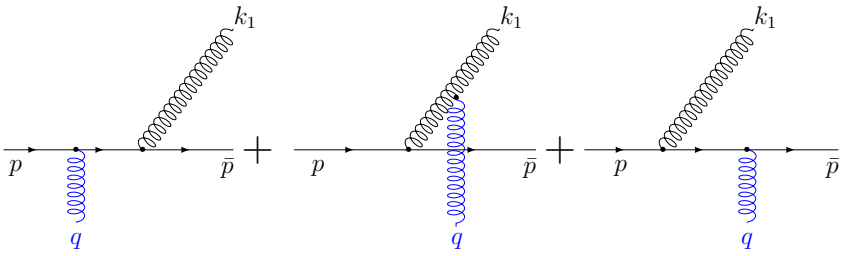

Figure 7.1: Gluon absorption induced gluon radiation.

7.1 Gluon radiation induced by gluon absorption

Let us first consider the case for a single gluon emission. As shown in Fig. 7.1, let the momentum of the highly energetic quark be denoted by p, the momentum of the quasi particle denoted by q, the momentum of the radiated gluon denoted by k_1, and $\bar{p}$ be the final momentum of the quark after the emission. The emission current associated with the induced gluon emission is obtained from the factorization of the radiated gluon out of the amplitude $\mathcal{M}_{gg}$ associated with $qg \to qg$,

$$\begin{aligned}\mathcal{M}_{gg}(q^-,1^+) &= \tilde{g}^2 T_{a_1} T_{a_q} \frac{\langle pq\rangle^3\langle \bar{p}q\rangle}{\langle p1\rangle\langle 1q\rangle\langle q\bar{p}\rangle\langle \bar{p}p\rangle} + \tilde{g}^2 T_{a_q} T_{a_1} \frac{\langle pq\rangle^3\langle \bar{p}q\rangle}{\langle pq\rangle\langle q1\rangle\langle 1\bar{p}\rangle\langle \bar{p}p\rangle} \\ &= \tilde{g}\frac{\langle pq\rangle^3\langle \bar{p}q\rangle}{\langle pq\rangle\langle q\bar{p}\rangle\langle \bar{p}p\rangle}\left(\tilde{g}T_{a_1}T_{a_q}\frac{\langle pq\rangle}{\langle p1\rangle\langle 1q\rangle} + \tilde{g}T_{a_q}T_{a_1}\frac{\langle q\bar{p}\rangle}{\langle q1\rangle\langle 1\bar{p}\rangle}\right) \\ &= A(p,q^-,\bar{p})J(1^+).\end{aligned} \tag{7.1}$$

In the first line, we start with the MHV amplitude where the helicity of the incoming gluon is "-1". In the second line, we factorize the color and kinematic dependence of the radiated gluon. In this factorization, we are left with the partial amplitude of the Born process, $A(p,q^-,\bar{p})$, and the current of the induced radiated gluon, $J(1^+)$. This factorization is different from the case of radiation induced from photon absorption: in the photon case the factorization is total, where the full amplitude is factorized from the current

$$\mathcal{M}_{g\gamma} = \mathcal{M}_{\gamma} J(1^+). \tag{7.2}$$

In our QCD set-up, the absorption of the gluon provides the necessary kick to induce radiation in a way similar to the photon case. But in addition to the kick, this gluon will also rotate the color of the quark and make the factorization partial. This partial factorization is reflected by the fact that the color charges can not be disentangled from each other,

$$J(1) \equiv \tilde{g}\left(T_{a_1}T_{a_q}\frac{\langle pq\rangle}{\langle p1\rangle\langle 1q\rangle} + T_{a_q}T_{a_1}\frac{\langle q\bar{p}\rangle}{\langle q1\rangle\langle 1\bar{p}\rangle}\right). \tag{7.3}$$

From Eq. (7.3), we can recover the vacuum current from photon decoupling in Eq. (5.14), by replacing the QCD generator T_{a_q} associated with the incoming gluon with the QED generator associated with a photon.

In the case of multiple emissions, the factorization in Eq. (7.2) can be generalized, in the same way where the Born amplitude can be partially factorized from the process $qg \to q(ng)$. This partiality of the factorization is related to the fact that only the kinematics of the Born amplitude can be factorized from the current; thus

$$\begin{aligned}\mathcal{M} &= \sum_{\mathcal{P}_{n+1}} (T_{a_1}T_{a_2}\cdots T_{a_n}T_{a_q})A(p,1^+,\ldots,n^+,q^-,\bar{p}) \\ &= A(p,q^-,\bar{p})J_n(1,\ldots,n;q)\end{aligned} \tag{7.4}$$

In Eq. (7.4), we recall the color decomposition of the full amplitude Eq. (2.29) in which we summed over the $(n+1)$ gluon permutations $\mathcal{P}_{n+1}$ of the partial amplitudes. To separate the Born amplitude $A(p,q^-,\bar{p})$ from the radiative term, we use the MHV expression in Eq. (3.57) and perform the following factorization for each term in the decomposition

$$A(p,\ldots,m,q^-,m{+}1,\ldots,\bar{p}) = A(p,q^-,\bar{p})\frac{\tilde{g}^n\langle pq\rangle\langle q\bar{p}\rangle}{\langle p1\rangle\langle 12\rangle\cdots\langle m\,q\rangle\langle q\,m{+}1\rangle\cdots\langle n\bar{p}\rangle}. \tag{7.5}$$

Taking Eq. (7.5) back into the first equality of Eq. (7.4), allows us to identify the multiple emission current

$$J_n \equiv \tilde{g}^n\sum_{m=0}^{n}\sum_{\mathcal{P}_n}\frac{(T_{a_1}T_{a_2}\cdots T_{a_m}T_{a_q}T_{a_{m+1}}\cdots T_{a_n})\langle pq\rangle\langle q\bar{p}\rangle}{\langle p1\rangle\langle 12\rangle\cdots\langle m\,q\rangle\langle q\,m{+}1\rangle\cdots\langle n\bar{p}\rangle}. \tag{7.6}$$

In addition to the permutation of soft gluons, we also have the sum over the different ways to attach the incoming gluon illustrated by the sum over m; see Fig. 7.2. Running from 0 to n, we can also think of m as the number of generators placed on the left of T_{a_q}, the generator associated with the incoming gluon.

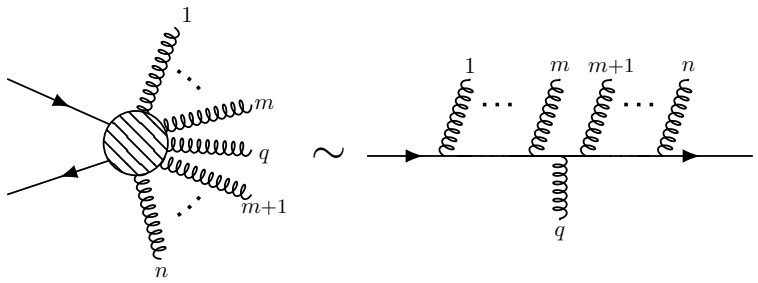

Figure 7.2: Illustration of the configuration m.

7.2 Color flip induced radiation

In this section, we are going to study the radiation of gluons induced from the rotation of color, what we will call a color flip. We still consider the same process where a highly energetic quark absorbs a gluon. The difference is that the incoming gluon has a very small transverse momentum $k_\perp$ compared to p^z. Thus the quark will not be deflected much from its direction of motion. The outgoing quark momentum will be

$$\bar{p} = xp + \mathcal{O}(\bar{p}_\perp). \tag{7.7}$$

In this expression x is the fraction of the momentum carried by the outgoing quark, and $\bar{p}_\perp$ is the transverse momentum of the outgoing quark, which will be negligible compared to the longitudinal component $\bar{p}_\parallel$. Therefore the multiple gluon emission current Eq. (7.6) will become

$$J_n = \tilde{g}^n \sum_{m=0}^{n} \sum_{\mathcal{P}_n} \frac{(T_{a_1} T_{a_2} \cdots T_{a_m} T_{a_q} T_{a_{m+1}} \cdots T_{a_n}) \langle pq \rangle \langle qp \rangle}{\langle p1 \rangle \langle 12 \rangle \cdots \langle m\, q \rangle \langle q\, m{+}1 \rangle \cdots \langle np \rangle}, \tag{7.8}$$

where instead of $\bar{p}$ we have xp; and since the angle brackets are linear, see Eq. (3.13), then the momentum fraction x from the numerator cancels with the one from the denominator.

7.2.1 Induced single gluon emission

First let us consider the single gluon emission. Under the approximation Eq. (7.7) the spinor bracket $\langle p\bar{p} \rangle$ will vanish due the antisymmetric property of brackets. Therefore the vacuum current in Eq. (5.14), produced from photon absorption, vanishes in

that condition. A vanishing current means no radiation, which can explained from the fact that massless particles have to travel at the speed of light. At that speed, the particle cannot feel any acceleration along the longitudinal direction. The only way to make massless Abelian charged particles radiate is to make it deviate from its direction with some transverse impulse.

However in the non-Abelian case, radiation can also be induced from a color flip. To show that let us consider the single emission current from Eq. (7.3) and impose the condition where $\bar{p} \propto p$,

$$J_1 = \tilde{g}\left(T_{a_1}T_{a_q}\frac{\langle pq\rangle}{\langle p1\rangle\langle 1q\rangle} + T_{a_q}T_{a_1}\frac{\langle q\bar{p}\rangle}{\langle q1\rangle\langle 1\bar{p}\rangle}\right) = \tilde{g}[T_{a_1}, T_{a_q}]\frac{\langle pq\rangle}{\langle p1\rangle\langle 1q\rangle}. \tag{7.9}$$

In the second equality we used Eq. (3.14) to express the condition in Eq. (7.7) in terms of spinor variables, that is $\lambda_{\bar{p}} \propto \lambda_p$. The radiation in Eq. (7.9) is purely non-Abelian, in the sense that it is only possible in the presence of the color charge T_{a_q}. In the Abelian limit, where $T_{a_q} \to \mathbb{1}$, we can see that the commutator factor vanishes and no radiation can be produced.

7.2.2 Induced two gluon emissions

Let us first introduce some new notation that will simplify expressions and will make the transition from 2 to n emissions easier. Define

$$\begin{cases} T_{n,m}(1,\cdots,n) \equiv T_{a_1}T_{a_2}\cdots T_{a_m}T_{a_q}T_{a_{m+1}}\cdots T_{a_n} \\ J_{n,m}(1,\cdots,n) \equiv \tilde{g}^n \dfrac{\langle pq\rangle}{\langle p1\rangle\langle 12\rangle\cdots\langle mq\rangle}\dfrac{\langle qp\rangle}{\langle q,m{+}1\rangle\cdots\langle n{-}1,n\rangle\langle np\rangle}. \end{cases} \tag{7.10}$$

Under the approximation where we have $\bar{p} \propto p$, combined with the new notation, the multiple radiation current introduced in Eq. (7.8) can be simply written as

$$J_n = \sum_{m=0}^{n}\sum_{\mathcal{P}_n} T_{n,m}(1,\ldots,n)J_{n,m}(1,\ldots,n) \tag{7.11}$$

Now, let us look at the main subject of this section, two gluon emissions stimulated by a color flip. Inspired by the vacuum calculation in Eq. (6.2), we split the permutation sum of the two emitted gluons into symmetric and antisymmetric pieces,

$$\begin{aligned} J_2 &= \sum_{m=0}^{2} \sum_{\mathcal{P}_2} T_{2,m}(1,2) J_{2,m}(1,2) \\ &= \frac{1}{2} \sum_{m=0}^{2} T^s_{2,m}(1,2) J^s_{2,m}(1,2) + \frac{1}{2} \sum_{m=0}^{2} T^a_{2,m}(1,2) J^a_{2,m}(1,2) \end{aligned} \tag{7.12}$$

The superscripts "s" and "a" stand respectively for symmetric and antisymmetric projection under the permutation of emitted gluons.

First let us investigate the symmetric piece. We will study the different configurations where $m = 0, 1, 2$:

$$\begin{cases} J^s_{2,0} = \tilde{g}^2 \left(\dfrac{\langle qp \rangle}{\langle q1 \rangle \langle 12 \rangle \langle 2p \rangle} + \dfrac{\langle qp \rangle}{\langle q2 \rangle \langle 21 \rangle \langle 1p \rangle} \right) = \tilde{g}^2 \displaystyle\prod_{I=\{1,2\}} \dfrac{\langle pq \rangle}{\langle pI \rangle \langle Iq \rangle} \\ J^s_{2,1} = \tilde{g}^2 \left(\dfrac{\langle pq \rangle \langle qp \rangle}{\langle p1 \rangle \langle 1q \rangle \langle q2 \rangle \langle 2p \rangle} + \dfrac{\langle pq \rangle \langle qp \rangle}{\langle p2 \rangle \langle 2q \rangle \langle q1 \rangle \langle 1p \rangle} \right) = -2\tilde{g}^2 \displaystyle\prod_{I=\{1,2\}} \dfrac{\langle pq \rangle}{\langle pI \rangle \langle Iq \rangle} \\ J^s_{2,2} = \tilde{g}^2 \left(\dfrac{\langle pq \rangle}{\langle p1 \rangle \langle 12 \rangle \langle 2q \rangle} + \dfrac{\langle pq \rangle}{\langle p2 \rangle \langle 21 \rangle \langle 1q \rangle} \right) = \tilde{g}^2 \displaystyle\prod_{I=\{1,2\}} \dfrac{\langle pq \rangle}{\langle pI \rangle \langle Iq \rangle}. \end{cases} \tag{7.13}$$

In the above results, we can see that the symmetric projection of the different configurations are proportional to each other. This allows us to factorize the kinematics of the symmetric part,

$$\sum_{m=0}^{2} T^s_{2,m}(1,2) J^s_{2,m}(1,2) = C^s_2(1,2) J^s_{2,2}(1,2). \tag{7.14}$$

We have chosen $J^s_{2,2}$ to be the common factor where the factor C^s_2 depends only on the color degrees of freedom. The color factor C^s_2 can be written in term of commutators,

$$C^s_2(1,2) = \big(\mathbf{1} T^s_{2,0}(1,2) - \mathbf{2} T^s_{2,1}(1,2) + \mathbf{1} T^s_{2,2}(1,2) \big) = \sum_{\mathcal{P}_2} [T_{a_1}, [T_{a_2}, T_{a_q}]]. \tag{7.15}$$

If the color flip incucing absorbed gluon was rather a photon, then $T_{a_q} \propto \mathbb{1}$ and $C^s_2 = 0$. Similarly to the single emission, this factorization makes the non-Abelian nature of the radiation manifest.

For the antisymmetric piece, we proceed by the same steps. We find

$$\begin{cases} J^a_{2,0} = \tilde{g}^2 \left(\dfrac{\langle qp \rangle}{\langle q1 \rangle \langle 12 \rangle \langle 2p \rangle} - \dfrac{\langle qp \rangle}{\langle q2 \rangle \langle 21 \rangle \langle 1p \rangle} \right) \\ J^a_{2,1} = \tilde{g}^2 \left(\dfrac{\langle pq \rangle \langle qp \rangle}{\langle p1 \rangle \langle 1q \rangle \langle q2 \rangle \langle 2p \rangle} - \dfrac{\langle pq \rangle \langle qp \rangle}{\langle p2 \rangle \langle 2q \rangle \langle q1 \rangle \langle 1p \rangle} \right) = 0 \\ J^a_{2,2} = \tilde{g}^2 \left(\dfrac{\langle pq \rangle}{\langle p1 \rangle \langle 12 \rangle \langle 2q \rangle} - \dfrac{\langle pq \rangle}{\langle p2 \rangle \langle 21 \rangle \langle 1q \rangle} \right) = -J^a_{2,0}. \end{cases} \tag{7.16}$$

Eq. (7.16) shows that the different antisymmetric configurations are also proportional to each other. And to be consistent with the symmetric case we choose $J^a_{2,2}$ to be the fundamental current which will be generated by the antisymmetrized color factor C^a_2,

$$C^a_2(1,2) = \big(-\mathbf{1}T^a_{2,0}(1,2)+\mathbf{0}T^a_{2,1}(1,2)+\mathbf{1}T^a_{2,2}(1,2)\big) = \sum_{\mathcal{P}_2} \epsilon_{\mathbf{12}}[T_{a_1},[T_{a_2},T_{a_q}]]. \quad (7.17)$$

This color factor again makes the non-Abelian nature of the radiation manifest.

Eq. (7.15) and Eq. (7.17) show that the color factor of the symmetric and antisymmetric parts are respectively the antisymmetric and symmetric projections of $[T_{a_1},[T_{a_2},T_{a_q}]]$. The kinematics, on the other hand, are the symmetric/antisymmetric projection of $J_{2,2}(1,2)$.

Taking everything, symmetric and antisymmetric pieces, back into Eq. (7.12) leads to a current with a sum over the different configurations

$$J_2 = \tilde{g}^2 \sum_{\mathcal{P}_2} [T_{a_1},[T_{a_2},T_{a_q}]] \frac{\langle pq\rangle}{\langle p1\rangle\langle 12\rangle\langle 2q\rangle}. \quad (7.18)$$

Here the sum over the different configurations are absorbed into the commutator, which makes the non-Abelian nature of the radiation manifest and makes J_2 have the same structure as the vacuum radiation Eq. (6.1).

7.3 Induced three gluon emissions

Understanding the three gluon emissions is necessary to extend the symmetric-antisymmetric decomposition, performed in the two gluon emissions computation. In the case of three gluons we have to deal to the mixed symmetry case. This mixed symmetry can be introduced from the decomposition into the different irreducible representations of the permutation group $\mathcal{P}_n$ for $n > 2$.

We first recall the case of two gluons, where the symmetric and antisymmetric projection are the two irreducible representations of $\mathcal{P}_2$. To symmetrize and antisymmetrize a function one can use respectively the projectors $\hat{P}_s$ and $\hat{P}_a$ such that

$$\hat{P}_s J_{2,m}(1,2) = \frac{1}{2} J^s_{2,m}(1,2) \quad \text{and} \quad \hat{P}_a J_{2,m}(1,2) = \frac{1}{2} J^a_{2,m}(1,2). \quad (7.19)$$

The 1/2 factors follows from the definition of $J^s_{2,m}$ and $J^a_{2,m}$ in Eq. (7.12), and the projectors satisfy the following conditions

$$\hat{P}_s + \hat{P}_a = 1 \quad \text{and} \quad \hat{P}_s \hat{P}_a = 0. \tag{7.20}$$

However, in the 3 gluons case we have a larger permutation group; and in addition to the symmetric and antisymmetric representations we can expect a mixed symmetry representation. This mixed representation is a representation that is partially symmetric under the swap of two indices and antisymmetric under the swap of the other two indices; for a review on the different representations of the permutation group see [93]. In this derivation, we are interested in the projection operator $\hat{P}_x$ associated to the mixed symmetry representation. With the symmetric and antisymmetric representations, $\hat{P}_x$ can be constructed from the following conditions

$$\hat{P}_s + \hat{P}_a + \hat{P}_x = 1 \quad \text{and} \quad \hat{P}_s \hat{P}_a = \hat{P}_s \hat{P}_x = \hat{P}_a \hat{P}_x = 0. \tag{7.21}$$

In terms of these projection operators the emission current associated to the induced 3 gluon emissions, from Eq. (7.11), can be decomposed as

$$J_3 = \sum_{m=0}^{3} \sum_{\mathcal{P}_3} \left(\hat{P}_s + \hat{P}_a + \hat{P}_x \right) T_{3,m}(1,2,3) J_{3,m}(1,2,3). \tag{7.22}$$

Here we need to recall that the action of the projection is distributive on the product of two functions, i.e.

$$\hat{P}_s \left[T_{3,m}(1,2,3) J_{3,m}(1,2,3) \right] = \hat{P}_s \left[T_{3,m}(1,2,3) \right] \hat{P}_s \left[J_{3,m}(1,2,3) \right]. \tag{7.23}$$

The manipulation of the symmetric and antisymmetric pieces are very much similar to the examination in the 2 gluons case. We find that the kinematic terms $J^s_{3,m}$ and $J^a_{3,m}$ are respectively proportional to $J^s_{3,3}$ and $J^a_{3,3}$. Therefore

$$\begin{aligned}
\sum_{m=0}^{3} \sum_{\mathcal{P}_3} \left(\hat{P}_s T_{3,m}(1,2,3) \right) \left(\hat{P}_s J_{3,m}(1,2,3) \right) &= \sum_{m=0}^{3} U^s_{3,m} \sum_{\mathcal{P}_3} \left(\hat{P}_s T_{3,m}(1,2,3) \right) \hat{P}_s J_{3,3}(1,2,3) \\
&= 3! \sum_{m=0}^{3} U^s_{3,m} \hat{P}_s \left[T_{3,m}(1,2,3) \right] \hat{P}_s \left[J_{3,3}(1,2,3) \right] \\
&= \frac{1}{3!} C^s_3(1,2,3) J^s_{3,3}(1,2,3).
\end{aligned}$$

In the first line, $U^s_{3,m}$ is a constant that depends only on m and is defined from the relation $J^s_{3,m} = U^s_{3,m} J^s_{3,3}$, which reflects the proportionality between the kinematics. In the second line, we consider the fact that symmetric projections are invariant under any permutation of $\mathcal{P}_3$; then the sum over the full permutation leads to the factor "3!", the dimension of $\mathcal{P}_3$. And the last line comes from the following definition

$$\begin{aligned} \hat{P}_s \left[J_{3,3}(1,2,3) \right] &\equiv \frac{1}{3!} J^s_{3,3}(1,2,3), \\ \hat{P}_s \left[T_{3,3}(1,2,3) \right] &\equiv \frac{1}{3!} T^s_{3,3}(1,2,3), \end{aligned} \tag{7.24}$$

with the new color factor

$$C^s_3(1,2,3) \equiv \sum_{m=0}^{3} U^s_{3,m} T^s_{3,m}(1,2,3). \tag{7.25}$$

The exact same steps can be done for the antisymmetric case, which leads to

$$J_3 = \frac{1}{3!} C^s_3(1,2,3) J^s_{3,3}(1,2,3) + \frac{1}{3!} C^a_3(1,2,3) J^a_{3,3}(1,2,3) + \text{Mixed-Sym}. \tag{7.26}$$

Eq. (7.26) is similar to the 2 gluons case in Eq. (7.12). In the derivation above, we claimed that $U^s_{3,m}$ and $U^a_{3,m}$ exist and can be determined to show that C^s_3 and C^a_3 are respectively the symmetric and antisymmetric projection a color factor C_3,

$$C_3(1,2,3) = [T_{a_1}, [T_{a_2}, [T_{a_3}, T_{a_q}]]]. \tag{7.27}$$

This claim will be proven in section 7.4 and 7.5, since these section are dedicated to the understanding of the symmetric and antisymmetric case for any n number of gluon emissions.

Now let us look at the mixed symmetry case. It is important to remind ourselves that the main ingredient for the symmetric and antisymmetric pieces was that the projected kinematics are proportional to each other, that is $J^{s/a}_{3,m} \propto J^{s/a}_{3,m'}$. For the mixed symmetry case, an explicit calculation shows that the mixed symmetry kinematics are not proportional to each other. Therefore we are going to treat this projection with a different approach using properties of the permutation group $\mathcal{P}_3$.

In this analysis, we start by looking at the relation between the different kinematics $J_{3,m}$. Then we give a short review of the permutation group in order to express the relations between the kinematics in terms of some permutation group action on

the kinematics. Then last, we use these relations to understand the mixed-symmetry projection of the 3 gluon emissions.

First, let us show that $J_{3,0}$ and $J_{3,3}$ and that $J_{3,2}$ and $J_{3,1}$ are related. Recall the antisymmetric property of the angular brackets, $\langle ij\rangle = -\langle ji\rangle$. Then,

$$\begin{aligned} J_{3,0}(1,2,3) &= \tilde{g}^3 \frac{\langle pq\rangle}{\langle q1\rangle\langle 12\rangle\langle 23\rangle\langle 3p\rangle} = -J_{3,3}(3,2,1) \\ J_{3,2}(1,2,3) &= \tilde{g}^3 \frac{\langle pq\rangle\langle qp\rangle}{\langle p1\rangle\langle 1q\rangle\langle q2\rangle\langle 23\rangle\langle 3p\rangle} = -J_{3,1}(3,2,1) \end{aligned} \tag{7.28}$$

The second relation comes from a photon decoupling relation similar to what we have done in Eq. (4.20), where

$$\begin{aligned} &\frac{\langle pq\rangle}{\langle p1\rangle\langle 13\rangle\langle 32\rangle\langle 2q\rangle} + \frac{\langle pq\rangle}{\langle p3\rangle\langle 31\rangle\langle 12\rangle\langle 2q\rangle} + \frac{\langle pq\rangle}{\langle p3\rangle\langle 32\rangle\langle 21\rangle\langle 1q\rangle} \\ &\quad = \frac{\langle pq\rangle\langle pq\rangle}{\langle p1\rangle\langle 1q\rangle\langle p3\rangle\langle 32\rangle\langle 2q\rangle} = -\frac{\langle pq\rangle\langle qp\rangle}{\langle p1\rangle\langle 1q\rangle\langle p2\rangle\langle 23\rangle\langle 3q\rangle}. \end{aligned} \tag{7.29}$$

Then by translating this relation (7.29) in terms of J's through the definition Eq. (7.10), we will obtain a relation expressing $J_{3,1}$ as a superposition of the different permutations of $J_{3,3}$,

$$J_{3,1}(1,2,3) = -J_{3,3}(3,2,1) - J_{3,3}(1,3,2) - J_{3,3}(3,1,2). \tag{7.30}$$

Therefore, Eq. (7.28) and Eq. (7.30) relate the different kinematics $J_{3,m}$ to themselves as an action of some permutations, which leads us to a brief review of the action of the permutation group.

Let σ_{ij} be an element of the permutation group $\mathcal{P}_3$, such that the action of σ_{ij} on a regular function with 3 entries, say $F(1,2,3)$, is to swap the label i of the function with the label j. Similarly σ_{ijk} be an element of $\mathcal{P}_3$ that permutes the three indices in such a way the label i will be set to be j, j to be k, and k to be i. For example,

$$\begin{aligned} &\sigma_{13}\left[F(1,2,3)\right] = F(3,2,1) \\ &\sigma_{123}\left[F(1,2,3)\right] = F(2,3,1) \\ &\sigma_{12}\left[\sigma_{321}\left[F(1,2,3)\right]\right] = \sigma_{12}\left[F(3,1,2)\right] = F(3,2,1) \end{aligned} \tag{7.31}$$

The third example shows that a composition of two permutations is a permutation, which is a manifestation of the group closure. The identity element is the action of

	1	σ_{12}	σ_{13}	σ_{23}	σ_{123}	σ_{321}
1	1	σ_{12}	σ_{13}	σ_{23}	σ_{123}	σ_{321}
σ_{12}	σ_{12}	1	σ_{123}	σ_{321}	σ_{13}	σ_{23}
σ_{13}	σ_{13}	σ_{321}	1	σ_{123}	σ_{23}	σ_{12}
σ_{23}	σ_{23}	σ_{123}	σ_{321}	1	σ_{12}	σ_{13}
σ_{123}	σ_{123}	σ_{23}	σ_{12}	σ_{13}	σ_{321}	1
σ_{321}	σ_{321}	σ_{13}	σ_{23}	σ_{12}	1	σ_{123}

Table 7.1: Composition table of the permutation group $\mathcal{P}_3$

no permutation, and the inverse actions are: σ_{ij} for σ_{ij} and σ_{kji} for σ_{ijk}. And last, the composition action of σ's are summarized in Tab. 7.1.

Let us go back into the study of the 3 gluon emissions in which the permutation group will act on the label of the radiated gluons. Starting with the relations (7.28) and (7.30), we would like to construct some operators that transforms the kinematic term $J_{3,3}$ into $J_{3,m}$. Let $\hat{Q}_m$ be the operators such that

$$J_{3,m}(1,2,3) = \hat{Q}_m J_{3,3}(1,2,3). \tag{7.32}$$

In terms of the permutation group action, we are able to find $\hat{Q}_m$ as a superposition of the different elements of the permutation group. The $\hat{Q}_m$ are given by

$$\begin{aligned} \hat{Q}_0 &\equiv -\sigma_{13}, & \hat{Q}_1 &\equiv \sigma_{13} + \sigma_{23} + \sigma_{321}, \\ \hat{Q}_2 &\equiv -1 - \sigma_{23} - \sigma_{321}, & \hat{Q}_3 &\equiv 1. \end{aligned} \tag{7.33}$$

The point of these operators is to provide to the mixed symmetry case a relation equivalent to the one in the symmetric case where $J^s_{3,m} = U^s_{3,m} J^s_{3,3}$. Therefore it is necessary to understand how the action of the projector $\hat{P}_x$ will interfere with $\hat{Q}_m$. In terms of permutations, as shown in [93], the projection operator $\hat{P}_x$ defined in Eq. (7.21) can be written as

$$\hat{P}_x = \frac{1}{3}(2 - \sigma_{123} - \sigma_{321}). \tag{7.34}$$

The projector $\hat{P}_x$ and the operator $\hat{Q}_m$ are now written in terms of permutation operators. Then based on Eq. (7.33) and Eq. (7.34), it can be checked that the

actions on $J_{3,3}$ do not interfere, specifically with Tab. 7.1 one can check the following commutation relation

$$[\hat{P}_x, \hat{Q}_m] = 0. \tag{7.35}$$

Therefore with Eq. (7.32), the mixed symmetry kinematics can be written as

$$J^x_{3,m}(1,2,3) = \hat{P}_x \hat{Q}_m J_{3,3}(1,2,3) = \hat{Q}_m J^x_{3,3}(1,2,3). \tag{7.36}$$

At this stage, it seems the only point of having $\hat{Q}_m$ is just to simplify the computation, that is to say instead of computing the four kinematics $J^x_{3,m}$ we just have to compute $J^x_{3,3}$ and then use $\hat{Q}_m$ to generate the solution for different m. However the goal of this derivation is to provide a solution that requires only $J^x_{3,3}$ with some color factor C^x_3 that absorbs the contribution of the different configuration m. The crucial step is to introduce the set of dual operators $\hat{Q}^\sharp_m$ such that under the permutation sum: "the action of $\hat{Q}_m$ on the kinematics leaving the color term intact is equal to the action of $\hat{Q}^\sharp_m$ on the color term leaving the kinematics intact".

$$\sum_{\mathcal{P}_3} T^x_{3,m}(1,2,3)\hat{Q}_m J^x_{3,3}(1,2,3) = \sum_{\mathcal{P}_3} \left(\hat{Q}^\sharp_m T^x_{3,m}(1,2,3)\right) J^x_{3,3}(1,2,3). \tag{7.37}$$

We computed the set of operators $\hat{Q}^\sharp_m$ dual to $\hat{Q}_m$, see Appendix F.2, that satisfy the commutation relation $[\hat{P}_x, \hat{Q}^\sharp_m] = 0$,

$$\begin{aligned} \hat{Q}^\sharp_0 &= -\sigma_{13}, & \hat{Q}^\sharp_1 &= \sigma_{13} + \sigma_{23} + \sigma_{123}, \\ \hat{Q}^\sharp_2 &= -1 - \sigma_{23} - \sigma_{123}, & \hat{Q}^\sharp_3 &= 1. \end{aligned} \tag{7.38}$$

The dual operator $\hat{Q}^\sharp$, as defined in Eq. (7.37), of any operator $\hat{Q}$ which is a linear combination of permutations is given by the same operator $\hat{Q}$ with the exception where σ_{123} and σ_{321} are interchanged; see Appendix F.2. Therefore the mixed symmetry piece can be written as

$$\sum_{m=0}^{3} \sum_{\mathcal{P}_3} T^x_{3,m}(1,2,3) J^x_{3,m}(1,2,3) = \sum_{\mathcal{P}_3} \hat{P}_x \left(\sum_{m=0}^{3} \hat{Q}^\sharp_m T_{3,m}(1,2,3) \right) J^x_{3,3}(1,2,3). \tag{7.39}$$

The term in brackets is the new color factor for the mixed case; a color factor that contains all the contributions of the different configurations m. With the expression of $\hat{Q}^\sharp_m$ in terms of permutations and with the definition of $T_{n,m}$ in terms of T_a's,

one can compare the following expression by expanding both sides of the equality in terms of color charge products

$$\sum_{m=0}^{3} \hat{Q}_m^\sharp T_{3,m}(1,2,3) = [T_{a_1},[T_{a_2},[T_{a_3},T_{a_q}]]]. \tag{7.40}$$

Therefore the mixed symmetry terms of the Eq. (7.26) are equal to

$$\text{Mixed-Sym} = \sum_{\mathcal{P}_3} C_3^x(1,2,3) J_{3,3}^x(1,2,3), \tag{7.41}$$

where C_3^x is the mixed symmetry projection of the new color factor introduced in Eq. (7.40).

In conclusion, the 3 gluon emissions current induced from a color flip can be decomposed into symmetric, antisymmetric and mixed symmetry terms under the permutation of the 3 gluons. The kinematic piece $J_{3,3}$ was chosen to be the fundamental term in which all the kinematics $J_{3,m}$ are expressed. In the symmetric and antisymmetric projections $J_{3,m}^{s/a}$ are proportional to $J_{3,3}^{s/a}$ which does not hold for the mixed symmetry case. We then introduced a set of operators $\hat{Q}_m$ that act on $J_{3,3}^x$ in order to generate all the mixed symmetry kinematic factors $J_{3,m}^x$.

The fascinating observation is that the action of these operators on the mixed case plays the roles of the proportionality between the kinematic respectively on the symmetric and antisymmetric case, and leads to a common color factor Eq. (7.27) projected respectively into the irreducible representation of $\mathcal{P}_3$. Therefore as for the single and two gluon emission the radiation current can be written in the form where the non-Abelian nature of the radiation is explicitly manifest as a commutation of the color charges

$$J_3 = \tilde{g}^3 \sum_{\mathcal{P}_3} [T_{a_1},[T_{a_2},[T_{a_3},T_{a_q}]]] \frac{\langle pq\rangle}{\langle p1\rangle\langle 12\rangle\langle 23\rangle\langle 3q\rangle}. \tag{7.42}$$

7.4 Conjectured current

Based on the 1,2,3-gluon emission results, in this section, we are going to conjecture the analytical expression for the multiple emissions current induced from a color flip interaction. In the previous calculations, for $n = 1,2,3$, we found that the

sum over the different configurations (sum over m) are absorbed into a new color factor, denoted by C_n. And the commutator structure of this color factor makes the non-Abelian nature of the radiation manifest. On the other hand the respective kinematics from these calculations (7.9, 7.18, 7.42) present also a pattern,

$$\begin{aligned} C_1(1) &= [T_{a_1}, T_{a_q}] \\ C_2(1,2) &= [T_{a_1}, [T_{a_2}, T_{a_q}]] \\ C_3(1,2,3) &= [T_{a_1}, [T_{a_2}, [T_{a_3}, T_{a_q}]]]. \end{aligned} \tag{7.43}$$

We therefore conjecture the multiple emission current J_n induced from a color flip to be

$$J_n = \tilde{g}^n \sum_{\mathcal{P}_n} [T_{a_1}, [T_{a_2}, [\cdots, [T_{a_n}, T_{a_q}] \cdots]]] \frac{\langle pq \rangle}{\langle p1 \rangle \langle 12 \rangle \cdots \langle nq \rangle}. \tag{7.44}$$

This conjectured current is then equivalent to the current that we introduced in Eq. (7.8). The claim is that the nontrivial sum over the different configurations in Eq. (7.8) is absorbed into the color factor that makes the non-Abelian structure manifest,

$$C_n(1, \ldots, n) = [T_{a_1}, [T_{a_2}, [\cdots, [T_{a_n}, T_{a_q}] \cdots]]]. \tag{7.45}$$

The Eq. (7.44) will be easy to manipulate compared to Eq. (7.8), since it is very natural to decompose Eq. (7.44) into the various irreducible representation of the symmetric group in order to simplify the squaring of the current without the configuration over m in Eq. (7.8). Therefore we need to prove that Eq. (7.44) is correct. The main obstacle is that, we are not be able to perform a brute force calculation going from Eq. (7.8) to derive Eq. (7.44). Instead, we plan to project the two currents into the irreducible representation of the gluon-permutation group. Then we will complete the proof for the fully symmetric and fully antisymmetric cases by comparing the different irreducible projections of the two currents.

Similarly with the three induced gluon emissions in Eq. (7.26), the multiple gluon emission can be expanded as

$$J_n = \frac{1}{n!} C_n^s J_{n,n}^s + \frac{1}{n!} C_n^a J_{n,n}^a + \text{Mixed-Sym}. \tag{7.46}$$

In this section, the mixed symmetry case will not be discussed due to the following technical reason. The different irreducible representations of the permutation group

$\mathcal{P}_3$ can be represented in terms of the Young diagrams; see e.g. [94]. In terms of Young diagrams the mixed symmetry for $\mathcal{P}_3$ is represented with  . However for a general group $\mathcal{P}_n$, the mixed symmetry is a collection of more than one irreducible representation; for example for $n = 4$ the mixed symmetry is a collection of three irreducible representations

$$\text{Mixed-Sym} : \left\{ \text{  } \right\}. \tag{7.47}$$

This higher number of representations introduces significantly more complexity for the mixed symmetry computation.

7.4.1 Symmetric case

Let us start with the purely symmetric case, where both kinematic and color factors are individually invariant under gluon permutations. As in Eq. (7.15) and Eq. (7.25) the color factor C_n^s can be expanded as a linear combination of $T_{n,m}$ by an explicit expansion of the commutation structure in Eq. (7.45). Let $U_{n,m}^s$ be the coefficient associated with the factor $T_{n,m}^s$ in this expansion, where the upper index s will stand for symmetric, n for the number of emissions and m to be the expansion index. Therefore

$$C_n^s(1,\dots,n) = \sum_{m=0}^{n} U_{n,m}^s T_{n,m}^s(1,\dots,n). \tag{7.48}$$

Here $U_{n,m}^s$ is only defined for $0 \leq m \leq n$. In order to determine the expression of $U_{n,m}^s$ it is useful to find a relation between C_n^s and C_{n-1}^s then use Eq. (7.48) on both C_n^s and C_{n-1}^s to generate a recursion for $U_{n,m}^s$.

Starting with Eq. (7.45), we can see that the color factor C_n can be expressed in terms of C_{n-1} as

$$C_n(1,2,\dots,n) = [T_1, C_{n-1}(2,\dots,n)]. \tag{7.49}$$

The next step is to symmetrize both sides of this relation. In the following expression, $C_{n-1}(1,\dots,\hat{\imath},\dots,n)$ represent the color factor related to $n-1$ emissions, in which a hat denotes the omission of that element since C_{n-1} has one less element compare to C_n,

$$C_n^s(1,\dots,n) = \sum_{S_n} [T_1, C_{n-1}(2,\dots,n)] = \sum_{i=1}^{n} [T_i, C_{n-1}^s(1,\dots,\hat{\imath},\dots,n)]. \tag{7.50}$$

Then we expand the C^s_{n-1} in terms of $T^s_{n-1,m}$ as in Eq. (7.48). Recall that the second index in $T_{n,m}$ represents the number of color charges to the left of T_{a_q}. Therefore multiplying $T_{n-1,m}(2,\ldots,n)$ on the left by the color charge T_1 or on the right by the same color charge T_1 will give respectively $T_{n,m+1}(1,2,\ldots,n)$ or $T_{n,m}(2,\ldots,n,1)$, since

$$\begin{aligned} T_{a_1}T_{n-1,m}(2,\ldots,n) &= T_{a_1}\underbrace{T_{a_2}\cdots T_{a_{m+1}}}_{m \text{ terms}}T_{a_q}\cdots T_{a_n} = T_{n,m+1}(1,2,\ldots,n) \\ T_{n-1,m}(2,\ldots,n)T_{a_1} &= \underbrace{T_{a_2}\cdots T_{a_{m+1}}}_{m \text{ terms}}T_{a_q}\cdots T_{a_n}T_{a_1} = T_{n,m}(2,\ldots,n,1), \end{aligned} \tag{7.51}$$

Eq. (7.51) leads to the following:

$$\begin{array}{lccccccccc} 0 & \longrightarrow & & & & & & & & 1 \\ 1 & & & & & & -1 & & 1 & \\ 2 & \longrightarrow & & 1 & & -2 & & 1 & & \\ 3 & & -1 & & 3 & & -3 & & 1 & \\ 4 & \longrightarrow & 1 & & -4 & & 6 & & -4 & & 1 \end{array}$$

Figure 7.3: Integer sequences generated from $U^s_{n,m}$.

$$\begin{aligned} C^s_n(1,\ldots,n) &= \sum_{m=0}^{n-1} U^s_{n-1,m}\sum_{i=1}^{n}[T_i, T^s_{n-1,m}(\ldots,\hat{\imath},\ldots)] \\ &= \sum_{m=0}^{n-1} U^s_{n-1,m}(T^s_{n,m+1}(1,\ldots,n) - T^s_{n,m}(1,\ldots,n)) \\ &= \sum_{m=0}^{n}(U^s_{n-1,m-1} - U^s_{n-1,m})T^s_{n,m}. \end{aligned} \tag{7.52}$$

The last line is just an index rearrangement that allows us to compare the coefficients of $T^s_{n,m}$ with $U^a_{n,m}$ in Eq. (7.48), which lead to the following recursion relation

$$U^s_{n,m} = U^s_{n-1,m-1} - U^s_{n-1,m}. \tag{7.53}$$

This recursion is similar to the Pascal's recursion with a negative sign difference, see Fig. 7.3 for a visualization of the integer sequences generated by Eq. (7.53). Based on Pascal's sequence we can see that $U^s_{n,m}$ will be proportional to the binomial, and given by

$$U^s_{n,m} = U^s_{0,0}\frac{(-1)^{n-m}n!}{(n-m)!m!}. \tag{7.54}$$

The initial condition, $U^s_{0,0}$, is fixed by the zero gluon emission case, which requires that

$$U^s_{0,0} = 1. \tag{7.55}$$

Therefore

$$U^s_{n,m} = (-1)^{n-m}\frac{n!}{(n-m)!m!}. \tag{7.56}$$

One can check that Eq. (7.56) correctly reproduces the 1, 2 and 3 gluon emission results in the symmetric configuration

$$\begin{cases} C^s_1 = -1T^s_{1,0}(1)+1T^s_{1,1}(1), \\ C^s_2 = 1T^s_{2,0}(1,2)-2T^s_{2,1}(1,2)+1T^s_{2,2}(1,2), \\ C^s_3 = -1T^s_{3,0}(1,2,3)+3T^s_{3,1}(1,2,3)-3T^s_{3,2}(1,2,3)+1T^s_{3,3}(1,2,3). \end{cases} \tag{7.57}$$

Before we show the comparison with the symmetric projection of the results from MHV Eq. (7.8), thereby proving from first principles that our conjectured current is necessarily correct for symmetric n gluon emission, let us examine the antisymmetric projection of the conjectured current.

7.4.2 Antisymmetric case

For the antisymmetric case, we will perform the exact same steps as in the symmetric case. First consider the explicit expansion of the commutation of C_n in its antisymmetric projection

$$C^a_n(1,\dots,n) = \sum_{m=0}^{n} U^a_{n,m}T^a_{n,m}(1,\dots,n), \tag{7.58}$$

where the coefficients $U^a_{n,m}$ are defined for $0 \leq m \leq n$. Then we recall the relation Eq. (7.49) which connects C_n to C_{n-1}, then we antisymmetrize this relation and expand them as in Eq. (7.58)

$$C^a_n(1,\dots,n) = \sum_{m=0}^{n}(U^a_{n-1,m-1} + (-1)^n U^a_{n-1,m})T^a_{n,m}(1,\dots,n). \tag{7.59}$$

This is similar to the symmetric case with the exception of the $(-1)^n$. Since $T^a_{n,m}$ is antisymmetric, then any swap of two variables will cost an extra negative sign.

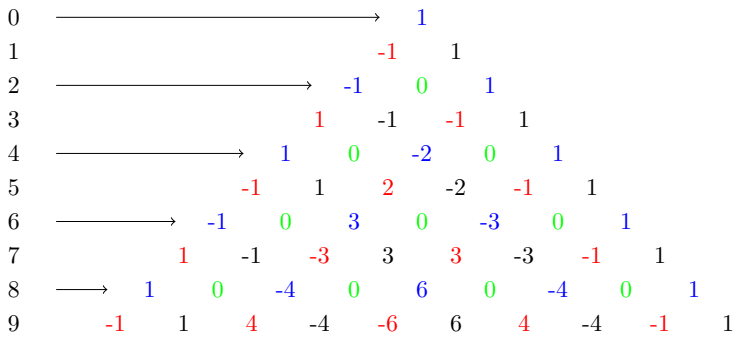

Figure 7.4: Integer sequences generated from $U^a_{n,m}$ for $n = \{0, \dots 9\}$.

Then the coefficient factors for the antisymmetric expansion are generated from a recursion,

$$U^a_{n,m} = U^a_{n-1,m-1} + (-1)^n U^a_{n-1,m}. \tag{7.60}$$

Solving this recursion is not as simple as the symmetric case, so in order to simplify the recursion into something we know how to solve let us look at the integer sequences generated from the recursion in Fig. 7.4. In this triangle we can find patterns for some partial sequences which will guide us on how to obtain a generic expression for $U^a_{n,m}$.

First, the sequence in blue spans the set of numbers with both n and m even. This sequence is the same sequence we had for the symmetric case; see Fig. 7.3. Second, the sequence in black reproduces the exact same sequence as the blue one but for n and m both odd integers. Third, the one in red in which n is odd and m is even, is the same sequence that solved the symmetric recursion but with a -1 for initial condition. And finally the fourth sequence in green is those with n even and m odd which are all zero.

Based on these patterns we will split the recursion in four regions depending on the parity of n and m:

- $(even,\ even)$: $\quad U^{\mathrm{a}}_{2k,2l} = U^{\mathrm{a}}_{2k-1,2l-1} + U^{\mathrm{a}}_{2k-1,2l}.$ (7.61)
- $(even,\ odd)$: $\quad U^{\mathrm{a}}_{2k,2l+1} = U^{\mathrm{a}}_{2k-1,2l} + U^{\mathrm{a}}_{2k-1,2l+1}.$ (7.62)
- $(odd,\ even)$: $\quad U^{\mathrm{a}}_{2k+1,2l} = U^{\mathrm{a}}_{2k,2l-1} - U^{\mathrm{a}}_{2k,2l}.$ (7.63)
- $(odd,\ odd)$: $\quad U^{\mathrm{a}}_{2k+1,2l+1} = U^{\mathrm{a}}_{2k,2l} - U^{\mathrm{a}}_{2k,2l+1}.$ (7.64)

In order to obtain an analytical expression we can play with these four recursions. Considering Eq. (7.61) we can expand the (odd, even) and (odd, odd) terms on its right hand side respectively using Eq. (7.63) and Eq. (7.64) and end up with a familiar recursion

$$U^{\mathrm{a}}_{2k,2l} = U^{\mathrm{a}}_{2(k-1),2(l-1)} - U^{\mathrm{a}}_{2(k-1),2l}. \tag{7.65}$$

This recursion relates the set of (even, even) to other (even, even) and it is analogous to Eq. (7.53) with a solution $U^{\mathrm{a}}_{2k,2l} = U^{\mathrm{s}}_{k,l}$. Then we do the same for the remaining recursions by considering the initial conditions: $U^{\mathrm{a}}_{0,0} = U^{\mathrm{a}}_{1,1} = -U^{\mathrm{a}}_{1,0} = 1$ and $U^{\mathrm{a}}_{2,1} = 0$. We therefore have the following general solutions,

$$\begin{aligned} U^{\mathrm{a}}_{2k,2l} &= (-1)^{l-k}\binom{k}{l}, & U^{\mathrm{a}}_{2k+1,2l+1} &= (-1)^{l-k}\binom{k}{l}, \\ U^{\mathrm{a}}_{2k+1,2l} &= (-1)^{l-k+1}\binom{k}{l}, & U^{\mathrm{a}}_{2k,2l+1} &= 0. \end{aligned} \tag{7.66}$$

7.5 Proof for the symmetric and antisymmetric cases

Now that the symmetric and antisymmetric projections of our conjectured current have been explored. Then the next step is to prove by comparison that the brute force MHV calculated current in Eq. (7.8) is the same as the conjectured. We will do so by decomposing the brute force calculated MHV current into symmetric and antisymmetric projections, then we will transform these to have the same structure as the conjectured currents and extract the spectrum coefficient $\hat{U}^{s/a}_{n,m}$ equivalent to those computed from the previous section.

Our goal is then reduced to a computation to show that the spectra $\hat{U}^{s/a}_{n,m}$ extracted from the calculated current are equal to the $U^{s/a}_{n,m}$ obtained from the conjectured current. In this section, we will start with the emission current expressed in Eq. (7.11), then similarly as for the conjectured in Eq. (7.46) we decompose the

current into the irreducible representation of $\mathcal{P}_n$,

$$\begin{aligned} J_n &= \sum_{m=0}^{n} \sum_{\mathcal{P}_n} T_{n,m}(1,\dots,n) J_{n,m}(1,\dots,n) \\ &= \frac{1}{n!} \sum_{m=0}^{n} T^s_{n,m} J^s_{n,m} + \frac{1}{n!} \sum_{m=0}^{n} T^a_{n,m} J^a_{n,m} + \text{Mixed-Sym} \\ &= \frac{1}{n!} J^s_n + \frac{1}{n!} J^a_n + \text{Mixed-Sym}. \end{aligned} \tag{7.67}$$

7.5.1 Symmetric case

Let us first consider the symmetric piece of Eq. (7.67). The goal is to compare this symmetric piece with the symmetric projection of the conjectured current Eq. (7.44). In order to have a comparable structure it is useful to factorize $J^s_{n,n}$,

$$\begin{aligned} J^s_n &= \frac{1}{n!} \sum_{m=0}^{n} T^s_{n,m}(1,\dots,n) J^s_{n,m}(1,\dots,n) \\ &= \frac{1}{n!} J^s_{n,n}(1,\dots,n) \sum_{m=0}^{n} \frac{J^s_{n,m}(1,\dots,n)}{J^s_{n,n}(1,\dots,n)} T^s_{n,m}(1,\dots,n). \end{aligned} \tag{7.68}$$

Now the relation above is of type $\hat{C}^s_n J^s_{n,n}$ where the $\hat{C}^s_n$ play the role of the symmetrized color factor in Eq. (7.48). We can then define the spectrum coefficient $\widehat{U}^s_{n,m}$, equivalent to the conjectured spectrum $U^s_{n,m}$, such that

$$\widehat{U}^s_{n,m}(1,\dots,n) = \frac{J^s_{n,m}(1,\dots,n)}{J^s_{n,n}(1,\dots,n)}. \tag{7.69}$$

Here, the coefficients $\widehat{U}^s_{n,m}$ are not necessarily constant numbers. However, we will see that the structure of the symmetric piece leads to a fascinating result in which the ratio $\widehat{U}^s_{n,m}(1,\dots,n)$ is nothing more than a combinatorial way to order the n radiated gluons. To show this, let us first introduce some mathematical notation:

- S_n: is the set of n integers from 1 to n; usually written as $S_n = \{1,\dots,n\}$.
- $S_{n,m}$: is a subset of S_n composed by m integers , $S_{n,m} \subset S_n$ with $m \leq n$.
- $\overline{S}_{n,m}$: is the complement of $S_{n,m}$ defined as $S_{n,m} \cup \overline{S}_{n,m} = S_n$.
- $\text{split}_{n,m}$: is the set of different ways to factorise S_n into $S_{n,m} \cup \overline{S}_{n,m}$.

- $\mathcal{P}_{[\mathcal{A}]}$: represents the permutation group that act on the element of the set $\mathcal{A}$.

We start from the first principle where we symmetrize the $J_{n,m}$ defined in Eq. (7.10) and try to sum over the full permutation $\mathcal{P}_{[S_n]} = \mathcal{P}_n$. The partial current $J_{n,m}$ is a product of two functions that depends respectively on two disjoint sets of gluons. We have m gluons emitted before and $(n-m)$ emitted after the absorption of the gluon that stimulates the radiation from the color flip.

Therefore, we can split the S_n into $S_{n,m}$ and its complement $\overline{S}_{n,m}$ in which we have to sum over all possible way to factorize S_n,

$$\begin{aligned} J^s_{n,m}(1,\dots,n) &= \tilde{g}^n \sum_{\mathcal{P}_{[S_n]}} \frac{\langle pq\rangle}{\langle p1\rangle\langle 12\rangle\cdots\langle mq\rangle} \frac{\langle qp\rangle}{\langle q,m{+}1\rangle\cdots\langle n{-}1,n\rangle\langle np\rangle} \\ &= \tilde{g}^n \sum_{\text{split}_{n,m}} \left(\sum_{\mathcal{P}_{[S_{n,m}]}} \frac{\langle pq\rangle}{\langle p1\rangle\cdots\langle mq\rangle} \right) \left(\sum_{\mathcal{P}_{[\overline{S}_{n,m}]}} \frac{\langle qp\rangle}{\langle q,m{+}1\rangle\cdots\langle np\rangle} \right). \end{aligned} \tag{7.70}$$

Then we recall the photon decoupling relation in Eq. (5.11) on these two partial symmetrized quantities in brackets. The photon decouplings will combine the terms in brackets into a single product over the full set S_n,

$$\begin{aligned} J^s_{n,m}(1,\dots,n) &= \tilde{g}^n \sum_{\text{split}_{n,m}} \left(\prod_{I\in S_{n,m}} \frac{\langle pq\rangle}{\langle pI\rangle\langle Iq\rangle} \right) \left(\prod_{J\in\overline{S}_{n,m}} \frac{\langle qp\rangle}{\langle qJ\rangle\langle Jp\rangle} \right) \\ &= \tilde{g}^n (-1)^{n-m} \sum_{\text{split}_{n,m}} \prod_{I\in S_n} \frac{\langle pq\rangle}{\langle pI\rangle\langle Iq\rangle} \\ &= (-1)^{n-m} \frac{n!}{(n-m)!n!} \tilde{g}^n \prod_{I\in S_n} \frac{\langle pq\rangle}{\langle pI\rangle\langle Iq\rangle} \end{aligned} \tag{7.71}$$

In the first equality of the Eq. (7.71), the two terms in brackets come respectively from the decoupling relation from the terms in brackets of the two sums in the previous equation. In the second equality the $(-1)^{n-m}$ factor is due to the antisymmetric property of the angle brackets when swapping terms in order to make it in a single products. This single product is independent from the way we split S_n. Therefore, the sum will give the number of way to split S_n into two, that is to say number of ways to have m gluons emitted before the color flip is

$$\widehat{U}^s_{n,m}(1,\dots,n) = \frac{J^s_{n,m}(1,\dots,n)}{J^s_{n,n}(1,\dots,n)} = (-1)^{n-m} \frac{n!}{(n-m)!n!}. \tag{7.72}$$

This result is amazing: the ratio between the two non trivial complex functions is reduced to a simple combinatorial factor and coincides exactly with the value of the one from the conjectured, $U^s_{n,m}$ in Eq. (7.56).

7.5.2 Antisymmetric case

This section is very similar to the symmetric case. We consider the antisymmetric projection of the current computed from the MHV calculation and compare it with the antisymmetric term of the conjectured current in Eq. (7.46). We first factorize $J^a_{n,n}$ from Eq. (7.67) in order the reproduce the structure of the antisymmetric piece in the conjectured current, then define the spectrum $\widehat{U}^a_{n,m}$ the same way as for the symmetric case,

$$J^a_n = \frac{1}{n!} J^a_{n,n}(1,\dots,n) \sum_{m=0}^{n} \frac{J^a_{n,m}(1,\dots,n)}{J^a_{n,n}(1,\dots,n)} T^a_{n,m}(1,\dots,n). \tag{7.73}$$

The spectrum associated with the antisymmetric case is then the ratio between two antisymmetric piece functions that depend on the different momenta of the emitted gluons; we have

$$\widehat{U}^a_{n,m}(1,\dots,n) \equiv \frac{J^a_{n,m}(1,\dots,n)}{J^a_{n,n}(1,\dots,n)}. \tag{7.74}$$

The difficulty in the antisymmetric case is that we do not have a relation similar to the photon decoupling, which allowed us to interpret the result of the symmetric case as a combinatorial factor. What we can do is to study the different properties of $\widehat{U}^a_{n,m}$ and then show that it is a solution of the antisymmetric recursion in Eq. (7.60). Here are some properties that we need to consider:

- The currents $J^a_{n,m}$ and $J^a_{n,n}$ are both antisymmetric. Thus the ratio is symmetric. Hence under an odd permutation the negative sign from the numerator cancels out with one from the denominator

$$\frac{1}{n!} \sum_{S_n} \widehat{U}^a_{n,m}(1,\dots,n) = \widehat{U}^a_{n,m}(1,\dots,n). \tag{7.75}$$

- Similarly both the numerator and the denominator scale the same way under momentum rescaling. Therefore for any complex number z we have

$$\widehat{U}^a_{n,m}(1,\dots,zi,\dots,n) = \widehat{U}^a_{n,m}(1,\dots,i,\dots,n). \tag{7.76}$$

Thus $\hat{U}^a_{n,m}$ is a scale invariant quantity.

One way to see that $\widehat{U}^a_{n,m}$ is a solution of the recursion relation associated to the antisymmetric is to find a relation between the coefficients $\widehat{U}^a_{n,m}$ and those from the lower number of emission coefficients $\widehat{U}^a_{n-1,m}$. To do so, we will use either soft or collinear limits which will suppress the dependence of one momentum from $\widehat{U}^a_{n,m}$. It can not be done with the soft limit since $\widehat{U}^a_{n,m}$ is scale invariant, and leave us no choice than using the collinear limits.

We consider the situation where the n-th gluon is not resolve from the parent momenta, that is to say k_n is collinear to p. In this situation the currents $J^a_{n,m}$ and $J^a_{n,n}$ will diverge since the bracket $\langle pn\rangle$ will tend to zero as the p and k_n tend to be collinear. However, we are going to show that such divergences cancel out in the ratio that defines $\widehat{U}^a_{n,m}$.

Let us start by considering $J^a_{n,m}$, we isolate the dependences of the momentum k_n by explicitly expand the different permutation of n in the analytic expression of $J^a_{n,m}$. Considering the fact that a odd permutation will cost a negative sign for an antisymmetrized quantity, therefore

$$\begin{aligned}
J^a_{n,m} &= \sum_{\mathcal{P}_n} \epsilon_{1,2,\ldots,n} \frac{\langle pq\rangle}{\langle p1\rangle\langle 12\rangle\cdots\langle mq\rangle} \frac{\langle qp\rangle}{\langle q,m{+}1\rangle\cdots\langle n{-}1,n\rangle\langle np\rangle} \\
&= \sum_{\mathcal{P}_{n-1}} \epsilon_{1,2,\ldots,n-1} \frac{\langle pq\rangle}{\langle p1\rangle\cdots\langle mq\rangle} \frac{\langle qp\rangle}{\langle q,m{+}1\rangle\cdots\langle n{-}1\,p\rangle} \left(\frac{\langle n{-}1\ \mathrm{p}\rangle}{\langle n{-}1\,n\rangle\langle np\rangle} + \cdots \right) \\
&+ \sum_{\mathcal{P}_{n-1}} \epsilon_{1,2,\ldots,n-1} \frac{\langle pq\rangle}{\langle p1\rangle\cdots\langle m{-}1\,q\rangle} \frac{\langle qp\rangle}{\langle q,m\rangle\cdots\langle n{-}1\,p\rangle} \left((-1)^{n-1} \frac{\langle p1\rangle}{\langle pn\rangle\langle n1\rangle} + \cdots \right)
\end{aligned} \tag{7.77}$$

$\epsilon_{1,2,\ldots,n}$ is the antisymmetric Levi-Civita symbol. Then from this relation above, under the limit $\langle pn\rangle$ goes to zero, we have $\langle *n\rangle \simeq \langle *p\rangle$ and we only keep the leading

singular terms,

$$
\begin{aligned}
J^a_{n,m} &= \sum_{\mathcal{P}_{n-1}} \epsilon_{1,2,\dots,n-1} \frac{\langle pq\rangle}{\langle p1\rangle\cdots\langle mq\rangle} \frac{\langle qp\rangle}{\langle q,m{+}1\rangle\cdots\langle n{-}1\,p\rangle} \frac{1}{\langle np\rangle} \\
&\quad + \sum_{\mathcal{P}_{n-1}} \epsilon_{1,2,\dots,n-1} \frac{\langle pq\rangle}{\langle p1\rangle\cdots\langle m{-}1\,q\rangle} \frac{\langle qp\rangle}{\langle q,m\rangle\cdots\langle n{-}1\,p\rangle} \frac{(-1)^{n-1}}{\langle pn\rangle} + \mathcal{O}(\langle np\rangle^0) \\
&\simeq \frac{1}{\langle np\rangle} \sum_{\mathcal{P}_{n-1}} \epsilon_{1,2,\dots,n-1} J_{n-1,m}(1,\dots,n-1) \\
&\qquad\qquad + \frac{(-1)^n}{\langle np\rangle} \sum_{\mathcal{P}_{n-1}} \epsilon_{1,2,\dots,n-1} J_{n-1,m-1}(1,\dots,n-1) \\
&\simeq \frac{(-1)^n}{\langle np\rangle} \Big((-1)^n J^a_{n-1,m}(1,\dots,n-1) + J^a_{n-1,m-1}(1,\dots,n-1) \Big).
\end{aligned}
\tag{7.78}
$$

Similarly for $J^a_{n,n}$, we have

$$
J^a_{n,n} = \sum_{\mathcal{P}_n} \epsilon_{1,2,\dots,n} \frac{\langle pq\rangle}{\langle p1\rangle\langle 12\rangle\cdots\langle nq\rangle} \simeq \frac{(-1)^n}{\langle np\rangle} J^a_{n-1,n-1}(1,\dots,n-1). \tag{7.79}
$$

From these two limit we can see how the coefficients $\widehat{U}^a_{n,m}$ will split into a linear combination of the lower emissions coefficients. The same thing will be produced if we choose different momentum than k_n to be collinear to p, since $\widehat{U}^a_{n,m}$ is symmetric. However we know that we are in the limit where all the gluons are collinear to p which leads to

$$
\widehat{U}^a_{n,m} = \widehat{U}^a_{n-1,m-1} + (-1)^n \widehat{U}^a_{n-1,m}, \tag{7.80}
$$

With the initial condition of no radiation where $n = 0$ we have $\widehat{U}^a_{0,0} = 1$. Therefore $\widehat{U}^a_{n,m}$ solves the same recursion as the antisymmetric case of the conjecture with the same initial condition. We can conclude that the two spectra $\widehat{U}^a_{n,m}$ is equal to the spectrum $U^a_{n,m}$ derived from Eq. (7.44).

7.6 Summary

In this chapter we would like to understand the radiation of gluons induced from a color flip of quark. We first consider the most general case where a gluon provides enough of a kick to an on-shell quark to induce gluon radiations. Then we consider the fact where the quark interact relatively soft with the medium compare to its initial energy. Then show for one, two, and three gluon emissions that in this soft medium interaction will induced radiation that is purely non-Abelian, color flip.

We then conjectured the analytic radiation current for any number of gluon radiations induced from a color flip, in such a way that the non-Abelian nature of the radiation is manifest. Since we didn't find a way to go from the radiation current derived from the MHV calculation Eq. (7.8) to the conjectured current Eq. (7.44), we projected the two currents into the different irreducible representations of $\mathcal{P}_n$. We then showed that the symmetric and antisymmetric color factor spectra $\hat{U}^{s/a}_{n,m}$ from the MHV calculation are indeed equal to the spectra $U^{s/a}_{n,m}$ from the conjectured current, which constitutes a partial proof.

Through this work we only consider the contribution of the MHV configurations in which all the emitted gluons/photons have a positive helicity. We could have considered the $\overline{\text{MHV}}$ case where all the emitted gluons/photons have a negative helicity. In that case we will obtain the same results with the exception that the angle brackets will be swapped with square brackets.

8 Conclusions

Understanding radiation in quantum chromodynamics (QCD) is necessary to develop a better model for parton energy loss in quark-gluon plasma (QGP). The number of gluons radiated by a high-p_T parton in medium has been estimated to be about 3. This estimation, being not less or equal to 1, leads us to take into account the possibility for multiple gluon emission. Despite the non-Abelian nature of QCD, in which gluons self-interact, energy loss calculations often approximate the distribution of emitted gluons to be Poisson. In this thesis the main objective is to understand multiple gluon emissions beyond this Poisson approximation.

The main framework used in this thesis was the maximal helicity violating (MHV) techniques. In Chapters 2 and 3 the two main foundations of the techniques were reviewed. First, the color kinematic decomposition was introduced in Chapter 2, which reduces the complexity of QCD amplitudes. QCD amplitudes are factorized into a sum over $SU(N)$ generators and purely kinematic partial amplitudes. Second, the spinor helicity variables were introduced in Chapter 3, which lead to a remarkably simple formula for MHV amplitudes.

The MHV techniques makes the computation of any $2 \to 2$ scattering amplitude trivial. In particular, in Chapter 4 we computed the cross section for a quark anti-quark annihilation to two gluons. Having the MHV amplitudes formula in hand, Eq. (3.57), makes the MHV computation simple and clean. We then derived for the first time an efficient method for finding splitting function using MHV, where the task of the computation is to consider the contribution of all different helicity configurations.

The introduction of the photon decoupling in Eq. (4.22) allowed us to accommodate photons in our calculations. We used this decoupling in Chapter 5 to rederive the multiple photon emission current and showed for the first time using MHV in a rigorous way that photon emissions are indeed independent and distributed according to the Poisson distribution. We recovered the distribution derived in [58] by considering only the contribution of the MHV helicity configuration, in which only one photon has a negative helicity. The standard derivation assumes collinearity of the emissions in which the photon are emitted at a very small angle. However, the contribution of MHV helicity configuration alone reproduced this standard distribution for small angle radiation, which implies that the non-MHV contribution would contain information on the large angle radiations which are not considered in this thesis.

We then generalized the computation of the multiple photon emissions current into the first ever derivation of the amplitude for multiple gluon vacuum emissions from an off-shell quark. We showed that under strong angular ordering the multiple gluon radiation current can be reduced into the product of individual, independent single gluon emission currents.

In Chapter 6, we squared our amplitude for two gluon emissions to study two gluon correlations for the first time beyond the Poisson approximation using MHV. We explicitly derived the non-Abelian correction that leads to the correlation between the two emitted gluons. As a result the correlation is a scale invariant quantity and can be expressed only in terms of the difference in angle $\Delta\phi$ and rapidity $\Delta\eta$ between the two emitted gluons. The results were then compared to the two particle correlation measured by ALICE from p-Pb collisions. The comparison shows a good qualitative agreement in which we see a tight correlation in angle and broad correlation in rapidity.

In Chapter 7 we studied for the first time the case of induced n-guon radiations at the amplitude level. We considered the case of an s-channel interaction between a high-p_T quark and the medium, where a gluon is absorbed and leads to multiple radiation. We computed the multiple radiation induced from the absorption of a gluon that provides enough of a kick to the on-shell quark to induce gluon radiations.

We showed that the quark will still radiate in the case where there is no momentum kick, which is induced by only a change in color. We explicitly computed the emission current for one, two, and three gluon emissions and then conjectured the current for a generic number of emissions. We proved our conjecture for the case where the amplitude is symmetric under interchange of emitted gluons and for the case where the amplitudes are antisymmetric under interchange of emitted gluons by comparing the symmetric and antisymmetric projections of the conjectured current with the MHV calculated current.

In future work, it is important to extend this partial proof of the color flip calculation into the mixed symmetry case. In Section 7.3, we already introduced the operator $\hat{Q}_m$ that connects the different kinematics $J_{3,m}$ into each other. This operator was constructed in order to simplify the calculation in the mixed symmetry case for the three gluon emission case. Finding a way to generalize this kind of operator into $\hat{Q}_m^{(n)}$ is the first step in our quest to complete the proof for the veracity of the conjectured current.

In this thesis we characterized the MHV radiation induced from a pure kinematic off-shellness of a high-p_T quark in Chapter 5, and separately the radiation induced from a purely color flip of an high-p_T quark in Chapter 7. Another important avenue of future research is then to extend our MHV calculations to gluon radiation induced from a scattering that produces both a kinematic virtuality and a color change at the same time to a high-p_T parton. Such understanding will provide a more realistic picture of induced radiation with which the in-medium particle correlations could be computed.

The MHV calculation is very powerful for dealing with multiple radiation in momentum space. However, to understanding radiation induced from multiple scattering, it is important to think about MHV in position space. In position space we can extract information on the mean free path between successive collisions, and on the formation time of the gluon radiation. The inverse Fourier transform is the standard method to go from momentum to position dependence. MHV amplitudes are not expressed in terms four momentum p_μ but instead in terms of spinor variables $(\lambda, \widetilde{\lambda})$. The inverse Fourier transform of spinor variables has been already studied

and is known as "twistor variables"; see [95]. Many open questions arise: How to describe the notion of mean free path and formation time in terms of twistor variables? Will such description lead to a simpler formulation of the radiation? Can we have a better understanding of the LPM effect in terms of twistor variables?

In this work, we limited our calculation to the use of the MHV configuration only; in other words we only considered the case where the helicities of the emitted gluons are all the same. This restriction is motivated by the fact that the contribution of the different helicity configurations, the NMHV, NNMHV, etc., are suppressed at small angles $\mathcal{O}(k_\perp/E)$. However, some research suggests that wide angle radiations are important despite the collinearity assumption; see [97]. Therefore, it is likely important to explore the contribution of gluon radiation beyond MHV; the corresponding amplitudes are called N^{k}MHV amplitudes. Such a study will provide us with a better understanding of the large angle radiation and three jet events using the spinor helicity formalism.

Lastly, here are the two most pressing issues for the MHV techniques that we think have the most potential impact on energy loss phenomenology: to include the t-channel gluon exchange with medium quasi-particles and to include mass for heavy quark jets. One can isolate the t-channel exchange in MHV by computing the scattering of two different quark flavors. Such a trick might simplify further the MHV calculation of in-medium, multiple gluon energy loss. Including mass in MHV calculations now appears possible through very recent advances [98, 99].

This thesis showed that MHV techniques present a very powerful tool for studying the structure of multiple gluon radiation in massless pQCD and has a promising future for further understanding of LHC physics.

Bibliography

[1] M. Planck, "On the Law of Distribution of Energy in the Normal Spectrum," Annalen Phys. **4**, 553 (1901). 1

[2] A. Einstein, "On the electrodynamics of moving bodies," Annalen Phys. **17**, 891 (1905) [Annalen Phys. **14**, 194 (2005)]. doi:10.1002/andp.200590006. 1

[3] S. Weinberg, "The Quantum theory of fields. Vol. 1: Foundations," (1995). 1

[4] R. P. Feynman, "Mathematical formulation of the quantum theory of electromagnetic interaction," Phys. Rev. **80**, 440 (1950). doi:10.1103/PhysRev.80.440. 1

[5] J. S. Schwinger, "On Quantum electrodynamics and the magnetic moment of the electron," Phys. Rev. **73**, 416 (1948). doi:10.1103/PhysRev.73.416. 1

[6] M. Gell-Mann and M. Levy, "The axial vector current in beta decay," Nuovo Cim. **16**, 705 (1960). doi:10.1007/BF02859738. 1

[7] S. Weinberg, "A Model of Leptons," Phys. Rev. Lett. **19**, 1264 (1967). doi:10.1103/PhysRevLett.19.1264. 1

[8] W. J. Marciano and H. Pagels, "Quantum Chromodynamics: A Review," Phys. Rept. **36**, 137 (1978). doi:10.1016/0370-1573(78)90208-9. 2

[9] J. Beringer *et al.* [Particle Data Group], "Review of Particle Physics (RPP)," Phys. Rev. D **86**, 010001 (2012). doi:10.1103/PhysRevD.86.010001. 2

[10] S. Chatrchyan *et al.* [CMS Collaboration], "Observation of a new boson at a mass of 125 GeV with the CMS experiment at the LHC," Phys. Lett. B **716**, 30 (2012) doi:10.1016/j.physletb.2012.08.021 [arXiv:1207.7235 [hep-ex]]. 2

[11] G. Aad *et al.* [ATLAS Collaboration], "Observation of a new particle in the search for the Standard Model Higgs boson with the ATLAS detector at the LHC," Phys. Lett. B **716**, 1 (2012) doi:10.1016/j.physletb.2012.08.020 [arXiv:1207.7214 [hep-ex]]. 2

[12] J. Chadwick, "Possible Existence of a Neutron," Nature **129**, 312 (1932). doi:10.1038/129312a0. 2

[13] H. Yukawa, "On the Interaction of Elementary Particles I," Proc. Phys. Math. Soc. Jap. **17**, 48 (1935) [Prog. Theor. Phys. Suppl. **1**, 1]. doi:10.1143/PTPS.1.1. 2

[14] C. M. G. Lattes, H. Muirhead, G. P. S. Occhialini and C. F. Powell, "Processes Involving Charged Mesons," Nature **159**, 694 (1947). doi:10.1038/159694a0. 2

[15] C. M. G. Lattes, G. P. S. Occhialini and C. F. Powell, "Observations on the Tracks of Slow Mesons in Photographic Emulsions. 2," Nature **160**, 486 (1947). doi:10.1038/160486a0. 2

[16] G. D. Rochester and C. C. Butler, "Evidence for the Existence of New Unstable Elementary Particles," Nature **160**, 855 (1947). doi:10.1038/160855a0. 2

[17] M. Gell-Mann, "Isotopic Spin and New Unstable Particles," Phys. Rev. **92**, 833 (1953). doi:10.1103/PhysRev.92.833. 2

[18] T. Nakano and K. Nishijima, "Charge Independence for V-particles," Prog. Theor. Phys. **10**, 581 (1953). doi:10.1143/PTP.10.581. 2

[19] M. Gell-Mann, "The Eightfold Way: A Theory of strong interaction symmetry," CTSL-20, TID-12608. 2

[20] Y. Ne'eman, "Derivation of strong interactions from a gauge invariance," Nucl. Phys. **26**, 222 (1961). doi:10.1016/0029-5582(61)90134-1. 2

[21] M. Gell-Mann and Y. Ne'eman, "Current-generated algebras," Annals Phys. **30**, 360 (1964). doi:10.1016/0003-4916(64)90122-8. 2

[22] M. Gell-Mann, "A Schematic Model of Baryons and Mesons," Phys. Lett. **8**, 214 (1964). doi:10.1016/S0031-9163(64)92001-3. 2

[23] G. Zweig, "An SU(3) model for strong interaction symmetry and its breaking. Version 1," (1964), CERN-TH-401. 2

[24] M. Y. Han and Y. Nambu, "Three Triplet Model with Double SU(3) Symmetry," Phys. Rev. **139**, B1006 (1965). doi:10.1103/PhysRev.139.B1006. 3

[25] Y. Miyamoto, Prog. Theor. Phys. Suppl. Extra number (1965), 187. 3

[26] H. Fritzsch, M. Gell-Mann and H. Leutwyler, "Advantages of the Color Octet Gluon Picture," Phys. Lett. **47B**, 365 (1973). doi:10.1016/0370-2693(73)90625-4 3

[27] D. P. Barber *et al.*, "Discovery of Three Jet Events and a Test of Quantum Chromodynamics at PETRA Energies," Phys. Rev. Lett. **43**, 830 (1979). doi:10.1103/PhysRevLett.43.830. 3

[28] J. R. Ellis and I. Karliner, "Measuring the Spin of the Gluon in e+ e- Annihilation," Nucl. Phys. B **148**, 141 (1979). doi:10.1016/0550-3213(79)90019-1. 3

[29] K. G. Wilson, "Confinement of Quarks," Phys. Rev. D **10**, 2445 (1974). doi:10.1103/PhysRevD.10.2445. 4

[30] D. J. Gross and F. Wilczek, "Asymptotically Free Gauge Theories. 1," Phys. Rev. D **8**, 3633 (1973). doi:10.1103/PhysRevD.8.3633. 4

[31] H. D. Politzer, "Reliable Perturbative Results for Strong Interactions?," Phys. Rev. Lett. **30**, 1346 (1973). doi:10.1103/PhysRevLett.30.1346. 4

[32] S. Bethke, "Experimental tests of asymptotic freedom," Prog. Part. Nucl. Phys. **58**, 351 (2007) doi:10.1016/j.ppnp.2006.06.001 [hep-ex/0606035]. x, 3

[33] A. Bazavov *et al.*, "The chiral and deconfinement aspects of the QCD transition," Phys. Rev. D **85**, 054503 (2012) doi:10.1103/PhysRevD.85.054503 [arXiv:1111.1710 [hep-lat]]. 4, 5

[34] F. Karsch, E. Laermann and A. Peikert, "Quark mass and flavor dependence of the QCD phase transition," Nucl. Phys. B **605**, 579 (2001) doi:10.1016/S0550-3213(01)00200-0 [hep-lat/0012023]. 5

[35] A. Bazavov *et al.* [HotQCD Collaboration], "Equation of state in (2+1)-flavor QCD," Phys. Rev. D **90**, 094503 (2014) doi:10.1103/PhysRevD.90.094503 [arXiv:1407.6387[hep-lat]]. x, 5

[36] K. Adcox *et al.* [PHENIX Collaboration], "Formation of dense partonic matter in relativistic nucleus-nucleus collisions at RHIC: Experimental evaluation by the PHENIX collaboration," Nucl. Phys. A **757**, 184 (2005) doi:10.1016/j.nuclphysa.2005.03.086 [nucl-ex/0410003]. 5

[37] J. Adams *et al.* [STAR Collaboration], "Experimental and theoretical challenges in the search for the quark gluon plasma: The STAR Collaboration's critical assessment of the evidence from RHIC collisions," Nucl. Phys. A **757**, 102 (2005) doi:10.1016/j.nuclphysa.2005.03.085 [nucl-ex/0501009]. 5

[38] K. Aamodt *et al.* [ALICE Collaboration], "Elliptic flow of charged particles in Pb-Pb collisions at 2.76 TeV," Phys. Rev. Lett. **105**, 252302 (2010) doi:10.1103/PhysRevLett.105.252302 [arXiv:1011.3914 [nucl-ex]]. 5

[39] B. Abelev [ALICE Collaboration], "Strangeness with ALICE: from pp to Pb-Pb," arXiv:1209.3285 [nucl-ex]. x, 6

[40] S. Chatrchyan *et al.* [CMS Collaboration], "Measurement of the elliptic anisotropy of charged particles produced in PbPb collisions at $\sqrt{s}_{NN}$=2.76 TeV," Phys. Rev. C **87**, no. 1, 014902 (2013) doi:10.1103/PhysRevC.87.014902 [arXiv:1204.1409 [nucl-ex]]. x, 7

[41] G. Aad *et al.* [ATLAS Collaboration], "Observation of a Centrality-Dependent Dijet Asymmetry in Lead-Lead Collisions at $\sqrt{s_{NN}}$ = 2.77 TeV with

the ATLAS Detector at the LHC," Phys. Rev. Lett. **105**, 252303 (2010) doi:10.1103/PhysRevLett.105.252303 [arXiv:1011.6182 [hep-ex]]. 5

[42] B. Betz, "Jet Quenching in Heavy-Ion Collisions - The Transition Era from RHIC to LHC," Eur. Phys. J. A P **48**, 164 (2012) doi:10.1140/epja/i2012-12164-8 [arXiv:1211.5897 [nucl-th]]. x, 8

[43] M. Gyulassy and X. n. Wang, "Multiple collisions and induced gluon Bremsstrahlung in QCD," Nucl. Phys. B **420**, 583 (1994) doi:10.1016/0550-3213(94)90079-5 [nucl-th/9306003]. 9

[44] R. Baier, D. Schiff and B. G. Zakharov, "Energy loss in perturbative QCD," Ann. Rev. Nucl. Part. Sci. **50**, 37 (2000) doi:10.1146/annurev.nucl.50.1.37 [hep-ph/0002198]. 9

[45] M. Gyulassy, I. Vitev, X. N. Wang and B. W. Zhang, "Jet quenching and radiative energy loss in dense nuclear matter," In *Hwa, R.C. (ed.) et al.: Quark gluon plasma* 123-191 doi:10.1142/9789812795533-0003 [nucl-th/0302077]. 9

[46] E. Wang and X. N. Wang, "Jet tomography of dense and nuclear matter," Phys. Rev. Lett. **89**, 162301 (2002) doi:10.1103/PhysRevLett.89.162301 [hep-ph/0202105]. 9

[47] M. Gyulassy, P. Levai and I. Vitev, "Jet quenching in thin quark gluon plasmas. 1. Formalism," Nucl. Phys. B **571**, 197 (2000) doi:10.1016/S0550-3213(99)00713-0 [hep-ph/9907461]. 9, 10

[48] M. Gyulassy, P. Levai and I. Vitev, "NonAbelian energy loss at finite opacity," Phys. Rev. Lett. **85**, 5535 (2000) doi:10.1103/PhysRevLett.85.5535 [nucl-th/0005032]. 9, 10

[49] H. Song and U. W. Heinz, "Causal viscous hydrodynamics in 2+1 dimensions for relativistic heavy-ion collisions," Phys. Rev. C **77**, 064901 (2008) doi:10.1103/PhysRevC.77.064901 [arXiv:0712.3715 [nucl-th]]. 9

[50] W. A. Horowitz, "Testing pQCD and AdS/CFT Energy Loss at RHIC and LHC," AIP Conf. Proc. **1441**, 889 (2012) doi:10.1063/1.3700710 [arXiv:1108.5876 [hep-ph]]. 9

[51] P. Romatschke and U. Romatschke, "Viscosity Information from Relativistic Nuclear Collisions: How Perfect is the Fluid Observed at RHIC?," Phys. Rev. Lett. **99**, 172301 (2007) doi:10.1103/PhysRevLett.99.172301 [arXiv:0706.1522 [nucl-th]]. 9

[52] A. Buchel and J. T. Liu, "Universality of the shear viscosity in supergravity," Phys. Rev. Lett. **93**, 090602 (2004) doi:10.1103/PhysRevLett.93.090602 [hep-th/0311175]. 9

[53] A. Majumder and M. Van Leeuwen, "The Theory and Phenomenology of Perturbative QCD Based Jet Quenching," Prog. Part. Nucl. Phys. **66**, 41 (2011) doi:10.1016/j.ppnp.2010.09.001 [arXiv:1002.2206 [hep-ph]]. 9

[54] M. Djordjevic and M. Djordjevic, "Generalization of radiative jet energy loss to non-zero magnetic mass," Phys. Lett. B **709**, 229 (2012) doi:10.1016/j.physletb.2012.02.019 [arXiv:1105.4359 [nucl-th]]. 9

[55] S. Wicks, W. Horowitz, M. Djordjevic and M. Gyulassy, "Elastic, inelastic, and path length fluctuations in jet tomography," Nucl. Phys. A **784**, 426 (2007) doi:10.1016/j.nuclphysa.2006.12.048 [nucl-th/0512076]. 9

[56] N. Armesto, C. A. Salgado and U. A. Wiedemann, "Medium induced gluon radiation off massive quarks fills the dead cone," Phys. Rev. D **69**, 114003 (2004) doi:10.1103/PhysRevD.69.114003 [hep-ph/0312106]. 10

[57] M. Gyulassy, P. Levai and I. Vitev, "Jet tomography of Au+Au reactions including multigluon fluctuations," Phys. Lett. B **538**, 282 (2002) doi:10.1016/S0370-2693(02)01990-1 [nucl-th/0112071]. 10

[58] M. E. Peskin and D. V. Schroeder, "An Introduction to quantum field theory," 1995. 10, 15, 17, 42, 46, 50, 51, 95, 109, 110, 128

[59] N. Armesto *et al.*, "Comparison of Jet Quenching Formalisms for a Quark-Gluon Plasma 'Brick'," Phys. Rev. C **86**, 064904 (2012) doi:10.1103/PhysRevC.86.064904 [arXiv:1106.1106 [hep-ph]]. 10

[60] N. Armesto, L. Cunqueiro and C. A. Salgado, "Q-PYTHIA - a Monte Carlo implementation for jet quenching," arXiv:0906.0754 [hep-ph]. 10

[61] R. Baier, Y. L. Dokshitzer, A. H. Mueller and D. Schiff, "Quenching of hadron spectra in media," JHEP **0109**, 033 (2001) doi:10.1088/1126-6708/2001/09/033 [hep-ph/0106347]. 10

[62] P. B. Arnold, G. D. Moore and L. G. Yaffe, "Transport coefficients in high temperature gauge theories. 1. Leading log results," JHEP **0011**, 001 (2000) doi:10.1088/1126-6708/2000/11/001 [hep-ph/0010177]. 10

[63] S. Caron-Huot and C. Gale, "Finite-size effects on the radiative energy loss of a fast parton in hot and dense strongly interacting matter," Phys. Rev. C **82**, 064902 (2010) doi:10.1103/PhysRevC.82.064902 [arXiv:1006.2379 [hep-ph]]. 10

[64] X. N. Wang and X. f. Guo, "Multiple parton scattering in nuclei: Parton energy loss," Nucl. Phys. A **696** (2001) 788 doi:10.1016/S0375-9474(01)01130-7 [hep-ph/0102230]. 11

[65] A. Majumder, "The In-medium scale evolution in jet modification," arXiv:0901.4516 [nucl-th]. 11

[66] A. Bassetto, M. Ciafaloni, G. Marchesini and A. H. Mueller, "Jet Multiplicity and Soft Gluon Factorization," Nucl. Phys. B **207**, 189 (1982). doi:10.1016/0550-3213(82)90161-4 11, 55, 57

[67] A. Bassetto, M. Ciafaloni and G. Marchesini, "Jet Structure and Infrared Sensitive Quantities in Perturbative QCD," Phys. Rept. **100**, 201 (1983). doi:10.1016/0370-1573(83)90083-2 11, 55, 57

[68] P. Arnold, H. C. Chang and S. Iqbal, "The LPM effect in sequential bremsstrahlung 2: factorization," JHEP **1609**, 078 (2016) doi:10.1007/JHEP09(2016)078 [arXiv:1605.07624 [hep-ph]]. 11

[69] P. Arnold, H. C. Chang and S. Iqbal, "The LPM effect in sequential bremsstrahlung: dimensional regularization," JHEP **1610**, 100 (2016) doi:10.1007/JHEP10(2016)100 [arXiv:1606.08853 [hep-ph]]. 11

[70] P. Arnold, H. C. Chang and S. Iqbal, "The LPM effect in sequential bremsstrahlung: 4-gluon vertices," JHEP **1610**, 124 (2016) doi:10.1007/JHEP10(2016)124 [arXiv:1608.05718 [hep-ph]]. 11

[71] L. Xiong and E. V. Shuryak, "Gluon multiplication in high-energy heavy ion collisions," Phys. Rev. C **49**, 2203 (1994) doi:10.1103/PhysRevC.49.2203 [hep-ph/9309333]. 11

[72] S. J. Parke and T. R. Taylor, "An Amplitude for n Gluon Scattering," Phys. Rev. Lett. **56**, 2459 (1986). doi:10.1103/PhysRevLett.56.2459 12

[73] F. A. Berends and W. T. Giele, "Recursive Calculations for Processes with n Gluons," Nucl. Phys. B **306**, 759 (1988). doi:10.1016/0550-3213(88)90442-7 12

[74] S. Weinberg, "Nonabelian Gauge Theories of the Strong Interactions," Phys. Rev. Lett. **31**, 494 (1973). doi:10.1103/PhysRevLett.31.494 15

[75] J. M. Henn and J. C. Plefka, "Scattering Amplitudes in Gauge Theories," Lect. Notes Phys. **883**, pp.1 (2014). doi:10.1007/978-3-642-54022-6 20, 34

[76] F. Maltoni, K. Paul, T. Stelzer and S. Willenbrock, "Color flow decomposition of QCD amplitudes," Phys. Rev. D **67**, 014026 (2003) doi:10.1103/PhysRevD.67.014026 [hep-ph/0209271]. 22

[77] R. Britto, "Introduction to Scattering Amplitudes," lecture notes available at http://http://www.maths.tcd.ie/~britto/lecture-notes.pdf (2011). 24, 26

[78] H. Elvang and Y. t. Huang, "Scattering Amplitudes in Gauge Theory and Gravity," Cambridge University Press, 2015. 24, 26, 111

[79] N. Arkani-Hamed, J. L. Bourjaily, F. Cachazo, A. B. Goncharov, A. Postnikov and J. Trnka, "Grassmannian Geometry of Scattering Amplitudes," arXiv:1212.5605 [hep-th]. 29

[80] R. Britto, F. Cachazo, B. Feng and E. Witten, "Direct proof of tree-level recursion relation in Yang-Mills theory," Phys. Rev. Lett. **94**, 181602 (2005) doi:10.1103/PhysRevLett.94.181602 [hep-th/0501052]. 36

[81] R. Britto, F. Cachazo and B. Feng, "New recursion relations for tree amplitudes of gluons," Nucl. Phys. B **715**, 499 (2005) doi:10.1016/j.nuclphysb.2005.02.030 [hep-th/0412308]. 36

[82] C. Duhr and F. Maltoni, "Antenna functions from MHV rules," JHEP **0811**, 002 (2008) doi:10.1088/1126-6708/2008/11/002 [arXiv:0808.3319 [hep-ph]]. 40

[83] H. Baer and R. N. Cahn, "Cross-section formulae for specific processes," (427-435) Phys. Rev. D **86**, 010001 (2012). doi:10.1103/PhysRevD.86.010001 42

[84] R. K. Ellis, W. J. Stirling and B. R. Webber, "QCD and collider physics," Camb. Monogr. Part. Phys. Nucl. Phys. Cosmol. **8**, 1 (1996). 46

[85] S. J. Parke and M. L. Mangano, "The Structure of Gluon Radiation in QCD," AIP Conf. Proc. **201**, 91 (1990). 46, 52

[86] K. J. Ozeren and W. J. Stirling, "MHV techniques for QED processes," JHEP **0511**, 016 (2005) doi:10.1088/1126-6708/2005/11/016 [hep-th/0509063]. 52

[87] Y. Jia, R. Huang and C. Y. Liu, "$U(1)$-decoupling, KK and BCJ relations in $\mathcal{N} = 4$ SYM," Phys. Rev. D **82**, 065001 (2010) doi:10.1103/PhysRevD.82.065001 [arXiv:1005.1821 [hep-th]]. 46

[88] B. C. Odom, D. Hanneke, B. D'Urso and G. Gabrielse, "New Measurement of the Electron Magnetic Moment Using a One-Electron Quantum Cyclotron,"

Phys. Rev. Lett. **97**, 030801 (2006) Erratum: [Phys. Rev. Lett. **99**, 039902 (2007)]. doi:10.1103/PhysRevLett.97.030801 49

[89] D. Y. Bardin, P. Christova, M. Jack, L. Kalinovskaya, A. Olchevski, S. Riemann and T. Riemann, "ZFITTER v.6.21: A Semianalytical program for fermion pair production in e+ e- annihilation," Comput. Phys. Commun. **133**, 229 (2001) doi:10.1016/S0010-4655(00)00152-1 [hep-ph/9908433]. 49

[90] G. Curci and M. Greco, "Large Infrared Corrections in QCD Processes," Phys. Lett. **92B**, 175 (1980). doi:10.1016/0370-2693(80)90331-7 54

[91] A. Sabio Vera and M. A. Vazquez-Mozo, "The Double Copy Structure of Soft Gravitons," JHEP **1503**, 070 (2015) doi:10.1007/JHEP03(2015)070 [arXiv:1412.3699 [hep-th]]. 54

[92] B. Abelev *et al.* [ALICE Collaboration], "Long-range angular correlations on the near and away side in p-Pb collisions at $\sqrt{s_{NN}} = 5.02$ TeV," Phys. Lett. B **719**, 29 (2013) doi:10.1016/j.physletb.2013.01.012 xi, 66

[93] G. De B. Robinson, "On the Representations of the Symmetric Group," American Journal of Mathematics 60, no.3 (1938): 745-760. doi:10.2307/2371609. 76, 79

[94] W. K. Tung, "Group theory in Physics," World Scientific Publishing Co. Pte. Ltd. (1985). ISBN 9971-966-56-5 83

[95] N. Arkani-Hamed, F. Cachazo, C. Cheung and J. Kaplan, "The S-Matrix in Twistor Space," JHEP **1003**, 110 (2010) doi:10.1007/JHEP03(2010)110 [arXiv:0903.2110 [hep-th]]. 97

[96] V. Shtabovenko, "FeynCalc 9," J. Phys. Conf. Ser. **762**, no. 1, 012064 (2016) doi:10.1088/1742-6596/762/1/012064 [arXiv:1604.06709 [hep-ph]]. 125, 126

[97] W. A. Horowitz and B. A. Cole, Phys. Rev. C **81**, 024909 (2010) doi:10.1103/PhysRevC.81.024909 [arXiv:0910.1823 [hep-ph]]. 97

[98] N. Craig, H. Elvang, M. Kiermaier and T. Slatyer, "Massive amplitudes on the Coulomb branch of N=4 SYM," JHEP **1112**, 097 (2011) doi:10.1007/JHEP12(2011)097 [arXiv:1104.2050 [hep-th]]. 97

[99] N. Arkani-Hamed, T. C. Huang and Y. t. Huang, "Scattering Amplitudes For All Masses and Spins," arXiv:1709.04891 [hep-th]. 97

$SU(N)$

A

The group $SU(N)$ is the special unitary Lie group with N^2-1 real parameters, represented by $N \times N$ complex unitary matrices with determinant 1. Basic reviews on $SU(N)$ Lie algebra can be found in [58]. In a given representation an element $U(\vec{\alpha})$ of the group can be written as

$$U(\vec{\alpha}) = e^{i\alpha_a T_a}, \tag{A.1}$$

where $\vec{\alpha} = (\alpha_1, \ldots, \alpha_{N^2-1})$ is the N^2-1 dimensional vector of the independent real parameters α_a, and T_a are the traceless Hermitian matrices that form the basis of the Lie algebra $su(N)$. To generate a group element of $SU(N)$, the generators T_a have to satisfy the following Lie bracket (commutator)

$$[T_a, T_b] = i f_{abc} T_c, \tag{A.2}$$

and normalized by

$$\mathrm{tr}\,(T_a T_b) = \frac{1}{2}\delta_{ab}. \tag{A.3}$$

The antisymmetric constant f_{abc} are the structure constants of the algebra. The Jacobi identity for the generators, $[T_a, [T_b, T_c]] + \text{cyclic} = 0$, implies

$$f_{dab} f_{dce} + f_{dbc} f_{dae} + f_{dca} f_{dbe} = 0. \tag{A.4}$$

In the adjoint representation of the group, the generators are given by the structure constants, $(T_a^{\mathrm{adj}})_{bc} \equiv -i f_{abc}$, while in that representation the Jacobi identity Eq. (A.4) can be written as

$$[T_a^{\mathrm{adj}}, T_b^{\mathrm{adj}}] = i f_{abc} T_c^{\mathrm{adj}}. \tag{A.5}$$

Here are some useful relations and definitions derived from the different properties of the generators, also derived in [58],

1. Fierz identity
$$(T_a)_{ij}(T_a)_{kl} = \frac{1}{2}\left(\delta_{il}\delta_{kj} - \frac{1}{N}\delta_{ij}\delta_{kl}\right). \tag{A.6}$$

2. Casimir operator in the fundamental representation
$$(T_a T_a)_{ij} = C_F \delta_{ij}, \tag{A.7}$$
where $CF = (N^2 - 1)/2N$, which is equal to 4/3 for QCD.

3. Casimir operator in the adjoint representation
$$\left(T_c^{\text{adj}} T_c^{\text{adj}}\right)_{ab} = C_A \delta_{ab}. \tag{A.8}$$
where $C_A = N$, and equal to 3 for QCD.

Spinor helicity *B*

B.1 Helicity formalism

This section follows closely Appendix A in [78]. In the helicity formalism we defined

$$p_{a\dot{b}} \equiv p^{\mu}(\sigma_{\mu})_{a\dot{b}}, \tag{B.1}$$

where with the metric convention diag$(+,-,-,-)$ the Pauli matices σ_{μ} are

$$\sigma_{\mu} = \left\{ \begin{pmatrix} 1 & 0 \\ 0 & 1 \end{pmatrix}, \begin{pmatrix} 0 & 1 \\ 1 & 0 \end{pmatrix}, \begin{pmatrix} 0 & -i \\ i & 0 \end{pmatrix}, \begin{pmatrix} 1 & 0 \\ 0 & -1 \end{pmatrix} \right\}, \tag{B.2}$$

also written as $\sigma_{\mu} = (1, \vec{\sigma})$. One can show that

$$\det p_{a\dot{b}} = p_{\mu}p^{\mu} \tag{B.3}$$

The spinor indices a and $\dot{b}$ are raised and lowered using

$$\epsilon^{ab} = \epsilon^{\dot{a}\dot{b}} = -\epsilon_{ab} = -\epsilon_{\dot{a}\dot{b}} = \begin{pmatrix} 0 & 1 \\ -1 & 0 \end{pmatrix} \tag{B.4}$$

where $\epsilon_{ac}\epsilon^{cb} = \delta_a^b$. With those definitions combined with $\tilde{\sigma}_{\mu} = (1, -\vec{\sigma})$, the following will be true as shown in [78]

$$\begin{aligned} (\tilde{\sigma}_{\mu})^{\dot{a}b} &= \epsilon^{ab}\epsilon^{\dot{a}\dot{b}}(\sigma_{\mu})_{a\dot{b}}, \\ (\sigma^{\mu})_{a\dot{a}}(\sigma_{\mu})_{b\dot{b}} &= 2\epsilon_{ab}\epsilon_{\dot{a}\dot{b}}, \\ \mathrm{tr}\,(\sigma_{\mu}\tilde{\sigma}_{\nu}) &= 2g_{\mu\nu}. \end{aligned} \tag{B.5}$$

Define $q^{\dot{a}b} \equiv q^{\mu}(\tilde{\sigma}_{\mu})^{\dot{a}b}$, then it follows

$$\mathrm{tr}\left(p_{a\dot{c}}\, q^{\dot{c}b}\right) = p_{a\dot{c}}q^{\dot{c}a} = p_{\mu}q_{\nu}\mathrm{tr}\,(\sigma^{\mu}\tilde{\sigma}^{\nu}) = 2p.q. \tag{B.6}$$

B.2 Spinor variables

For a massless theory, $\det p_{a\dot{b}} = p_\mu p^\mu = 0$ which is equivalent to the rank of $p_{a\dot{b}}$ being equal to one. Thus $p_{a\dot{b}}$ (similarly for $q^{\dot{a}b}$) can be parametrized in terms of spinors as follows

$$p_{a\dot{b}} = \lambda_a \widetilde{\lambda}_{\dot{b}} \quad \text{and} \quad q^{\dot{a}b} = \tilde{\mu}^{\dot{a}} \mu^b. \tag{B.7}$$

Then the following trace becomes

$$\text{tr}\left(p_{a\dot{c}}\, q^{\dot{c}b}\right) = \lambda_a \mu^a \widetilde{\lambda}_{\dot{a}} \tilde{\mu}^{\dot{a}} = \langle pq \rangle [pq], \tag{B.8}$$

where the angle and square brackets are defined by

$$\langle pq \rangle \equiv \lambda_a \mu^a = \epsilon^{ab} \lambda_a \mu_b \quad \text{and} \quad [pq] \equiv \widetilde{\lambda}_{\dot{a}} \tilde{\mu}^{\dot{a}} = \epsilon^{\dot{a}\dot{b}} \widetilde{\lambda}_{\dot{a}} \tilde{\mu}_{\dot{b}}. \tag{B.9}$$

The Levi-Civita symbol, being the metric of angle and square brackets, makes the products antisymmetric.

B.3 Schouten identity

The spinor variables live in a two dimensional space. Therefore three non-zero spinors cannot be independent; i.e.

$$\lambda_{1a} = \alpha \lambda_{2a} + \beta \lambda_{3a}. \tag{B.10}$$

To determine α and β, one can use the antisymmetric property of the brackets by contracting the equation above respectively with λ_{2a} and λ_{3a}. Then we find

$$\langle 12 \rangle = \beta \langle 32 \rangle \Longrightarrow \beta = -\frac{\langle 12 \rangle}{\langle 23 \rangle}, \quad \text{and} \quad \langle 13 \rangle = \alpha \langle 23 \rangle \Longrightarrow \alpha = -\frac{\langle 31 \rangle}{\langle 23 \rangle}. \tag{B.11}$$

Then leads to the Schouten identity, by taking α and β into the original equation

$$\lambda_{1a} \langle 23 \rangle + \lambda_{2a} \langle 31 \rangle + \lambda_{3a} \langle 12 \rangle = 0. \tag{B.12}$$

It is very common to contract the free index a of this identity with an arbitrary spinor λ_{ra},

$$\langle r1 \rangle \langle 23 \rangle + \langle r2 \rangle \langle 31 \rangle + \langle r3 \rangle \langle 12 \rangle = 0. \tag{B.13}$$

An extension of the Schouten identity is the following triangle relation:

$$\frac{\langle ab \rangle}{\langle ac \rangle \langle cb \rangle} + \frac{\langle bb' \rangle}{\langle bc \rangle \langle cb' \rangle} = \frac{\langle ab \rangle \langle cb' \rangle + \langle ac \rangle \langle b'b \rangle}{\langle cb \rangle \langle ac \rangle \langle cb' \rangle} = \frac{\langle ab' \rangle}{\langle ac \rangle \langle cb' \rangle} \tag{B.14}$$

Scattering Amplitudes

C

In this chapter we will compute scattering using the BCFW recursion introduced in Section 3.4. The qqg initial conditions for the recursion are given by

$$A(p,1^-,\bar{p}) = i\tilde{g}\frac{\langle p1\rangle^3\langle\bar{p}1\rangle}{\langle p1\rangle\langle 1\bar{p}\rangle\langle\bar{p}p\rangle} \quad \text{and} \quad A(p,1^+,\bar{p}) = -i\tilde{g}\frac{[p1]^3[\bar{p}1]}{[p1][1\bar{p}][\bar{p}p]}. \tag{C.1}$$

And the ggg initial conditions are given by

$$A_n(1^-,2^-,3^+) = i\tilde{g}\frac{\langle 12\rangle^4}{\langle 12\rangle\langle 23\rangle\langle 31\rangle} \quad \text{and} \quad A_n(1^+,2^+,3^-) = -i\tilde{g}\frac{[12]^4}{[12][23][31]}. \tag{C.2}$$

C.1 $q\bar{q} \to gg$ amplitude

To compute this amplitude we are going to use the BCFW recursion Eq. (3.54), where in the case of $q\bar{q} \to gg$, the recursion is

$$A(p,1,2,\bar{p}) = A(p,\hat{1},\hat{\bar{q}}_1)\,\frac{1}{q_1^2}\,A(\hat{q}_1,\hat{2},\bar{p})\Big|_{\hat{q}_1^2=0}. \tag{C.3}$$

Diagrammatically represented by Fig. C.1, we have $\hat{q}_1 = -\hat{k}_1 + p = -\bar{p} - \hat{k}_2$ and we use $\hat{\bar{q}}_1$ as opposed to $-\hat{q}_1$ to emphasize that the object with momentum $\hat{\bar{q}}_1$ is an antiquark. We use the following shift to complexify the momenta

$$\begin{aligned} \lambda_1(z) &= \lambda_1 & \lambda_2(z) &= \lambda_2 - z\lambda_1 \\ \widetilde{\lambda}_1(z) &= \widetilde{\lambda}_1 + z\widetilde{\lambda}_2 & \widetilde{\lambda}_2(z) &= \widetilde{\lambda}_2, \end{aligned} \tag{C.4}$$

where z is fixed by the on-shell condition of $\hat{q}_1$. With the fact that the brackets $\langle p1\rangle$ and $[\bar{p}2]$ are the products between generic momenta and then $\langle p1\rangle$ and $[\bar{p}2]$ cannot

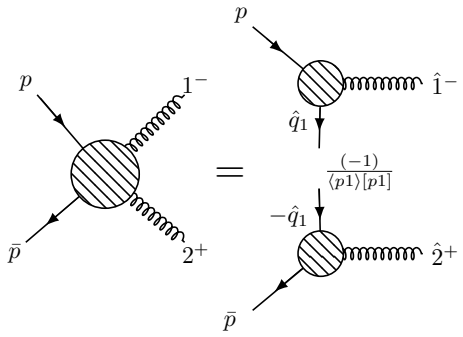

Figure C.1: BCFW term for $q\bar{q} \to gg$.

be necessary equal to zero, the on-shellness of $\hat{q}_1$ gives

$$\hat{q}_1^2 = \begin{cases} -\langle p1\rangle[p\hat{1}] = 0 \\ -\langle \bar{p}\hat{2}\rangle[\bar{p}2] = 0 \end{cases} \Longrightarrow \begin{cases} [p\hat{1}] = [p1] + z[p2] = 0 \\ \langle \bar{p}\hat{2}\rangle = \langle \bar{p}2\rangle - z\langle \bar{p}1\rangle = 0. \end{cases} \tag{C.5}$$

Hence

$$z = \frac{[p1]}{[2p]} = \frac{\langle \bar{p}2\rangle}{\langle \bar{p}1\rangle}. \tag{C.6}$$

Now that the shift is fixed, let us consider the different helicity configurations of Eq. (3.54):

1. Partial amplitude $A(p, 1^-, 2^+, \bar{p})$ with $q_1^2 = -\langle \bar{p}2\rangle[\bar{p}2]$

$$\begin{aligned} A(p, 1^-, 2^+, \bar{p}) &= A(p, \hat{1}^-, \hat{\tilde{q}}_1)\frac{(-1)}{\langle \bar{p}2\rangle[\bar{p}2]}A(\hat{q}_1, \hat{2}^+, \bar{p}) \\ &= -(i\tilde{g})^2\frac{\langle p\hat{1}\rangle^3\langle \hat{\tilde{q}}_1\hat{1}\rangle}{\langle p\hat{1}\rangle\langle \hat{1}\hat{\tilde{q}}_1\rangle\langle \hat{\tilde{q}}_1 p\rangle}\frac{(-1)}{\langle \bar{p}2\rangle[\bar{p}2]}\frac{[\bar{p}\hat{2}]^3[\hat{q}_1\hat{2}]}{[\hat{q}_1 2][\hat{2}\bar{p}][\bar{p}\hat{q}_1]} \\ &= -(i\tilde{g})^2\frac{\langle p1\rangle^3\langle \hat{q}_1 1\rangle}{\langle p1\rangle\langle 1\hat{q}_1\rangle\langle \hat{q}_1 p\rangle}\frac{1}{\langle \bar{p}2\rangle[\bar{p}2]}\frac{[\bar{p}2]^3[\hat{q}_1 2]}{[\hat{q}_1 2][2\bar{p}][\bar{p}\hat{q}_1]} \\ &= -(i\tilde{g})^2\frac{\langle p1\rangle^3}{\langle p1\rangle\langle \bar{p}2\rangle}\frac{[\bar{p}2]}{[\bar{p}\hat{q}_1]\langle \hat{q}_1 p\rangle} \end{aligned} \tag{C.7}$$

In the second line we substitute the three point amplitudes by their respective expressions from Eq. (3.55). In the third line we considered the shifts where $\lambda_1(z) = \lambda_1$ and $\widetilde{\lambda}_2(z) = \widetilde{\lambda}_2$, then any angle brackets $\langle *\hat{1}\rangle$ are equal to $\langle *1\rangle$ and similarly any square brackets $[*\hat{2}]$ are equal to $[*2]$. We also use momentum conservation to substitute $\hat{q}_1 = -\hat{\tilde{q}}_1$. With the relation $\hat{q}_1 = \bar{p} - \hat{k}_2$ we have

$$[\bar{p}\hat{q}_1]\langle \hat{q}_1 p\rangle = -[\bar{p}2]\langle \hat{2}p\rangle. \tag{C.8}$$

Then the amplitude is

$$A(p, 1^-, 2^+, \bar{p}) = -(i\tilde{g})^2 \frac{\langle p1\rangle^3}{\langle p1\rangle\langle \bar{p}2\rangle\langle p\hat{2}\rangle}, \tag{C.9}$$

where one of the momenta is still shifted. With the shifts Eq. (C.4) and with the on-shell condition Eq. (C.6) we can write

$$\begin{aligned}\langle p\hat{2}\rangle &= \langle p2\rangle - z\langle p1\rangle \\ &= \langle p2\rangle - \frac{\langle \bar{p}2\rangle}{\langle \bar{p}1\rangle}\langle p1\rangle \\ &= -\frac{\langle 12\rangle\langle p\bar{p}\rangle}{\langle \bar{p}1\rangle},\end{aligned} \tag{C.10}$$

in the last step we put the expressions in a common denominator, and use the Schouten identity in the numerator. Taking this relation above into the expression of the amplitude we obtain

$$A(p, 1^-, 2^+, \bar{p}) = (i\tilde{g})^2 \frac{\langle p1\rangle^3\langle \bar{p}1\rangle}{\langle p1\rangle\langle 12\rangle\langle 2\bar{p}\rangle\langle \bar{p}p\rangle}. \tag{C.11}$$

2. Consider the same amplitude where via momentum conservation we are going to choose $q_1^2 = -\langle p1\rangle[p1]$. With the exact same steps as in Eq. (C.7), we find

$$\begin{aligned}A(p, 1^-, 2^+, \bar{p}) &= -(i\tilde{g})^2 \frac{[\bar{p}2]^3\langle p1\rangle}{[p1][2\bar{p}][\bar{p}\hat{q}_1]\langle \hat{q}_1 p\rangle} \\ &= -(i\tilde{g})^2 \frac{[\bar{p}2]^3(-1)}{[p1][2\bar{p}][\bar{p}\hat{1}]},\end{aligned} \tag{C.12}$$

where the second equality is obtained from $[\bar{p}\hat{q}_1]\langle \hat{q}_1 p\rangle = [\bar{p}2]\langle \hat{2}p\rangle$. Now to get rid of the shifted momentum we use again Eq. (C.4) and Eq. (C.6),

$$\begin{aligned}[\bar{p}\hat{1}] &= [\bar{p}1] + z[\bar{p}2] \\ &= [\bar{p}1] + \frac{[p1]}{[2p]}[\bar{p}2] \\ &= -\frac{[\bar{p}p][12]}{[2p]}.\end{aligned} \tag{C.13}$$

Taking this expression back into the amplitude leads to

$$A(p, 1^-, 2^+, \bar{p}) = (i\tilde{g})^2 \frac{[\bar{p}2]^3[p2]}{[p1][12][2\bar{p}][\bar{p}p]}. \tag{C.14}$$

Then the amplitude can be either written only in terms of angle brackets Eq. (C.11) or only in terms of square brackets Eq. (C.14).

Similarly it can be shown that

$$A(p,1^+,2^-,\bar{p}) = (i\tilde{g})^2 \frac{\langle p2\rangle^3\langle\bar{p}2\rangle}{\langle p1\rangle\langle 12\rangle\langle 2\bar{p}\rangle\langle\bar{p}p\rangle} = -(i\tilde{g})^2 \frac{[p2]^3[\bar{p}2]}{[p1][12][2\bar{p}][\bar{p}p]}. \tag{C.15}$$

3. For the case of $A(p,1^+,2^+,\bar{p})$, we have

$$\begin{aligned} A(p,1^+,2^+,\bar{p}) &= -(i\tilde{g})^2 \frac{[\hat{\bar{q}}_1\hat{1}]^3[p\hat{1}]}{[p\hat{1}][\hat{1}\hat{\bar{q}}_1][\hat{\bar{q}}_1 p]} \frac{(-1)}{\langle\bar{p}2\rangle[\bar{p}2]} \frac{[\bar{p}\hat{2}]^3[\hat{q}_1\hat{2}]}{[\hat{q}_1 2][\hat{2}\bar{p}][\bar{p}\hat{q}_1]} \\ &= -(i\tilde{g})^2 \frac{[\hat{q}_1\hat{1}]^2[\bar{p}2]}{[\hat{q}_1 p][\hat{q}_1\bar{p}]\langle\bar{p}2\rangle}. \end{aligned} \tag{C.16}$$

To remove $\hat{q}_1$ we are going to use the following relations

$$\frac{\langle 2\hat{q}_1\rangle[\hat{q}_1\hat{1}]}{\langle 2\hat{q}_1\rangle[\hat{q}_1 p]} = \frac{\langle 2p\rangle[p\hat{1}]}{\langle 2\bar{p}\rangle[\hat{p}p]} \quad \text{and} \quad \frac{\langle\hat{1}\hat{q}_1\rangle[\hat{q}_1\hat{1}]}{\langle\hat{1}\hat{q}_1\rangle[\hat{q}_1\bar{p}]} = \frac{\langle\hat{1}p\rangle[p\hat{1}]}{\langle\hat{1}p\rangle[p\hat{p}]}. \tag{C.17}$$

Then the amplitude becomes

$$A(p,1^+,2^+,\bar{p}) = -(i\tilde{g})^2 \frac{[p\hat{1}]^2[\bar{p}2]\langle 2p\rangle}{[\bar{p}p]^2\langle\bar{p}2\rangle^2}. \tag{C.18}$$

Once again the amplitude ends up with one shifted momentum after simplifications. To write the amplitude in terms of the physical momenta we replace the complex shift z using the condition $\hat{q}_1^2 = 0$. Here the amplitude is proportional to $[p\hat{1}]^2$ which is zero according the on-shell condition in Eq. (C.6); therefore

$$A(p,1^+,2^+,\bar{p}) = 0. \tag{C.19}$$

Similarly $A(p,1^+,2^+,\bar{p}) = 0$.

C.2 n-point amplitudes

In addition to the three point amplitude $q\bar{q} \to g$ in Eq. (3.39), to prove the general formula of MHV amplitude for $q\bar{q} \to ng$, we need to consider the following amplitudes that are computed from the original BCFW

$$\begin{aligned} &A_n^{gluon}(1^\pm,2^\pm,\ldots,n^\pm) = 0, \\ &A_n^{gluon}(1^\pm,\ldots,i^\mp,\ldots,n^\pm) = 0. \end{aligned} \tag{C.20}$$

C.2.1 Vanishing amplitudes

The result in Eq. (C.19), showed that the amplitude $A(p, 1, 2, \bar{p})$ vanished if the helicities of the two gluons are both equal to $+1$. This is similar to the relation in Eq. (C.20) for multiple gluon amplitudes.

The generalization of Eq. (C.19) is that $A(p, 1^+, \ldots, n^+, \bar{p}) = 0$. To prove this relation, it is better to begin with the case for $n = 3$. In terms of the BCFW recursion, the amplitude $A(p, 1^+, 2^+, 3^+, \bar{p})$ can be expended as in Fig. C.2. In this expansion the amplitude is given by the sum of four BCFW terms.

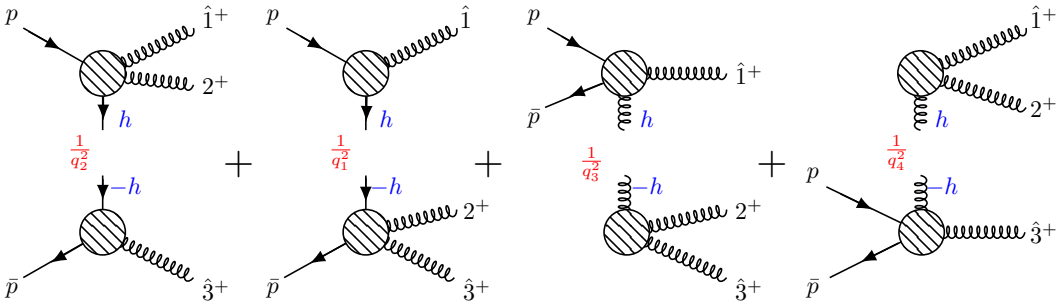

Figure C.2: BCFW terms for $A(p, 1^+, 2^+, 3^+, \bar{p})$.

- The first and second terms are both made with three point amplitudes and a four point amplitude, respectively, of the $A(p, 1, \bar{p})$ and $A(p, 1, 2, \bar{p})$; according to Eq. (C.19) the the 4-point amplitude vanishes here since the helicities of the gluons are both equal to $+1$.

- For the third BCFW term in Fig. C.2 we need to consider two cases. The first case is for the helicity of the mediator gluon been equal to $+1$; this will make the 4-point amplitude $A(p, 1, q, \bar{p})$ vanishes. The second case occurs when the mediator helicity is -1. In this case, the 4-point amplitude of the third terms is non-zero however the 3-point A_3^{gluon} amplitude vanishes since the helicities of the 3 gluons are all equal to $+1$.

- The same argument as above can applied to the fourth BCFW term.

Therefore the 5-point amplitude $A(p, 1, 2, 3, \bar{p})$ is equal to zero for the case where

the three gluons have all helicities equal to +1. Therefore we have

$$A(p, 1^+, 2^+, 3^+, \bar{p}) = 0. \tag{C.21}$$

For $n = 4$, one can check that the BCFW terms of the amplitude are made with sub amplitudes of the type $A(p, 1, 2, 3, \bar{p})$ and $A(p, 1, 2, \bar{p})$, and also of the gluonic type $A_4^{gluon}(1, 2, 3, 4)$ and $A_4^{gluon}(1, 2, 3)$. According to Eq. (C.19), Eq. (C.20), and Eq. (C.21) all the sub-amplitudes will vanish if the helicities of the 4-gluons are all equal to +1 the same way as for Eq. (C.21). Therefore the amplitude $A(p, 1^+, 2^+, 3^+, 4^+, \bar{p})$ will be zero. The same argument can be made for $n = 5$, $n = 6$ and so on and so forth. Hence

$$A(p, 1^+, \ldots, n^+, \bar{p}) = 0. \tag{C.22}$$

C.2.2 MHV amplitudes

Here we want to show that the MHV amplitude, in which only one of the gluons has a negative helicity, for $q\bar{q} \to ng$ is given by

$$A(p, 1^+, \ldots, i^-, \ldots, n^+, p) = (i\tilde{g})^n \frac{\langle pi\rangle^3 \langle \bar{p}i\rangle}{\langle p1\rangle\langle 12\rangle \cdots \langle n\bar{p}\rangle\langle \bar{p}p\rangle}. \tag{C.23}$$

To show Eq. (C.23) we are going use proof by induction. First we assume that this formula is true for $n-1$ gluons, i.e.

$$A(p, 1^+, \ldots, i^-, \ldots, (n{-}1)^+, p) = (i\tilde{g})^n \frac{\langle pi\rangle^3 \langle \bar{p}i\rangle}{\langle p1\rangle\langle 12\rangle \cdots \langle n{-}1\,\bar{p}\rangle\langle \bar{p}p\rangle}. \tag{C.24}$$

To compute the result for n gluons we are going to use the recursion in which the non trivial BCFW terms are given shown in Fig. C.3. All other BCFW terms not shown in Fig. C.3 are zero because of their helicity configuration.

Let us evaluate the each BCFW terms represented by the diagrams (a) to (d):

(a): Here the on-shell condition for the exchanged momentum leads to

$$\begin{aligned} &\hat{q}_{n-1}^2 = (\hat{k}_n - \bar{p})^2 = -\langle \hat{n}\bar{p}\rangle[n\bar{p}] = 0 \\ &\Longrightarrow \langle \hat{n}\bar{p}\rangle = \langle n\bar{p}\rangle - z\langle 1\bar{p}\rangle = 0 \\ &\Longrightarrow z = \frac{\langle n\bar{p}\rangle}{\langle 1\bar{p}\rangle}. \end{aligned} \tag{C.25}$$

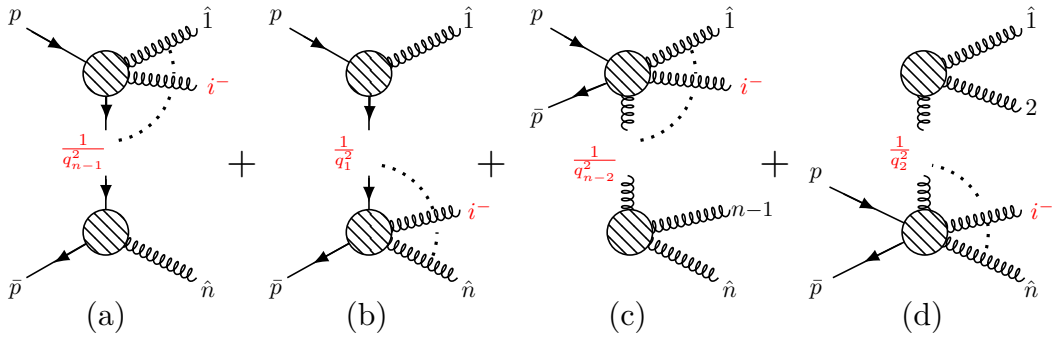

Figure C.3: Non-vanishing BCFW terms for MHV amplitudes with a $q\bar{q}$ and n gluons.

The BCFW term is given by

$$(\mathrm{a}) = (i\tilde{g})^n \frac{\langle pi\rangle^3\langle \hat{q}i\rangle}{\langle p\hat{1}\rangle\langle \hat{1}2\rangle\cdots\langle n{-}1\,\hat{q}\rangle\langle \hat{q}p\rangle}\frac{1}{\langle \bar{p}n\rangle[\bar{p}n]}\frac{[\bar{p}\hat{n}]^3[\hat{q}\hat{n}]}{[\hat{q}\hat{n}][\hat{n}\bar{p}][\bar{p}\hat{q}]}, \tag{C.26}$$

where q is shorthand for q_{n-1}. Recalling that $\hat{q} = \hat{k}_n - \bar{p}$ leads to

$$\begin{aligned}
\langle i\hat{q}\rangle[\hat{q}\hat{n}] &= -\langle i\bar{p}\rangle[\bar{p}\hat{n}] = -\langle i\bar{p}\rangle[\bar{p}n] \\
\langle p\hat{q}\rangle[\hat{q}\bar{n}] &= -\langle p\bar{p}\rangle[\bar{p}\hat{n}] = -\langle p\bar{p}\rangle[\bar{p}n] \\
\langle n{-}1\,\hat{q}\rangle[\hat{q}\bar{p}] &= \langle n{-}1\,\hat{n}\rangle[\hat{n}\bar{p}] = \langle n{-}1\,\hat{n}\rangle[n\bar{p}].
\end{aligned} \tag{C.27}$$

Thus the BCFW term becomes

$$\begin{aligned}
(\mathrm{a}) &= (i\tilde{g})^n \frac{\langle pi\rangle^3\langle \bar{p}i\rangle}{\langle p1\rangle\langle 12\rangle\cdots\langle n{-}1\,\hat{n}\rangle\langle n\bar{p}\rangle\langle \bar{p}p\rangle} \\
&= (i\tilde{g})^n \frac{\langle pi\rangle^3\langle \bar{p}i\rangle}{\langle p1\rangle\langle 12\rangle\cdots\langle n{-}1\,n\rangle\langle n\bar{p}\rangle\langle \bar{p}p\rangle}\frac{\langle n{-}1\,n\rangle\langle 1\bar{p}\rangle}{\langle n{-}1\,\bar{p}\rangle\langle 1n\rangle}.
\end{aligned} \tag{C.28}$$

The second equality is obtained by applying the on-shell condition in Eq. (C.25) to remove the shift on the bracket $\langle n{-}1\,\hat{n}\rangle$,

$$\begin{aligned}
\langle n{-}1\,\hat{n}\rangle &= \langle n{-}1\,n\rangle - z\langle n{-}1, 1\rangle \\
&= \langle n{-}1\,n\rangle - \frac{\langle n\bar{p}\rangle}{\langle 1\bar{p}\rangle}\langle n{-}1, 1\rangle \\
&= \frac{\langle n{-}1\,\bar{p}\rangle\langle 1n\rangle}{\langle 1\bar{p}\rangle} \longleftarrow \text{(Schoutten)}
\end{aligned} \tag{C.29}$$

(b): The on-shell condition for $\hat{q}_1$ gives

$$\begin{aligned}
\hat{q}_1^2 = (\hat{k}_1 - p)^2 &= -\langle 1p\rangle[\hat{1}p] = 0 \\
\Longrightarrow [\hat{1}p] &= [1p] + z[np] = 0 \\
\Longrightarrow z &= \frac{[p1]}{[np]}.
\end{aligned} \tag{C.30}$$

The BCFW term is

$$(\text{b}) = (i\tilde{g})^n \frac{[\hat{q}\hat{1}]^3[p\hat{1}]}{[p\hat{1}][\hat{1}\hat{q}][\hat{q}p]} \frac{1}{\langle p1\rangle[p1]} \frac{\langle \hat{q}i\rangle^3\langle \bar{p}i\rangle}{\langle \hat{q}2\rangle\cdots\langle n{-}1\,\hat{n}\rangle\langle \hat{n}\bar{p}\rangle\langle \bar{p}\hat{q}\rangle}. \tag{C.31}$$

With q a shorthand for q_1, and if we recall that $\hat{q}_1 = \hat{k}_1 - p$, then we have

$$\begin{aligned} [\hat{1}\hat{q}]\langle \hat{q}i\rangle &= -[\hat{1}p]\langle pi\rangle \\ [p\hat{q}]\langle \hat{q}\bar{p}\rangle &= [p\hat{1}]\langle \hat{1}\bar{p}\rangle = [p\hat{1}]\langle 1\bar{p}\rangle \\ [\hat{1}\hat{q}]\langle \hat{q}2\rangle &= -[\hat{1}p]\langle p2\rangle, \end{aligned} \tag{C.32}$$

the BCFW term becomes

$$(\text{b}) = (i\tilde{g})^n \frac{\langle pi\rangle^3\langle \bar{p}i\rangle}{\langle p1\rangle\langle 12\rangle\cdots\langle n{-}1\,\hat{n}\rangle\langle \hat{n}\bar{p}\rangle\langle \bar{p}p\rangle} \frac{[p\hat{1}]}{[p1]} = 0. \tag{C.33}$$

To see why this is zero, one can check first that the brackets $\langle n{-}1\,\hat{n}\rangle$ and $\langle \hat{n}\bar{p}\rangle$ are finite and non zero under the on-shell condition, but indeed from the condition Eq. (C.30) we have $[p\hat{1}] = 0$, and therefore (b)=0.

(c): The on-shell condition for $\hat{q}_{n-2}$ is given by

$$\begin{aligned} &\hat{q}_{n-2}^2 = (\hat{k}_n + k_{n-1})^2 = \langle \hat{n}\,n{-}1\rangle[n\,n{-}1] = 0 \\ &\Longrightarrow \langle \hat{n}\,n{-}1\rangle = \langle n\,n{-}1\rangle - z\langle 1\,n{-}1\rangle = 0 \\ &\Longrightarrow z = \frac{\langle n\,n{-}1\rangle}{\langle 1\,n{-}1\rangle} \end{aligned} \tag{C.34}$$

The BCFW term is

$$(\text{c}) = \frac{(i\tilde{g})^n[n{-}1\,\hat{n}]^4}{[\hat{q}\,n{-}1][n{-}1\,\hat{n}][\hat{n}\hat{q}]} \frac{1}{\langle n\,n{-}1\rangle[n\,n{-}1]} \frac{\langle pi\rangle^3\langle \bar{p}i\rangle}{\langle p\hat{1}\rangle\langle \hat{1}2\rangle\cdots\langle n{-}2\,\hat{q}\rangle\langle \hat{q}\bar{p}\rangle\langle \bar{p}p\rangle}. \tag{C.35}$$

With q a shorthand for q_{n-2}, and if we recall that $\hat{q}_{n-2} = -(\hat{k}_n + k_{n-1})$, then we have

$$\begin{aligned} [\hat{n}\hat{q}]\langle \hat{q}\,n{-}2\rangle &= -[\hat{n}\,n{-}1]\langle n{-}1\,n{-}2\rangle = -[n\,n{-}1]\langle n{-}1\,n{-}2\rangle \\ [n{-}1\,\hat{q}]\langle \hat{q}\bar{p}\rangle &= -[n{-}1\,\hat{n}]\langle \hat{n}\bar{p}\rangle = -[n{-}1\,n]\langle \hat{n}\bar{p}\rangle. \end{aligned} \tag{C.36}$$

Then the BCFW term becomes

$$\begin{aligned} (\text{a}) &= (i\tilde{g})^n \frac{\langle pi\rangle^3\langle \bar{p}i\rangle}{\langle p1\rangle\langle 12\rangle\cdots\langle n{-}1\,n\rangle\langle \hat{n}\bar{p}\rangle\langle \bar{p}p\rangle} \\ &= (i\tilde{g})^n \frac{\langle pi\rangle^3\langle \bar{p}i\rangle}{\langle p1\rangle\langle 12\rangle\cdots\langle n{-}1\,n\rangle\langle n\bar{p}\rangle\langle \bar{p}p\rangle} \frac{\langle 1\,n{-}1\rangle\langle n\bar{p}\rangle}{\langle n{-}1\,\bar{p}\rangle\langle 1n\rangle}. \end{aligned} \tag{C.37}$$

Where the second equality is obtained from the on-shell condition in Eq. (C.34),

$$\begin{aligned}\langle \hat{n}\bar{p}\rangle &= \langle n\bar{p}\rangle - z\langle 1\bar{p}\rangle \\ &= \langle n\bar{p}\rangle - \frac{\langle n\, n{-}1\rangle}{\langle 1\, n{-}1\rangle}\langle 1\bar{p}\rangle \\ &= \frac{\langle n1\rangle\langle \bar{p}\, n{-}1\rangle}{\langle 1\, n{-}1\rangle}.\end{aligned} \tag{C.38}$$

(d): The on-shell condition for $\hat{q}_2$ is given by

$$\begin{aligned}&\hat{q}_1 = (\hat{k}_1 + k_2)^2 = \langle 12\rangle[\hat{1}2] = 0 \\ &\implies [\hat{1}2] = [12] + z[n2] = 0 \\ &\implies z = \frac{[12]}{[2n]}.\end{aligned} \tag{C.39}$$

The corresponding BCFW term is

$$\text{(d)} = \frac{[\hat{1}2]^4}{[\hat{1}2][2\hat{q}][\hat{q}\hat{1}]}\frac{1}{\langle 12\rangle[12]}\frac{\langle pi\rangle^3\langle \bar{p}i\rangle}{\langle p\hat{q}\rangle\langle \hat{q}3\rangle\cdots\langle n{-}1\,\hat{n}\rangle\langle \hat{n}\bar{p}\rangle\langle \bar{p}p\rangle}. \tag{C.40}$$

With q the shorthand for q_2, we recall that $\hat{q}_2 = -(\hat{k}_1 + k_2)$, then

$$\begin{aligned}[2\hat{q}]\langle \hat{q}p\rangle - [2\hat{1}]\langle \hat{1}p\rangle &= -[2\hat{1}]\langle 1p\rangle \\ [\hat{1}\hat{q}]\langle \hat{q}3\rangle &= -[\hat{1}2]\langle 23\rangle,\end{aligned} \tag{C.41}$$

then the BCFW term becomes

$$\text{(d)} = (i\tilde{g})^n\frac{\langle pi\rangle^3\langle \bar{p}i\rangle}{\langle p1\rangle\langle 12\rangle\cdots\langle n{-}1\,\hat{n}\rangle\langle \hat{n}\bar{p}\rangle\langle \bar{p}p\rangle}\frac{[\hat{1}2]}{[12]} = 0. \tag{C.42}$$

One can check that the brackets $\langle n{-}1\,\hat{n}\rangle$ and $\langle \hat{n}\bar{p}\rangle$ do not vanish when we impose the on-shell condition Eq. (C.39), while $[\hat{1}2] = 0$ in that condition, therefore (d)$= 0$.

The MHV amplitude for $A(p, 1, \ldots, n, \bar{p})$ is then given by the sum of (a) and (b),

$$\text{(a)+(b)} = \frac{(i\tilde{g})^n\langle pi\rangle^3\langle \bar{p}i\rangle}{\langle p1\rangle\langle 12\rangle\cdots\langle n{-}1\, n\rangle\langle n\bar{p}\rangle\langle \bar{p}p\rangle}\left(\frac{\langle n{-}1\, n\rangle\langle 1\bar{p}\rangle}{\langle n{-}1\,\bar{p}\rangle\langle 1n\rangle} + \frac{\langle 1\, n{-}1\rangle\langle n\bar{p}\rangle}{\langle n{-}1\,\bar{p}\rangle\langle 1n\rangle}\right). \tag{C.43}$$

Using the Schoutten identity we obtain

$$\frac{\langle n{-}1\, n\rangle\langle 1\bar{p}\rangle}{\langle n{-}1\,\bar{p}\rangle\langle 1n\rangle} + \frac{\langle 1\, n{-}1\rangle\langle n\bar{p}\rangle}{\langle n{-}1\,\bar{p}\rangle\langle 1n\rangle} = -\frac{\langle n1\rangle\langle n{-}1\,\bar{p}\rangle}{\langle n{-}1\,\bar{p}\rangle\langle 1n\rangle} = 1. \tag{C.44}$$

Therefore

$$A(p,1^+,\ldots,i^-,\ldots,n^+,p) = (i\tilde{g})^n \frac{\langle pi\rangle^3\langle\bar{p}i\rangle}{\langle p1\rangle\langle 12\rangle\cdots\langle n{-}1\,n\rangle\langle n\bar{p}\rangle\langle\bar{p}p\rangle}. \tag{C.45}$$

The exact same steps with the exact same BCFW terms can be used for the $\overline{\text{MHV}}$ amplitude with the exception of instead of only one negative helicity for the i-th gluon, we have only one positive helicity. Then we obtain

$$A(p,1^-,\ldots,i^+,\ldots,n^-,p) = (i\tilde{g})^n \frac{[pi]^3[\bar{p}i]}{[p1][12]\cdots[n{-}1\,n][n\bar{p}][\bar{p}p]}. \tag{C.46}$$

Squaring $\mathcal{M}(q\bar{q} \to gg)$ D

In this chapter, we present the computation of the squaring of the amplitude associated to $q\bar{q} \to gg$ with explicit details. Let us begin with the color kinematic decomposition introduced in Eq. (2.16),

$$\mathcal{M} = T_{a_1} T_{a_2} A(p, 1^-, 2^+, \bar{p}) + T_{a_2} T_{a_1} A(p, 2^+, 1^-, \bar{p}). \tag{D.1}$$

The associated color average of the absolute square of the amplitude in Eq. (D.1) is given by the following trace

$$\begin{aligned} \mathrm{tr}\left(|\mathcal{M}|^2\right) =& C_1 \left|A(p, 1^-, 2^+, \bar{p})\right|^2 + C_1 \left|A(p, 2^+, 1^-, \bar{p})\right|^2 \\ &+ 2C_2 \,\mathrm{Re}\left(A(p, 1^-, 2^+, \bar{p}) A^*(p, 2^+, 1^-, \bar{p})\right), \end{aligned} \tag{D.2}$$

where C_1 and C_2 are the color factors defined by

$$C_1 \equiv \mathrm{tr}\left(T_{a_1} T_{a_1} T_{a_2} T_{a_2}\right) \quad \text{and} \quad C_2 \equiv \mathrm{tr}\left(T_{a_1} T_{a_2} T_{a_1} T_{a_2}\right). \tag{D.3}$$

In order to evaluate the different expressions in Eq. (D.2), it is necessary and useful to specify the different helicities of the particles in the process. Thus, let us

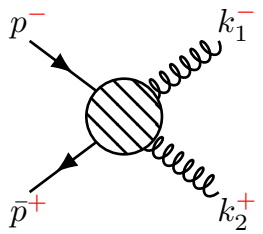

Figure D.1: Amplitude for $q\bar{q} \to gg$.

consider the helicity configuration as in Fig. D.1 where the helicity of the quark is $-1/2$, the antiquark has helicity $+1/2$, the gluon with momentum k_1 has helicity -1, and the gluon with momentum k_2 has helicity $+1$. Then we have

$$A(p,1^-,2^+,\bar{p}) = \frac{\tilde{g}^2\langle p1\rangle^3\langle\bar{p}1\rangle}{\langle p1\rangle\langle 12\rangle\langle 2\bar{p}\rangle\langle\bar{p}p\rangle} \text{ and } A^*(p,1^-,2^+,\bar{p}) = \frac{\tilde{g}^2[p1]^3[\bar{p}1]}{[p1][12][2\bar{p}][\bar{p}p]}. \quad \text{(D.4)}$$

It is also important to introduce the associated Mandelstam variables in terms of angle and square brackets:

$$\begin{aligned} s &= (p+\bar{p})^2 = (k_1+k_2)^2 = \langle p\bar{p}\rangle[p\bar{p}] = \langle 12\rangle[12] \\ t &= (p-k_1)^2 = (\bar{p}-k_2)^2 = -\langle p1\rangle[p1] = -\langle\bar{p}2\rangle[\bar{p}2] \\ u &= (p-k_2)^2 = (\bar{p}-k_1)^2 = -\langle p2\rangle[p2] = -\langle\bar{p}1\rangle[\bar{p}1]. \end{aligned} \quad \text{(D.5)}$$

Therefore the different kinematics in Eq. (D.2) are given by

$$\left|A(p,1^-,2^+,\bar{p})\right|^2 = \tilde{g}^4\frac{\langle p1\rangle^3\langle\bar{p}1\rangle}{\langle p1\rangle\langle 12\rangle\langle 2\bar{p}\rangle\langle\bar{p}p\rangle}\frac{[p1]^3[\bar{p}1]}{[p1][12][2\bar{p}][\bar{p}p]} = \tilde{g}^4\frac{t^3u}{s^2t^2}, \quad \text{(D.6)}$$

$$\left|A(p,2^+,1^-,\bar{p})\right|^2 = \tilde{g}^4\frac{\langle p1\rangle^3\langle\bar{p}1\rangle}{\langle p2\rangle\langle 21\rangle\langle 1\bar{p}\rangle\langle\bar{p}p\rangle}\frac{[p1]^3[\bar{p}1]}{[p2][21][1\bar{p}][\bar{p}p]} = \tilde{g}^4\frac{t^3u}{s^2u^2}, \quad \text{(D.7)}$$

and the cross term is given by

$$A(p,1^-,2^+,\bar{p})A^*(p,2^+,1^-,\bar{p}) = \frac{\tilde{g}^4\langle p1\rangle^3\langle\bar{p}1\rangle}{\langle p1\rangle\langle 12\rangle\langle 2\bar{p}\rangle\langle\bar{p}p\rangle}\frac{[p1]^3[\bar{p}1]}{[p2][21][1\bar{p}][\bar{p}p]} = \frac{-\tilde{g}^4t}{s^2u}\langle p1\bar{p}2p]. \quad \text{(D.8)}$$

In order to compute the real part of Eq. (D.8) as required in Eq. (D.2), we recall the relation introduced in Eq. (3.37) which leads to

$$2\,\mathrm{Re}(\langle p1\bar{p}2p]) = \langle p1\bar{p}2p] + [p1\bar{p}2p\rangle = \mathrm{tr}\left(\not{p}\not{k}_1\not{\bar{p}}\not{k}_2\right) = t^2+u^2-s^2. \quad \text{(D.9)}$$

And then the averaged modulus square amplitude becomes

$$\mathrm{tr}\left(|\mathcal{M}|^2\right) = \tilde{g}^4\frac{t}{su}\left[C_1(t^2+u^2) - C_2(t^2+u^2-s^2)\right]. \quad \text{(D.10)}$$

To simplify the relation even further, we use the fact that $s+t+u=0$, then we have

$$s^2 = (t+u)^2 = t^2+u^2+2tu \Longrightarrow t^2+u^2 = s^2-2tu. \quad \text{(D.11)}$$

Therefore, after simplification we have

$$\mathrm{tr}\left(|\mathcal{M}|^2\right) = \tilde{g}^4C_1\left[\frac{t}{u} + 2\frac{C_2-C_1}{C_1}\frac{t^2}{s^2}\right]. \quad \text{(D.12)}$$

The value of the color factors can be computed using the FeynCalc package in Mathematica [96] and are given by $C_1 = C_A C_F^2$ and $C_2 = -C_F/2$. Therefore we find that

$$\mathrm{tr}\,|\mathcal{M}|^2 = \tilde{g}^4 C_A C_F^2 \left[\frac{t}{u} - \frac{C_A}{C_F}\frac{t^2}{s^2}\right]. \tag{D.13}$$

Current squaring

E

In this chapter we are going to compute the square of the two gluon emission current J_2,

$$J_2(1,2) = \tilde{g}^2 \left(\frac{T_{a_1} T_{a_2} \langle p\bar{p} \rangle}{\langle p1 \rangle \langle 12 \rangle \langle 2\bar{p} \rangle} + \frac{T_{a_2} T_{a_1} \langle p\bar{p} \rangle}{\langle p2 \rangle \langle 21 \rangle \langle 1\bar{p} \rangle} \right). \tag{E.1}$$

To square Eq. (E.1) we are going to consider the following decomposition

$$J_2(1,2) = \frac{\tilde{g}^2}{2} C^s_{1,2} J^s_2(1,2) + \frac{\tilde{g}^2}{2} C^a_{1,2} J^a_2(1,2), \tag{E.2}$$

where the upper scripts s and a stand respectively for symmetric and antisymmetric, and the new variables are given by

$$\begin{aligned} C^s_{1,2} &\equiv \{T_{a_1}, T_{a_2}\}, & C^a_{1,2} &\equiv [T_{a_1}, T_{a_2}], \\ J^s_2(1,2) &\equiv \sum_{\mathcal{P}_2} \frac{\langle p\bar{p} \rangle}{\langle p1 \rangle \langle 12 \rangle \langle 2\bar{p} \rangle}, & J^a_2(1,2) &\equiv \sum_{\mathcal{P}_2} \frac{\epsilon_{12} \langle p\bar{p} \rangle}{\langle p1 \rangle \langle 12 \rangle \langle 2\bar{p} \rangle}. \end{aligned} \tag{E.3}$$

Squaring the current in Eq. (E.2) leads to

$$|J_2(1,2)|^2 = \frac{\tilde{g}^4}{4} \left[\mathrm{tr}\left(C^s_{1,2} C^{s\dagger}_{1,2} \right) |J^s_2(1,2)|^2 + \mathrm{tr}\left(C^a_{1,2} C^{a\dagger}_{1,2} \right) |J^a_2(1,2)|^2 \right]. \tag{E.4}$$

To compute the traces of the color factors, we used FeynCalc [96], and we obtained

$$\begin{aligned} \mathrm{tr}\left(C^s_{1,2} C^{s\dagger}_{1,2} \right) &= 2C_F^2 C_A - C_F, \\ \mathrm{tr}\left(C^s_{1,2} C^{s\dagger}_{1,2} \right) &= C_A^2 C_F, \\ \mathrm{tr}\left(C^s_{1,2} C^{a\dagger}_{1,2} \right) &= \mathrm{tr}\left(C^a_{1,2} C^{s\dagger}_{1,2} \right) = 0. \end{aligned} \tag{E.5}$$

The computation of the square of the symmetric and antisymmetric kinematics are computed in the following sections.

E.1 Squaring J_2

Symmetric

From its definition the square of symmetric kinematic piece is given by

$$|J_2^s(1,2)|^2 = \left(\sum_{\mathcal{P}_2} \frac{\langle p\bar{p}\rangle}{\langle p1\rangle\langle 12\rangle\langle 2\bar{p}\rangle}\right)\left(\sum_{\mathcal{P}_2} \frac{[p\bar{p}]}{[p1][12][2\bar{p}]}\right). \tag{E.6}$$

And with the triangle relation in Eq. (B.14), we have

$$\begin{aligned}\sum_{\mathcal{P}_2} \frac{\langle p\bar{p}\rangle}{\langle p1\rangle\langle 12\rangle\langle 2\bar{p}\rangle} &= \frac{\langle p\bar{p}\rangle}{\langle p1\rangle\langle 12\rangle\langle 2\bar{p}\rangle} + \frac{\langle p\bar{p}\rangle}{\langle p2\rangle\langle 21\rangle\langle 1\bar{p}\rangle} \\ &= \frac{\langle p\bar{p}\rangle}{\langle p2\rangle\langle 2\bar{p}\rangle}\left(\frac{\langle p2\rangle}{\langle p1\rangle\langle 12\rangle} + \frac{\langle 2\bar{p}\rangle}{\langle 21\rangle\langle 1\bar{p}\rangle}\right) \\ &= \frac{\langle p\bar{p}\rangle}{\langle p2\rangle\langle 2\bar{p}\rangle}\frac{\langle p\bar{p}\rangle}{\langle p1\rangle\langle 1\bar{p}\rangle}.\end{aligned} \tag{E.7}$$

A similar derivation holds for the second sum, with the one difference that instead of angle brackets we will have square brackets. Therefore the squaring yields

$$|J_2^s(1,2)|^2 = \left(\prod_{i=\{1,2\}} \frac{\langle p\bar{p}\rangle}{\langle pi\rangle\langle i\bar{p}\rangle}\right)\left(\prod_{i=\{1,2\}} \frac{[p\bar{p}]}{[pi][i\bar{p}]}\right). \tag{E.8}$$

The very last step is to recall the relation between the brackets and the four vector products where $\langle ij\rangle[ij] = 2k_i.k_j$; thus we find

$$\begin{aligned}|J_2^s(1,2)|^2 &= \prod_{i=\{1,2\}} \frac{\langle p\bar{p}\rangle[p\bar{p}]}{\langle pi\rangle[pi]\langle i\bar{p}\rangle[i\bar{p}]} \\ &= \prod_{i=\{1,2\}} \frac{p.\bar{p}}{2(p.k_i)(\bar{p}.k_i)}.\end{aligned} \tag{E.9}$$

Antisymmetric

The computation for the antisymmetric case is different from the symmetric case. Starting with the definition of the antisymmetric kinematics, squaring will give

$$|J_2^a(1,2)|^2 = \left(\sum_{\mathcal{P}_2} \frac{\epsilon_{12}\langle p\bar{p}\rangle}{\langle p1\rangle\langle 12\rangle\langle 2\bar{p}\rangle}\right)\left(\sum_{\mathcal{P}_2} \frac{\epsilon_{12}[p\bar{p}]}{[p1][12][2\bar{p}]}\right). \tag{E.10}$$

Since we don't have a relation similar to the triangle relation in Eq. (B.14), we perform a brute force computation, in which we have

$$\begin{aligned}\sum_{\mathcal{P}_2}\frac{\epsilon_{12}\langle p\bar{p}\rangle}{\langle p1\rangle\langle 12\rangle\langle 2\bar{p}\rangle}&=\frac{\langle p\bar{p}\rangle}{\langle p1\rangle\langle 12\rangle\langle 2\bar{p}\rangle}-\frac{\langle p\bar{p}\rangle}{\langle p2\rangle\langle 21\rangle\langle 1\bar{p}\rangle},\\ \sum_{\mathcal{P}_2}\frac{\epsilon_{12}[p\bar{p}]}{[p1][12][2\bar{p}]}&=\frac{[p\bar{p}]}{[p1][12][2\bar{p}]}-\frac{[p\bar{p}]}{[p2][21][1\bar{p}]}.\end{aligned}\tag{E.11}$$

By expanding the brackets, then putting everything into a common denominator we obtain

$$|J_2^a(1,2)|^2=(p.\bar{p})\frac{(p.k_1)(\bar{p}.k_2)+(p.k_2)(\bar{p}.k_1)+\frac{1}{4}\langle p1\bar{p}2p]+\frac{1}{4}[p1\bar{p}2p\rangle}{4(k_1.k_2)(p.k_1)(p.k_2)(\bar{p}.k_1)(\bar{p}.k_2)}.\tag{E.12}$$

To obtain Eq. (E.12) we used $\langle ij\rangle[ij]=2k_i.k_j$ and also the relation in Eq. (3.35) where

$$\langle p1\bar{p}2p]=\langle p1\rangle[1\bar{p}]\langle\bar{p}2\rangle[2p]\quad\text{and}\quad[p1\bar{p}2p\rangle=[p1]\langle 1\bar{p}\rangle[\bar{p}2]\langle 2p\rangle.\tag{E.13}$$

The relation Eq. (3.37) will lead to

$$\langle p1\bar{p}2p]+[p1\bar{p}2p\rangle=\mathrm{tr}\left(\not{p}\not{k}_1\not{\bar{p}}\not{k}_2\right),\tag{E.14}$$

and with the property of gamma matrices as in [58], we will find

$$(p.k_1)(\bar{p}.k_2)+(p.k_2)(\bar{p}.k_1)=\frac{1}{4}\mathrm{tr}\left(\not{p}\not{k}_1\not{\bar{p}}\not{k}_2\right)+(p.\bar{p})(k_2.k_1).\tag{E.15}$$

Therefore Eq. (E.12) becomes

$$|J_2^a(1,2)|^2=\left(1+\frac{\mathrm{tr}\left(\not{p}\not{k}_1\not{\bar{p}}\not{k}_2\right)}{2(k_1.k_2)(p.\bar{p})}\right)\prod_{i=\{1,2\}}\frac{p.\bar{p}}{2(p.k_i)(\bar{p}.k_i)}.\tag{E.16}$$

Permutation Group $\mathcal{P}_3$ F

In Section 7.3, we recall some elementary properties of the permutation group $\mathcal{P}_3$ in order to describe the mixed symmetry case for three gluon emissions. In the same section, we construct the operators $\hat{Q}_m$ such that

$$J_{3,m}(1,2,3) = \hat{Q}_m J_{3,3}(1,2,3). \tag{F.1}$$

By construction the operators $\hat{Q}_m$ are defined in Eq. (7.33) where

$$\begin{aligned} \hat{Q}_0 &\equiv -\sigma_{13}, & \hat{Q}_1 &\equiv \sigma_{13} + \sigma_{23} + \sigma_{321}, \\ \hat{Q}_2 &\equiv -1 - \sigma_{23} - \sigma_{321}, & \hat{Q}_3 &\equiv 1, \end{aligned} \tag{F.2}$$

where $\{1, \sigma_{ij}, \sigma_{ijk}\}$ are the different elements of $\mathcal{P}_3$ for $\{i,j,k\} = \{1,2,3\}$.

In this appendix we review the properties of the elements of the permutation group $\mathcal{P}_3$, in order to compute the dual operator $\hat{Q}^\sharp$ of the operator $\hat{Q}$, such that

$$\sum_{\mathcal{P}_3} T^x_{3,m}(1,2,3)\hat{Q} J^x_{3,3}(1,2,3) = \sum_{\mathcal{P}_3} \left(\hat{Q}^\sharp T^x_{3,m}(1,2,3)\right) J^x_{3,3}(1,2,3). \tag{F.3}$$

F.1 Properties of the elements of $\mathcal{P}_3$

Let $F(1,2,3)$ be a function that depends on the labels $\{1,2,3\}$. The action of σ_{ij} on $F(1,2,3)$ is to swap the label i of the function with the label j. Similarly σ_{ijk} permutes the three indices in such a way the label i becomes j, j becomes k, and k becomes i.

$$\begin{aligned} \sigma_{ij} F(i,j,k) &= F(j,i,k) \\ \sigma_{ijk} F(i,j,k) &= F(j,k,i) \end{aligned} \tag{F.4}$$

It is straight forward to see from the above description that

$$\sigma_{ij} = \sigma_{ji} \quad \text{and} \quad \sigma_{ijk} = \sigma_{jki} = \sigma_{kij}. \tag{F.5}$$

The inverse action can be identified and given by

$$\sigma_{ij}\sigma_{ij} = 1 \quad \text{and} \quad \sigma_{ijk}\sigma_{kji} = 1. \tag{F.6}$$

F.2 Dual operator $\hat{Q}^\sharp$

In this section we want to compute the dual operator $\hat{Q}^\sharp$ to the operator $\hat{Q}$

$$\hat{Q} = a + b_{ij}\sigma_{ij} + c_{ijk}\sigma_{ijk}, \tag{F.7}$$

where a, b_{ij}, and c_{ijk} are some complex numbers. The dual operator is defined from the relation

$$\sum_{\mathcal{P}_3} T^x_{3,m}(1,2,3)\hat{Q}J^x_{3,3}(1,2,3) = \sum_{\mathcal{P}_3} \left(\hat{Q}^\sharp T^x_{3,m}(1,2,3)\right) J^x_{3,3}(1,2,3), \tag{F.8}$$

where under the sum over the permutation, the action of $\hat{Q}$ on $J^x_{3,3}(1,2,3)$ is equivalent to the action of $\hat{Q}^\sharp$ on $T^x_{3,m}(1,2,3)$. Before we derive the expression of the dual operator let us recall that under the full permutation sum we have

$$\sum_{\mathcal{P}_3} F(1,2,3) = \sum_{\mathcal{P}_3} \sigma F(1,2,3), \tag{F.9}$$

for any function $F(1,2,3)$ and for any $\sigma \in \mathcal{P}_3$.

Starting with the left hand side of Eq. (F.8) combined with the definition of the operator Eq. (F.7), we have

$$\begin{aligned}\sum_{\mathcal{P}_3} T^x_{3,m}(1,2,3)\hat{Q}J^x_{3,3}(1,2,3) = a\sum_{\mathcal{P}_3} T^x_{3,m}(1,2,3)J^x_{3,3}(1,2,3) \\ + b_{ij}\sum_{\mathcal{P}_3} T^x_{3,m}(1,2,3)\sigma_{ij}J^x_{3,3}(1,2,3) \\ + c_{ijk}\sum_{\mathcal{P}_3} T^x_{3,m}(1,2,3)\sigma_{ijk}J^x_{3,3}(1,2,3).\end{aligned} \tag{F.10}$$

The first term in the the left hand side a trivial duality in which a no action in $J^x_{3,3}$ is dual to a no action in $T^x_{3,m}$. For the second term we are going to use Eq. (F.9) in

order to undo the action of σ_{ij} on $J^x_{3,3}$ with the inverse action such that

$$\begin{aligned}\sum_{\mathcal{P}_3} T^x_{3,m}(1,2,3)\sigma_{ij}J^x_{3,3}(1,2,3) &= \sum_{\mathcal{P}_3} \sigma_{ij}\left[T^x_{3,m}(1,2,3)\sigma_{ij}J^x_{3,3}(1,2,3)\right] \\ &= \sum_{\mathcal{P}_3} \left(\sigma_{ij}T^x_{3,m}(1,2,3)\right) J^x_{3,3}(1,2,3).\end{aligned} \tag{F.11}$$

For the third term in Eq. (F.10), we will perform the same trick as for the second term. The inverse action of σ_{ijk} is σ_{kji}; we have

$$\begin{aligned}\sum_{\mathcal{P}_3} T^x_{3,m}(1,2,3)\sigma_{ijk}J^x_{3,3}(1,2,3) &= \sum_{\mathcal{P}_3} \sigma_{kji}\left[T^x_{3,m}(1,2,3)\sigma_{ijk}J^x_{3,3}(1,2,3)\right] \\ &= \sum_{\mathcal{P}_3} \left(\sigma_{kji}T^x_{3,m}(1,2,3)\right) J^x_{3,3}(1,2,3).\end{aligned} \tag{F.12}$$

By taking everything back into Eq. (F.10), we can find that the dual operator the a general operator Eq. (7.33) is given by

$$\hat{Q}^\sharp = a + b_{ij}\sigma_{ij} + c_{ijk}\sigma_{kji}. \tag{F.13}$$

The dual operator $\hat{Q}^\sharp$, as defined in Eq. (7.37), of any operator $\hat{Q}$ which is a linear combination of permutations is given by the same operator $\hat{Q}$ with the exception where σ_{ijk} and σ_{kji} are interchanged.